On Knot Floer Homology of Satellite $(1,1)$ Knots

Philip J.P. Ording

Submitted in partial fulfillment of the
requirements for the degree
of Doctor of Philosophy
in the Graduate School of Arts and Sciences

COLUMBIA UNIVERSITY

2006

ABSTRACT

On Knot Floer Homology of Satellite $(1,1)$ Knots

Philip J.P. Ording

A $(1,1)$ knot is a knot $K \subset S^3$ which intersects each solid torus H_i, $i = 1,2$, of a genus one Heegaard splitting $S^3 = H_1 \cup H_2$ in a single trivial arc. Goda, Matsuda and Morifuji recognized that K is a $(1,1)$ knot if and only if it admits a doubly pointed Heegaard diagram of genus one, as defined by Ozsváth and Szabó. In this case, Ozsváth and Szabó have shown that the knot Floer homology of K is accessible by a combinatorial algorithm. This thesis presents a complementary algorithm for producing a doubly pointed Heegaard diagram from a given $(1,1)$ knot and then applies it in the study of knot Floer homology of certain satellite knots with trefoil companion. The Heegaard diagram algorithm here depends on a parameterization of (1,1) knots by Choi and Ko. The subsequent investigation of satellite knots depends on the classification of satellite (1,1) knots by Morimoto and Sakuma, and a computer program written by Gabriel Doyle is instrumental in the calculations of knot Floer homology herein. There are two appendices: one to implement the Heegaard knot diagram algorithm using *Mathematica*, and one to catalogue the knot Floer homology data obtained.

Contents

Acknowledgements

I owe my sincerest thanks to my advisor Professor Walter Neumann, for his trust and support throughout my graduate studies and to Professor Peter Ozsváth for his generosity and enthusiasm. I am especially grateful to my friend and colleague Matthew Hedden for suggesting this thesis problem and for generously sharing his knowledge of the subject with me. Jacob Rasmussen sent me Gabriel Doyle's program for computing knot Floer homology, and I am very grateful to them both. Part of my graduate research was carried out while I was visiting Japan, first as a National Science Foundation summer research fellow at Gakushuin University and then as a Japan Society for the Promotion of Science visiting researcher at Osaka University. There, I benefited from discussions with Makoto Sakuma, Hiroshi Goda and Mikami Hirasawa on the subject of $(1,1)$ knots, and I would like to express my sincere thanks to them and to their students for their hospitality. My friend Eugene Massey made helpful suggestions about programming. Emmanuel, David, Gene, Dylan, Noah, Peter, Joe, Matt, PJ, Keiko, Troels, Sara, Vanessa, Johan, Alp, Eric, Morgan, Bart, Nate, and Alexandra have been wonderfully supportive.

To my parents, Marie-Claire and Jon

Chapter 1

Introduction

Knot Floer homology is a homological realization of a classical knot invariant, the Alexander polynomial. In its most basic form it is a bigraded Abelian group

$$\widehat{HFK}(K) = \bigoplus_{d,i\in\mathbb{Z}} \widehat{HFK}_d(K,i)$$

The gradings d, i are, respectively, the Maslov or homological grading and the filtration grading. A fundamental property of knot Floer homology is that its Euler characteristic is the symmetrized Alexander polynomial:

$$\sum_i \chi(\widehat{HFK}(K,i)) \cdot t^i = \Delta_K(t)$$

where χ is the filtered Euler characteristic

$$\chi(\widehat{HFK}(K,i)) = \sum_d (-1)^d \operatorname{rk}(HFK_d(K,i))$$

The basic input for knot Floer homology is a Heegaard knot diagram $(\Sigma, \alpha, \beta, w, z)$ consisting of a closed oriented genus g surface, $2g$ embedded loops α, β and a pair

of basepoints $w, z \in \Sigma - \alpha - \beta$.

The knot Floer homology is a significant refinement of the classical invariant. However, calculating the knot Floer homology is difficult. In particular, computing the differentials involves counting points in certain moduli spaces of pseudoholomorphic discs in a symplectic manifold. In [OS04c], Ozsváth and Szabó showed that for Heegaard knot diagrams in the torus, the analysis reduces to a combinatorial problem. In [GMM05] Goda, Matsuda and Morifuji extended Ozsváth and Szabó's examples and showed that every $(1,1)$ knot has a genus one Heegaard knot diagram, and thus their knot Floer homology admits a combinatorial calculation. A $(1,1)$ knot is a knot embedded in an unknotted torus, except at a boundary parallel arc, or bridge. See figure 1.1. The $(1,1)$ knots form a large family which

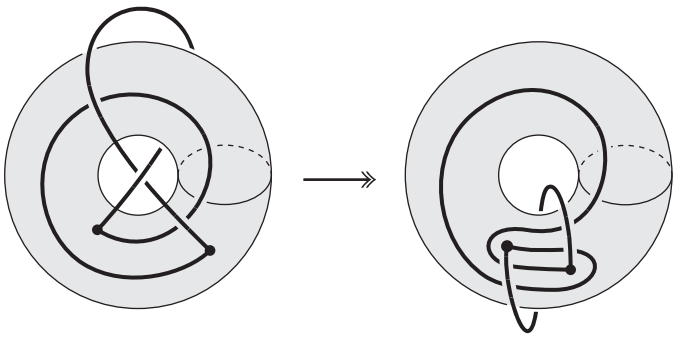

Figure 1.1: A $(1,1)$ knot, such as the figure eight knot above, admits a standard torus embedding, except at a bridge.

includes torus knots and 2-bridge knots as proper subfamilies. Hirozumi Fujii has shown [Fuj96] that every Laurent polynomial satisfying the properties of an Alexander polynomial appears as the Alexander polynomial of some $(1,1)$ knot.

In his survey article [Rasb], Jacob Rasmussen observes that a genus one Heegaard knot diagram can be put in a normal form represented by four integer parameters. His student Gabriel Doyle wrote a computer program [Doy05] that

takes the genus one Heegaard knot diagram parameters and calculates the knot Floer homology up to relative Maslov grading.

To calculate knot Floer homology according to the combinatorial examples found in [OS04c] and [GMM05], a genus one Heegaard diagram compatible with the knot is needed. Given a genus one Heegaard diagram, it is simple to find the knot associated with it. However, constructing a compatible genus one Heegaard diagram from a $(1,1)$ knot projection according to the known examples is complicated. Goda, Matsuda and Morifuji's examples [GMM05] involve isotoping the knot in the three-sphere while simultaneously isotoping an attaching circle in the torus. Each step in the isotopy of the knot determines the shape of the attaching curve, however this is the only regular aspect in the examples they construct. The knot isotopy is performed entirely "by hand." Unlike the genus one knot Floer homology calculation, an algorithm has been lacking in the construction of a genus one Heegaard knot diagram.

This thesis addresses this computational problem in knot Floer homology by presenting an algorithm for constructing a Heegaard diagram in the torus that is compatible with a $(1,1)$ knot. The difficulty inherent in the examples in [GMM05] is avoided by starting from a normalized projection of the $(1,1)$ knot to the flat torus. Doo Ho Choi and Ki Hyoung Ko showed [CK03] that $(1,1)$ knot projections in the torus can be put into a normal form $\mathfrak{d}(a,b,c,d)$ which is a generalization of the well-known Schubert normal form $\mathfrak{b}(a,b)$ for 2-bridge knots. Unlike Schubert normal form, however, it is not known what conditions to impose on the parameters a,b,c,d of $(1,1)$ normal form so that they classify $(1,1)$ knots. Projecting the knot to the torus allows for both the knot isotopy and the attaching curve isotopy to be performed in a rectangle. This is significantly more direct than the methods employed in [GMM05], and a computer implementation of the algorithm is included

in appendix A.

The algorithm is designed to produce a parameter indicating the absolute Maslov grading, in addition to producing the four parameters Rasmussen uses to describe a Heegaard diagram in the torus. This makes it possible to take advantage of Doyle's software and calculate the knot Floer homology groups exactly.

The algorithm starts with a Heegaard diagram for the unknot and ends with the Heegaard diagram for a given $(1,1)$ knot. Each step consists of a simple isotopy of an intermediate knot and attaching curve that either preserves or increases the total rank of the Floer homology. In particular, the absolute Maslov grading of generators is unchanged throughout the construction of the Heegaard diagram. It is due to this aspect of the algorithm that the the absolute Maslov grading of the generators in the desired Heegaard diagram may be deduced from the absolute Maslov grading of the single generator in the initial (unknot) Heegaard diagram.

This algorithm would have no advantage over the techniques of Goda, Matsuda and Morifuji were it not for the fact that the $(1,1)$ normal form can be determined for a large class of knots whose Floer homology is unknown. These are the satellite $(1,1)$ knots.

One outstanding question in knot Floer theory is how the invariants behave with respect to the satellite construction on knots. To construct a satellite knot, start with a knot C in the three-sphere S^3 and a knot P in the solid torus T. The *satellite knot with companion C and pattern P* is the image of P under an embedding $f : T \to S^3$ which maps T to a regular neighborhood of C. See figure 1.2. In general, the satellite knot will depend on the framing associated to the embedding of T. The Alexander polynomial of a satellite knot K has a simple expression in terms of the Alexander polynomials of its companion C and pattern

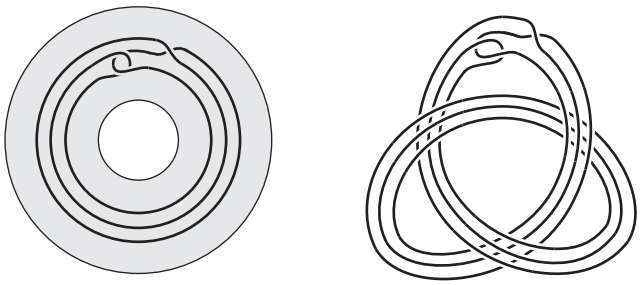

Figure 1.2: The satellite construction.

P

$$\Delta_K(t) = \Delta_C(t^n) \cdot \Delta_P(t)$$

where K represents n times a generator of $H_1(T)$. Given the correspondence between knot Floer homology and the Alexander polynomial, it is natural to expect that there is a generalization of this formula in homology.

Ozsváth and Szabó [OS04c] and Rasmussen [Ras03] proved that this is the case for composite knots, the simplest case of the satellite construction. The Alexander polynomial of a connect-sum is the product of the Alexander polynomials of its component knots. The knot Floer homology, for an appropriate choice of coefficients, is the tensor product of the component knot Floer homologies

$$\widehat{HFK}(K_1 \# K_2, i) \cong \bigoplus_{i=i_1+i_2} \widehat{HFK}(K_1, i_1) \otimes \widehat{HFK}(K_2, i_2)$$

Other special cases of the satellite construction have seen recent progress. Cabling was investigated by Matthew Hedden in his thesis [Hed05], and he has recently announced [Hed] a formula for the Floer homology of all Whitehead doubles of a knot. A t-twisted Whitehead double of a knot K is the satellite knot with companion K and unknot pattern as shown in figure 1.3. Hedden's results are

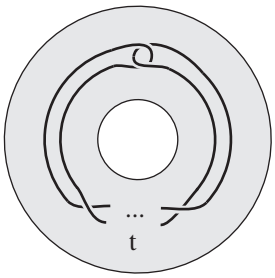

Figure 1.3: The pattern for a t-twisted Whitehead double.

informed, in part, by the work of Eaman Eftekhary [Eft05]. Unlike the Alexander polynomial, the knot Floer homology distinguishes the (untwisted) Whitehead double from the unknot. This fact is a corollary of a fundamental theorem of Ozsváth and Szabó [OS04b] which states that the degree of the knot Floer homology equals the Seifert genus of a knot, where the degree $\deg\widehat{HFK}(K)$ is defined as the largest integer $i > 0$ such that $\widehat{HFK}(K, i) \neq 0$.

Given the computational techniques available, satellite $(1, 1)$ knots are the next natural starting point for investigating the behavior of the knot Floer homology under the satellite construction. Morimoto and Sakuma completely classified satellite (1,1)-knots in [MS91]. A satellite $(1, 1)$ knot is denoted by the symbol $K(\alpha, \beta; p, q)$, and it is constructed from the 2-bridge link with Schubert normal form $b(\alpha, \beta)$ and has torus knot $t(p, q)$ companion.

As mentioned, there is a formula for the $(1, 1)$ normal form of a satellite $(1, 1)$-knot $K(\alpha, \beta; p, q)$. It is presented in lemma 4.1.

The algorithm is applied to construct Heegaard knot diagrams of several satellite knots with right-handed trefoil companion. Doyle's program is then used to calculate the knot Floer homology of the satellite and its pattern. The knot Floer homology of the right-handed trefoil is a basic and well-known example in the theory; it is reproduced in chapter 4. The Floer homology data for satellites and

their patterns is included in appendix B.

A particular example $K(8,3;3,2)$, the 6-twisted Whitehead double of the right-handed trefoil, proves to be especially useful. Khovanov homology is another knot homology theory that shares many formal properties with knot Floer homology (see Rasmussen's survey [Rasb]). Perhaps most interestingly, there exist smooth knot concordance invariants coming from both theories. The concordance invariants τ and s for knot Floer homology and Khovanov homology, respectively, coincided in every case where they had been computed, and they were conjectured to be equal [Rasa]. However, the Floer homology of $K(8,3;3,2)$ can be combined with Eftekhary's results for the untwisted Whitehead double [Eft05] to calculate τ of the 2-twisted Whitehead double of the trefoil, and here the knot Floer homology concordance invariant τ differs from the concordance invariant from Khovanov homology. This result is due to Hedden and the author and appears in [HO].

This thesis is organized as follows: Chapter 2 provides background on $(1,1)$ knots, Heegaard knot diagrams and knot Floer homology are provided. Knot Floer homology is one part a broader theory of 3- and 4-manifold invariants developed by Ozsváth and Szabó[1]. The aim of this thesis is focussed on calculating knot Floer homology in the special case of (classical) knots with genus one Heegaard diagrams. In order to keep the exposition contained, only the most basic form of the theory is presented. The various definitions are illustrated for the right-handed trefoil. The technique for constructing $(1,1)$ knot Heegaard diagrams found in [GMM05] is reviewed and illustrated in the case of $K(8,3;3,2)$. Normal forms for $(1,1)$ knots and genus one Heegaard diagrams are defined. Chapter 3 presents the algorithm for constructing a Heegaard diagram associated to a normal form of a $(1,1)$ knot. A torus knot example illustrates the various steps in the process. Chapter 4

[1]See Ozsváth and Szabó's survey [OS04a] for an overview of this greater context.

comprises the definition of satellite $(1,1)$ knots according to Morimoto and Sakuma and a presentation of the satellites' $(1,1)$ normal form. An explicit calculation of the knot Floer homology is included for $K(8,3;3,2)$, and the relevance for concordance invariants is discussed in more detail. Observations concerning the satellite knot Floer homology data conclude the chapter and the thesis. There are two appendices: appendix A to implement the Heegaard knot diagram algorithm using the software system *Mathematica* [Wol05], and appendix B to catalogue the knot Floer homology data obtained.

Chapter 2

Heegaard Knot Diagrams & Knot Floer Homology

2.1 Heegaard knot diagrams

A *knot* will mean an embedding of the circle in the 3-dimensional sphere S^3. A properly embedded arc t in a handlebody H is *trivial* if there is an embedded disk $D \subset H$ such that $D \cap t = t$ is a subarc of ∂D, and $D \cap \partial H = c\ell(\partial D - t, \partial D)$ is an arc $p(t)$ connecting the two points of $\partial t \subset \partial H$. The arc $p(t)$ is referred to as the *projection* of t onto ∂H, while D is called the *trace disk* of the projection.

Let Σ be a genus g Heegaard surface of a Heegaard decomposition $S^3 = H_\alpha \cup_\Sigma H_\beta$. A knot K is said to be in *b-bridge position* with respect to Σ if K intersects Σ transversely and meets each handlebody H_α, H_β in a collection of b mutually disjoint trivial arcs $K \cap H_\alpha = t_\alpha^1 \cup \cdots \cup t_\alpha^b$ and $K \cap H_\beta = t_\beta^1 \cup \cdots \cup t_\beta^b$. The union $(H_\alpha, t_\alpha^1 \cup \cdots \cup t_\alpha^b) \cup (H_\beta, t_\beta^1 \cup \cdots \cup t_\beta^b)$ is called a (g, b) *decomposition of* K. A (g, b) *knot* is a knot which admits a (g, b) decomposition. Notice that a $(0, b)$ decomposition corresponds to the usual b-bridge presentation of a knot. A diagram

of a (g, b) knot often projects the trivial arcs in one or the other handlebody to the Heegaard surface, as is the case in figure 1.1. Calling a $(1, 1)$ knot a "1-bridge torus knot" emphasizes this perspective.

A handlebody H with boundary Σ can be constructed from Σ by first attaching g 2-handles along g disjoint, simple closed curves $\{\gamma_1, \ldots, \gamma_g\}$ which are linearly independent in $H_1(\Sigma, \mathbb{Z})$, and then attaching a 3-handle. The curves $\{\gamma_1, \ldots, \gamma_g\}$ are called *attaching circles for* H. Notice that the three-handle is unique. This fact implies that H is determined by the attaching circles and allows us to characterize a Heegaard splitting by two sets of attaching circles. Let $M = H_\alpha \cup_\Sigma H_\beta$ be a genus g Heegaard splitting for a closed oriented three-manifold, M. A *Heegaard diagram for* M is a triple $(\Sigma,\boldsymbol{\alpha},\boldsymbol{\beta})$ consisting of the splitting surface Σ and two sets of g curves in Σ, $\boldsymbol{\alpha}= \{\alpha_1, \ldots, \alpha_g\}$ and $\boldsymbol{\beta}= \{\beta_1, \ldots, \beta_g\}$, which are attaching circles for the handlebodies H_α and H_β, respectively.

Two Heegaard diagrams may represent equivalent three-manifolds. In such a case, there is an isotopy, handleslide, stabilization or a sequence of the above which transforms one of the Heegaard diagrams into the other (cf. [GS99]). These transformations are referred to as *Heegaard moves*. A Heegaard move that preserves a point $u \in \Sigma$ will be referred to as a *u-pointed Heegaard move*.

There is another consequence of the uniqueness of the three-handle in the construction of a handlebody via attaching circles, and it invites the appearance of knots:

Definition 1. Let $\boldsymbol{\gamma}= \{\gamma_1, \ldots, \gamma_g\}$ be a set of attaching circles for a genus g handlebody H with boundary Σ, and let $B \subset H$ denote the three-ball cut from H by g properly embedded disks that the attaching circles bound. Then two basepoints $w, z \in \Sigma$ which do not lie on any of the attaching circles $\boldsymbol{\gamma}$ bound a unique (up to isotopy) arc t_γ in B. We call t_γ the *cut arc of* $\boldsymbol{\gamma}$ *based at* w, z.

Finally, we can state the main definition concerning this thesis, namely that of a Heegaard knot diagram.

Definition 2. Let $(\Sigma,\boldsymbol{\alpha},\boldsymbol{\beta})$ be a Heegaard diagram for S^3 and $w, z \in \Sigma$ two basepoints which do not lie on any of the attaching circles $\boldsymbol{\alpha},\boldsymbol{\beta}$. The union $t_\alpha \cup t_\beta$ of the cut arc t_α of $\boldsymbol{\alpha}$ based at w, z and t_β of $\boldsymbol{\beta}$ based at w, z is an embedded circle in S^3. If the union of the cut arcs based at w, z has knot type K we call the quintuple $(\Sigma, \boldsymbol{\alpha}, \boldsymbol{\beta}, w, z)$ a *Heegaard knot diagram for* K.

Figure 2.1 depicts a genus one Heegaard knot diagram for the trivial knot.

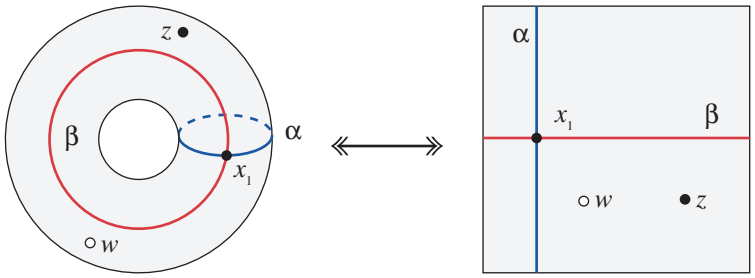

Figure 2.1: Heegaard knot diagram for the trivial knot.

Remark 1. The definition of a Heegaard knot diagram is slightly different than that of a doubly pointed Heegaard diagram compatible with a knot K, as defined in [OS04c]. For the latter, it is required that K is supported inside the β handlebody as an unknotted circle. Moreover, K meets the attaching disk bounded by β_1 transversely in one point, and none of the other attaching disks; β_1 is a meridian of the knot. Given a genus g Heegaard knot diagram $(\Sigma, \boldsymbol{\alpha}, \boldsymbol{\beta}, w, z)$ for K, as defined above, a stabilization produces a genus $g+1$ doubly pointed Heegaard diagram $(\Sigma', \boldsymbol{\alpha'}, \boldsymbol{\beta'}, w', z')$: Drill out a 1-handle $I \times D^2$ along the arc t_α. For w', z', choose two points in $\partial I \times \partial D^2$ at opposite ends of the 1-handle. The attaching circle ∂D^2 is a meridian, nominate it β_1' and define the rest of $\boldsymbol{\beta}$, as $\beta_i' := \beta_{i-1}$. In the other

handlebody, add to the beginning of $\boldsymbol{\alpha'}$ the boundary of the trace disk of t_β. The knot Floer homology of the two diagrams is equivalent [OS04c, Proposition 6.1].

2.2 Goda, Matsuda & Morifuji's construction

A doubly pointed genus g Heegaard diagram compatible with a knot K determines a $(g,1)$ decomposition of K since K is in 1-bridge position with respect to Σ. Given a $(g,1)$ decomposition for K there is, a priori, no well-defined associated Heegaard knot diagram for K; the definition of a (g,b) decomposition does not specify the placement of attaching circles. If K is a $(g,1)$ knot with respect to the surface Σ of a Heegaard splitting $S^3 = H_\alpha \cup H_\beta$, and $K \cap \Sigma = \{w,z\}$, then it is possible to find attaching circles $\boldsymbol{\alpha}$, $\boldsymbol{\beta}$ in $\Sigma - w - z$ such that $(\Sigma, \boldsymbol{\alpha}, \boldsymbol{\beta}, w, z)$ is a genus g Heegaard knot diagram for K. It suffices to take any set of attaching circles $\boldsymbol{\alpha}$ and $\boldsymbol{\beta}$ which are disjoint from the trace disks D_α of t_α and D_β of t_β respectively. This basic fact was proved in the genus one case [GMM05, Proposition 2.3] by Goda, Matsuda and Morifuji.

The examples of Heegaard knot diagrams appearing in [GMM05], for non-alternating knots with ten crossings and certain pretzel knots, are obtained by using a particular $(1,1)$ decomposition which is associated with an unknotting tunnel. An *unknotting tunnel* for a knot K is a properly embedded arc γ in the knot exterior, such that the complement of the graph $K \cup \gamma$ is an unknotted genus 2 handlebody. A graph whose complement in S^3 is an unknotted genus 2 handlebody is topologically a *theta graph* Θ, consisting of two vertices spanned by three edges $\delta_0, \delta_1, \delta_2$. A $(1,1)$ *tunnel for* K is an unknotting tunnel γ which meets K in such a way that a tubular neighborhood N of $\gamma \cup \delta_1$ or $\gamma \cup \delta_2$ in S^3 is a genus one Heegaard surface for S^3. In particular, $(N, K \cap N) \cup (S^3 - N, K \cap S^3 - N)$ is a $(1,1)$ decomposition of K. See figure 2.2. Every $(1,1)$ knot admits a $(1,1)$

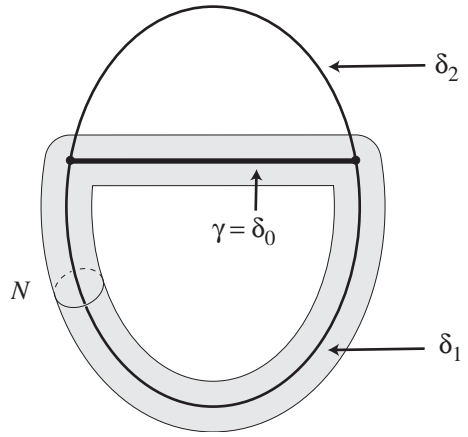

Figure 2.2: A $(1,1)$ tunnel $\gamma = \delta_0$ for a knot $K = \delta_1 \cup \delta_2$ and the associated $(1,1)$ decomposition. The graph $K \cup \gamma$ is a theta graph, so named for the shape of the embedding shown.

tunnel [MS91].

The Heegaard knot diagram constructions in [GMM05] begin with a Heegaard knot diagram for the trivial knot consisting of the Heegaard surface $\partial N \cong S^1 \times S^1$ associated to a given $(1,1)$ tunnel for a knot K, the standard meridian-longitude pair $S^1 \times 0$, $0 \times S^1$ and two basepoints $\{w, z\} = K \cap \partial N$. The diagram evolves according to a sequence of theta graph moves which realize the given tunnel as a $(1,1)$ tunnel for K. The beautiful illustrations of the constructions in [GMM05] make it clear that the diagrams so obtained are in fact Heegaard knot diagrams. (Figure 2.4 mimics their technique.) The general relationship between a theta graph move and a step in the evolution of the Heegaard knot diagram is implicit. The following description is meant to provide more detail and a setting for the general construction presented in chapter 3.

Let $f_t : \Theta \times I \to S^3 \times I$ be an ambient isotopy realizing γ as an unknotting tunnel for K; that is, f_t is a one parameter family of embeddings, such that $f_0|_{\delta_0} = \gamma$, $f_0|_{\delta_1 \cup \delta_2} = K$, and f_1 is a planar embedding of the theta graph. Assume

that f_t fixes, say, δ_1 for all $t \in I$ so that γ is a $(1,1)$ tunnel for K. Denote by T the genus one Heegaard surface of the associated $(1,1)$ decomposition for K. As previously, label w, z the points in T where the knot meets the splitting surface. Define a *projection of f_t to the Heegaard surface T* to be a one parameter family of surface automorphisms $pf_t : T \times I \to T \times I$ satisfying the following conditions: (i) The initial projection is the identity $pf_0 = \mathrm{id}$. (ii) For all $t \in I$, the image of the meridian $S^1 \times I \subset T$ under pf_t is a simple closed curve disjoint from w, z. (iii) The automorphism traces the movement of the basepoints w, z through out the tunnel isotopy; $pf_t|_{w,z} = \mathrm{Im} f_t \cap T$ for all $t \in I$.

Observe that the projection of the tunnel isotopy f_t, as defined, restricts to an isotopy on the meridian $S^1 \times 0$ starting with the identity and avoiding w, z throughout. In particular, this means that the cut arc of $S^1 \times 0$ based at w, z is well-defined for all $t \in I$ and coincides with the trivial arc of K in the solid torus with meridian $S^1 \times 0$. By the time $t = 1$, the image of the attaching circle $pf_1(S^1 \times 0)$ under the projection will generally fold around the basepoints in some complicated fashion; however, overhead the image of the trivial arc δ_2 is as simple as can be. Since $f_1(\Theta)$ is planar, there is some $x \in S^2$ such that $x \times S^1$ bounds a disk disjoint from the image of $f_1|_{d_2}$. Without loss of generality we assume $x = 0$, and $(T, pf_1(S^1 \times 0), 0 \times S^1, w, z)$ is a Heegaard knot diagram for K.

Figure 2.3 illustrates in stages the ambient isotopy realizing a $(1,1)$ tunnel for the 6-twisted Whitehead double of the right-handed trefoil, and each stage of the isotopy is projected to the torus in figure 2.4. This example is modeled on those appearing in [GMM05].

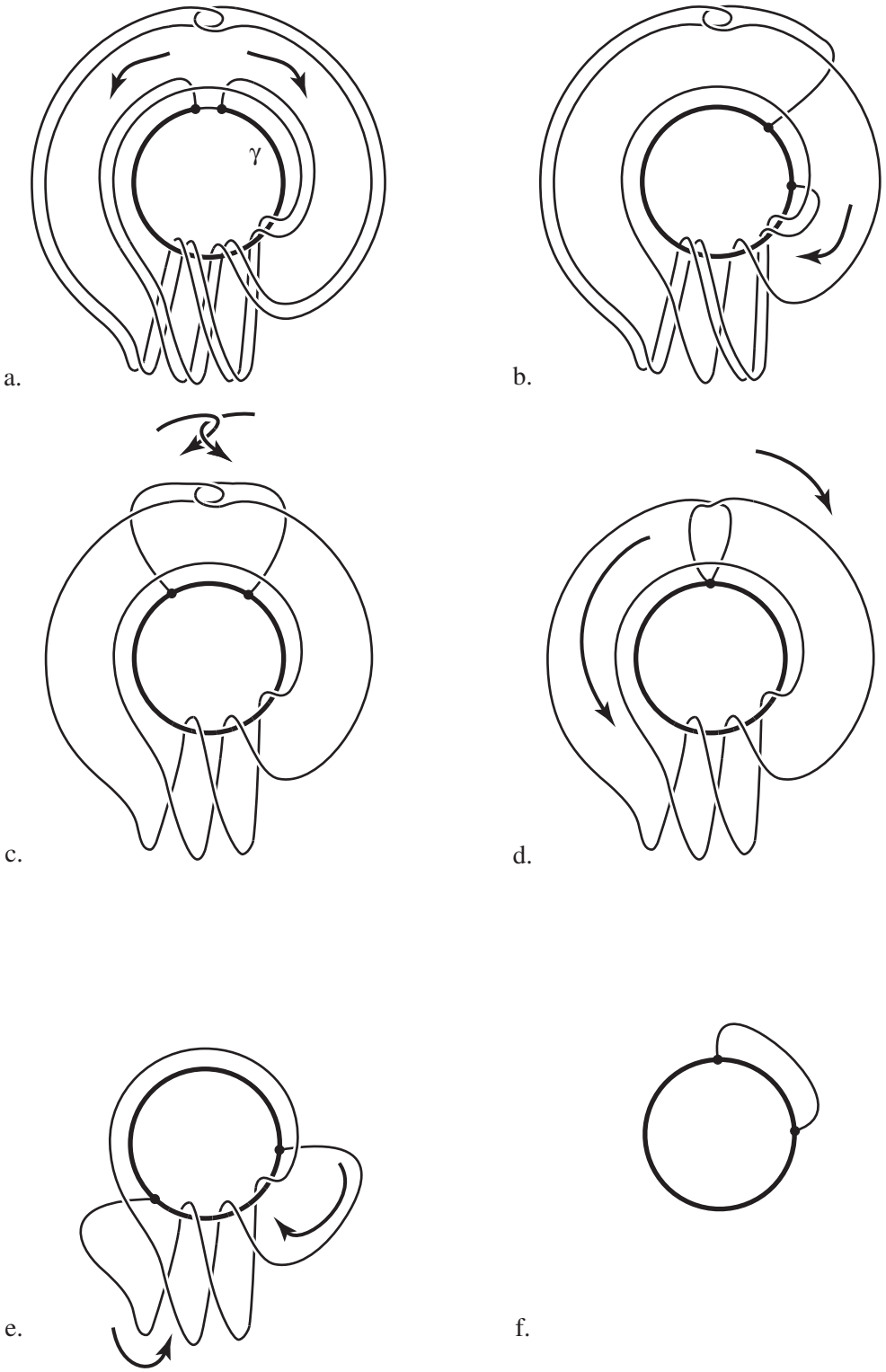

Figure 2.3: A $(1,1)$ tunnel γ for the 6-twisted Whitehead double of the right-handed trefoil.

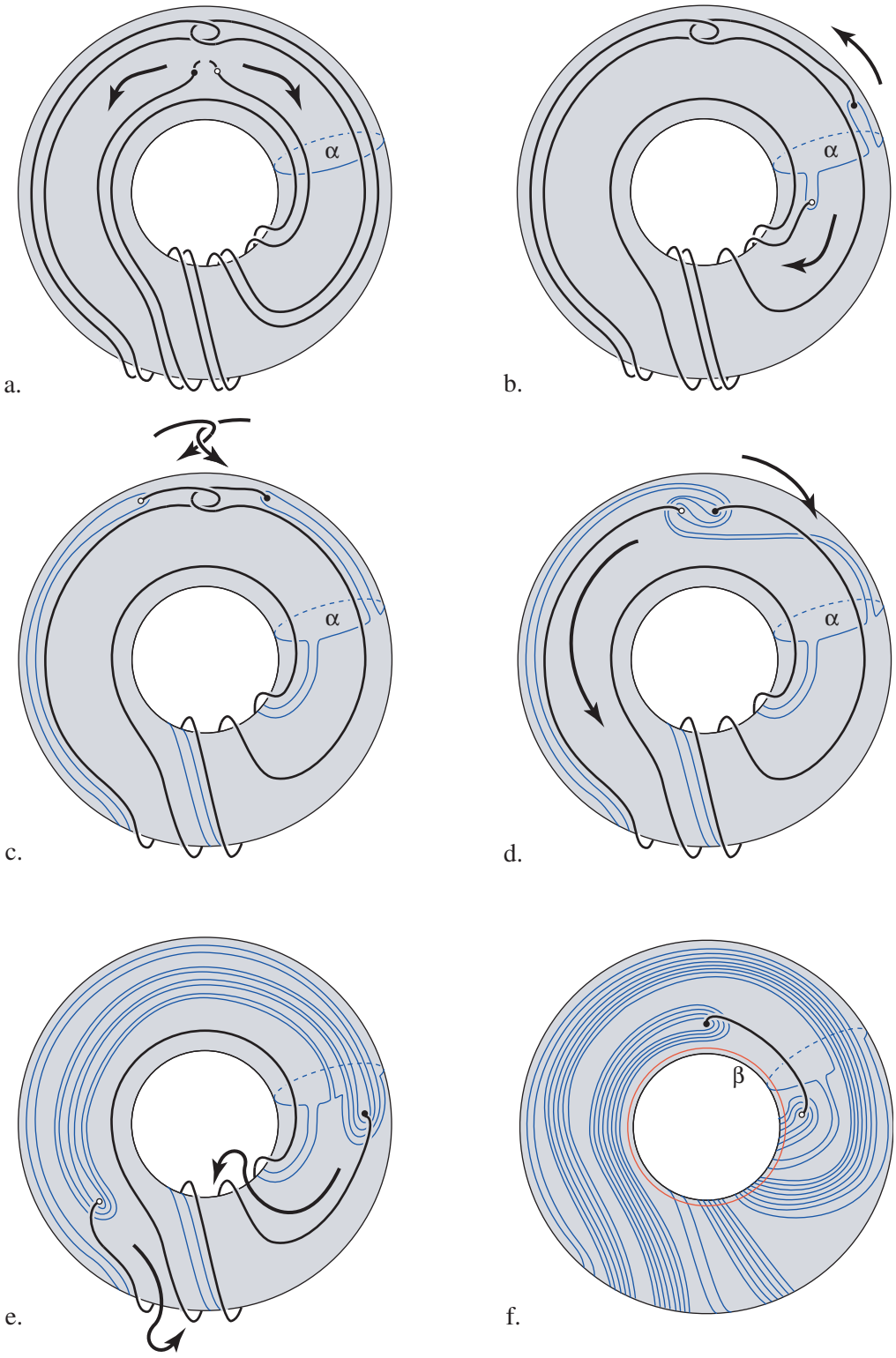

Figure 2.4: Constructing a Heegaard knot diagram for the 6-twisted Whitehead double of the right-handed trefoil, after Goda, Matsuda and Morifuji. The white and black circles are respectively w and z.

Remark 2. There is a paper [Sti79] by John Stillwell defining a geometrically natural invariant called the *compound crossing number* $C(K)$ of a knot K. The compound crossing number may be characterized as the smallest genus of all closed orientable surfaces F for which there is an embedding $K \hookrightarrow F$. As has been shown for other similar invariants (tunnel number, Heegaard genus, etc.), $C(K)$ provides an improvement over ordinary crossing number or bridge index in terms of bounding the number of generators and relations in the knot group [Sti79, Theorem 2]. What is of immediate relevance is the particular case, of knots having a "bridge" compound crossing. This case coincides exactly with $(g, 1)$ knots. Stillwell refines the bound on the generators of the knot group in this case and we interpret the result as: The knot group of a $(g, 1)$ knot has a presentation with $g + 1$ generators and g relations. From the geometric constructions of the proof, it is immediately observed [Sti79, Corollary] that a suitable cut — representing the single relation in the knot group — in an unknotted genus 2 handlebody produces a knotted torus whose knot is an arbitrary $(1, 1)$ knot K. This observation coincides with the aforementioned fact that $(1, 1)$ knots are those knots which admit genus one Heegaard knot diagrams [GMM05, Proposition 2.3]; a cut reversed in time is equivalent to attaching a 2-handle.

2.3 Normal form

At the expense of symmetry, it is sometimes useful to distinguish the trivial arcs to one side of the Heegaard surface from those on the other. The Schubert normal form used in the classification of 2-bridge knots [Sch56] is an example of a $(0, 2)$ decomposition which differentiates the pair of trivial arcs in one halfspace from the other; it is defined as follows: Let $(B_\alpha, t^1_\alpha \cup t^2_\alpha) \cup (B_\beta, t^1_\beta \cup t^2_\beta)$ denote the $(0, 2)$ decomposition of the 2-bridge knot K, where B_α, B_β are 3-balls bound by

a 2-sphere S^2. Project one pair of trivial arcs t^i_α onto two separate straight line segments $p(t^i_\alpha)$, and the other pair t^i_β onto two disjoint simple curves $p(t^i_\beta)$ where $i = 1, 2$. The projections can be arranged according to the diagrams in figure 2.5 where a, b are coprime integers satisfying $0 < a$ and $0 < |b| < a/2$. By *Schubert normal form* $\mathfrak{b}(a, b)$ is meant this diagram and the knot it describes. A pair of

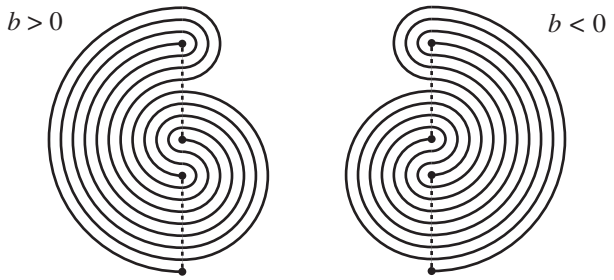

Figure 2.5: Schubert normal form for 2-bridge knots and links. On the left $\mathfrak{b}(8, 3)$, on the right $\mathfrak{b}(8, -3)$.

2-bridge knots $\mathfrak{b}(a, b)$, $\mathfrak{b}(a', b')$ are equivalent if and only if

$$a' = a \qquad \text{and} \qquad b' \equiv b^{\pm 1} \mod a$$

where b^{-1} is an integer satisfying $0 < |b^{-1}| < a$ and $bb^{-1} \equiv 1 \mod a$. The 2-bridge knot obtained by switching the over- and under-crossings — the mirror — of the normal form $\mathfrak{b}(a, b)$ is equivalent to the normal form $\mathfrak{b}(a, -b)$. Normal form $\mathfrak{b}(a, b)$ represents a two-component link if a is even, and a knot otherwise.

Knots with a $(1, 1)$ decomposition may be approached from a vantage point very similar to Schubert normal form for 2-bridge knots. Let $(H_\alpha, t_\alpha) \cup (H_\beta, t_\beta)$ be a $(1, 1)$ decomposition of a $(1, 1)$ knot K. Project the trivial arcs t_α, t_β to simple arcs $p(t_\alpha)$, $p(t_\beta)$ in the torus $T = \partial H_\alpha = \partial H_\beta$. Represent the torus T by a rectangle in the plane with sides labeled alternately M, L to indicate the standard meridian-longitude pair and the usual identifications. Assume $p(t_\alpha)$ is a straight line segment in T. Doo Ho Choi and Ki Hyoung Ko observed [CK03] that, after a

suitable isotopy, the arc $p(t_\beta)$ appears in one of the two forms shown in figure 2.6. A $(1,1)$ knot K in this position is said to be in $(1,1)$ *normal form* $\mathfrak{d}(a,b,c,d)$, where

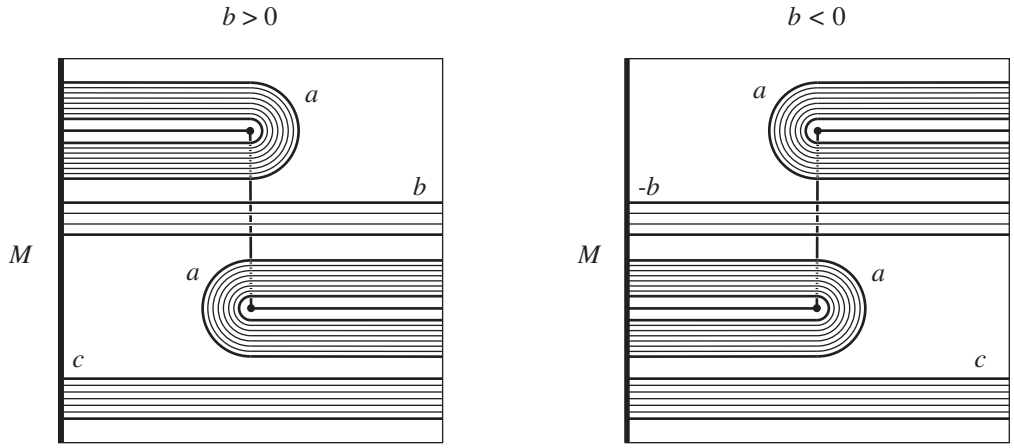

Figure 2.6: Normal form of a $(1,1)$ knot. The parameters a, b, c count the number of arcs in the bundles of strands, as shown. The square represents the flat torus with meridian M; top and bottom sides identified as usual. Identify left and right sides after twisting according to the parameter d. See the text.

$a, b, c, d \in \mathbb{Z}$. There are a strands in each of the rainbows that pass around the endpoints $\{w, z\} = K \cap T$. The parameter b counts the number of strands passing between the rainbows, and above $p(t_\alpha)$. The "slope" of these strands is defined according to the sign of b, as shown in figure 2.6. In addition, there are c strands running straight across the bottom of the diagram. The last parameter d is the *twist parameter*, and it indicates how the ends at the sides of the diagram match up: From top to bottom, number the strand ends on each side of the diagram $1, \ldots, 2a + |b| + c + 1$, then, identify the ith end on the right with the left end labeled $i + d \mod (2a + |b| + c + 1)$ by a $2\pi d/(2a + |b| + c + 1)$ twist. It should be noted that the sign convention chosen for d here is opposite the convention held in the original Choi-Ko parameterization of $(1,1)$ knots, as defined in [CK03]; the equivalence of Choi and Ko's *Schubert normal form of* 1*-bridge torus knots*

$(r, s, t, \rho)_\epsilon$ and $(1,1)$ normal form $\mathfrak{d}(a, b, c, d)$ is

$$\mathfrak{d}(r, \epsilon s, t, -\rho) = (r, s, t, \rho)_\epsilon$$

Notice in the following examples that one choice of orientation agrees with the convention for 2-bridge knots while the other, torus knots.

Example 2.3.1. $(1,1)$ normal form for 2-bridge knots. Since $(1,1)$ normal form is modeled on Schubert normal form, it is easy to see that any 2-bridge knot $\mathfrak{b}(\alpha, \epsilon\beta)$ normalized so that $0 < \beta < \alpha/2$ and $\epsilon = \pm 1$ is represented by

$$\mathfrak{d}(\beta - 1, \epsilon(\alpha - 2\beta + 1), 0, -\epsilon)$$

Example 2.3.2. Torus knots. These also have simple $(1,1)$ forms, since $(1,1)$ diagrams are torus diagrams. A $\mathfrak{t}(p, q)$ torus knot normalized so that $q > 0$, is represented by

$$\mathfrak{d}(0, 0, q - 1, p)$$

Notice that a $(1,1)$ normal form of type $b > 0$ can be transformed into a type $b < 0$ normal form, and vice versa, by sliding one of rainbows around the meridian. This implies that for $\epsilon = \pm 1$ and $b > 0$, the normal form $\mathfrak{d}(a, \epsilon b, c, d)$ represents the same knot as the normal form $\mathfrak{d}(a, -\epsilon c, b, d - \epsilon(2a + 1))$. Unlike Schubert normal form, it is not known what conditions to impose on the parameters of $(1,1)$ normal form so as to classify the knots they describe.

The two attaching circles α, β of a genus one Heegaard knot diagram (T, α, β, w, z) can be arranged in a shape very similar to $(1,1)$ normal form. Define *genus one Heegaard knot diagram normal form* $\mathfrak{D}(a, b, c, d)$, abbreviated as *Heegaard normal form*, as follows. The attaching circle α is represented by the meridian M bounding the flat torus diagram at the sides, and β, w and z take the form shown in figure 2.3. The parameters a, b, c, d are defined as for $(1,1)$ normal form, with

the following minor modification. There is one fewer strand end in the Heegaard knot diagram normal form than the $(1,1)$ normal form, and we identify the ith end on the right with the end labeled $i+d \mod (2a+b+c)$ on the left. This presentation of a genus one Heegaard knot diagram is equivalent to the one Rasmussen describes in [Rasb]. A genus one Heegaard knot diagram with normal form $\mathfrak{D}(a,b,c,d)$ represents the knot $K(p,q,r,s)$, as defined in [Rasb], for $p=2a+b+c$, $q=a$, $r=b$, $s=d$.

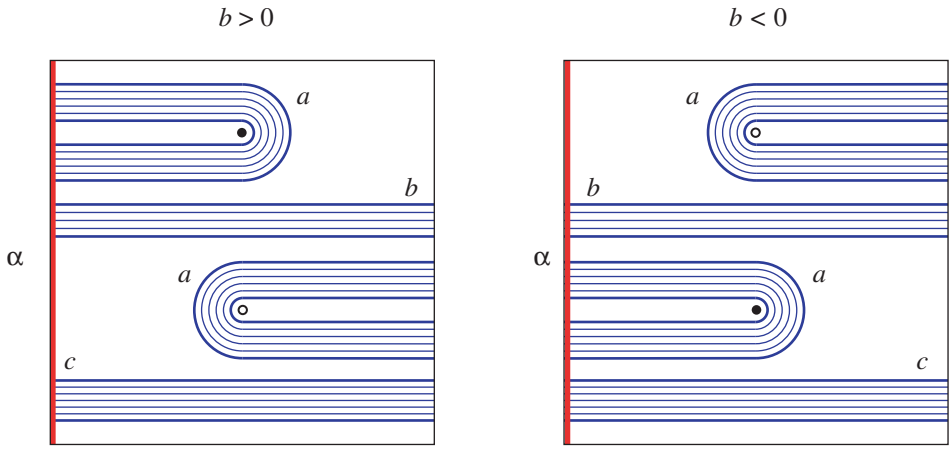

Figure 2.7: Genus one Heegaard knot diagram normal form. Attaching circles α, β are respectively in red and blue. The open and closed dots mark the basepoints w and z.

As already discussed, it is, in general, a difficult problem to find the Heegaard normal form corresponding to a given $(1,1)$ normal form. The case of 2-bridge knots is an exception.

Example 2.3.3. 2-bridge knots. The Heegaard normal form

$$\mathfrak{D}(\beta, \epsilon(\alpha - 2\beta), 0, 0)$$

where $0 < \beta < \alpha/2$ and $\epsilon = \pm 1$ is a Heegaard knot diagram for the 2-bridge knot with Schubert normal form $\mathfrak{b}(\alpha, \beta)$. This is immediate upon observing that the

$(1,1)$ normal form $\mathfrak{d}(\beta-1,\epsilon(\alpha-2\beta+1),0,-\epsilon)$ for $\mathfrak{b}(\alpha,\beta)$ represents an arc in $T-\beta$ connecting the basepoints w,z.

2.4 Knot Floer homology

Defining knot Floer homology in general — for $(g,1)$ knots — requires a significant amount of analysis. In order to discuss the differentials, for example, one must consider pseudoholomorphic disks in a $2g$ dimensional symplectic manifold. The geometry is sufficiently restricted (essentially, by the Riemann Mapping theorem) in the case $g=1$ that the basics of knot Floer homology may be characterized in a combinatorial way. This section summarizes the combinatorial calculation of the knot Floer homology $\widehat{HFK}(K)$ in the case of $(1,1)$ knots, as defined in [OS04c], and later developed in [GMM05].

Let (T,α,β,w,z) be a genus one Heegaard knot diagram for K. Lift the torus T to its universal cover $\tilde{T}\cong\mathbb{R}^2$. Pick two curves $\tilde{\alpha},\tilde{\beta}\subset\tilde{T}$ which project onto α,β respectively. Consider the free abelian group $CFK^\infty(K)$ generated by certain triples $[x,i,j]$ where x is an intersection point of $\tilde{\alpha}\cap\tilde{\beta}$ and $i,j\in\mathbb{Z}$.

For every pair of points $x,y\in\tilde{\alpha}\cup\tilde{\beta}$ there is a unique (up to homotopy) oriented closed path γ in $\tilde{\alpha}\cup\tilde{\beta}$ starting at x, going out along $\tilde{\alpha}$ to y and returning along $\tilde{\beta}$ back to x. If this path encloses a simply connected domain ϕ to its left, we[1] say x *is connected to* y *by a proper Whitney disk* $\phi(x,y)$. Let $\pi_2^1(x,y)$ denote the set of all proper Whitney disks ϕ connecting x to y.

Give $CFK^\infty(K)$ the differential

$$\partial^\infty[x,i,j]=\sum_{y\in\tilde{\alpha}\cap\tilde{\beta}}\sum_{\phi\in\pi_2^1(x,y)}[y,i-n_w(\phi),j-n_z(\phi)],$$

[1]The term "proper" is our own short-hand for unit Maslov index. See [OS04d] for details.

where $n_v(\phi)$ denotes the intersection number of ϕ with the lattice $\tilde{v} \subset \tilde{T}$ generated by lifts of a point $v \in T - \alpha - \beta$. The knot Floer homology $\widehat{HFK}(K)$ is equivalent to the homology of the chain complex $(CFK^\infty(K), \partial^\infty)$.

The knot Floer homology groups $\widehat{HFK}$ are graded by a homological grading and a filtration grading denoted gr and $\mathcal{F}$, respectively. The relative gradings of a pair of intersection points $x, y \in \{x_1, \ldots, x_n\}$ connected by a Whitney disk $\phi(x, y) \in \pi_2^1(x, y)$ is given by the relations

$$\mathrm{gr}(y) - \mathrm{gr}(x) = 2n_w(\phi(x, y)) - 1$$

$$\mathcal{F}(y) - \mathcal{F}(x) = n_w(\phi(x, y)) - n_z(\phi(x, y))$$

The absolute filtration grading can be determined by requiring that the rank of $\widehat{HFK}$ in filtration level i is the same as it is in filtration level $-i$. The absolute homological grading is defined for the trivial knot below. Later it will be described how to to determine the absolute grading of a generator of $CFK^\infty(K)$ of an arbitrary $(1, 1)$ knot K from the grading on the trivial knot.

Example 2.4.1. The trivial knot is a $(1, 1)$ knot with a Heegaard knot diagram (T, α, β, w, z) consisting of the torus T, attaching circles α, β bounding standard meridian disks in the solid tori T_α, T_β respectively, and basepoints $w, z \in T - \alpha - \beta$, as shown in Figure 2.1. There is a unique generator $[x_1, i, j]$ corresponding to the single intersection $\tilde{\alpha} \cap \tilde{\beta}$, and no differentials. Hence, $\widehat{HFK}(\text{unknot}) \cong \mathbb{Z}$. Since there is only one generator, it must lie in filtration level $\mathcal{F} = 0$, and the absolute homological grading is defined to be $\mathrm{gr}(x_1) = 0$. Hence,

$$\widehat{HFK}(\text{unknot}, i) = \begin{cases} \mathbb{Z}_{(0)}, & \text{if } i = 0 \\ 0 & \text{else} \end{cases}$$

Hedden has pointed out [Hed05] that the fact that a w-pointed Heegaard move preserves the absolute homological grading $\mathrm{gr}(x)$ can be used to determine the absolute homological grading. Since every Heegaard knot diagram can be transformed by a sequence of w-pointed Heegaard moves into a Heegaard knot diagram for the unknot, the absolute homological grading is determined by the absolute homological grading of the single generator (of $\widehat{HFK}(\text{unknot})$) left after this process. The algorithm in Chapter 3 constructs the required sequence of w-pointed Heegaard moves and isolates the intersection that persists throughout it.

Example 2.4.2. Knot Floer homology of the right-handed trefoil. The trefoil is a $(1,1)$ knot; figure 2.8 illustrates the $(1,1)$ normal form $\mathfrak{d}(0,-2,0,1)$ and a genus one Heegaard knot diagram $\mathfrak{D}(1,-1,0,0)$ obtained from the Schubert normal form $\mathfrak{b}(3,-1)$ for the right-handed trefoil. There are 2 proper Whitney disks connecting

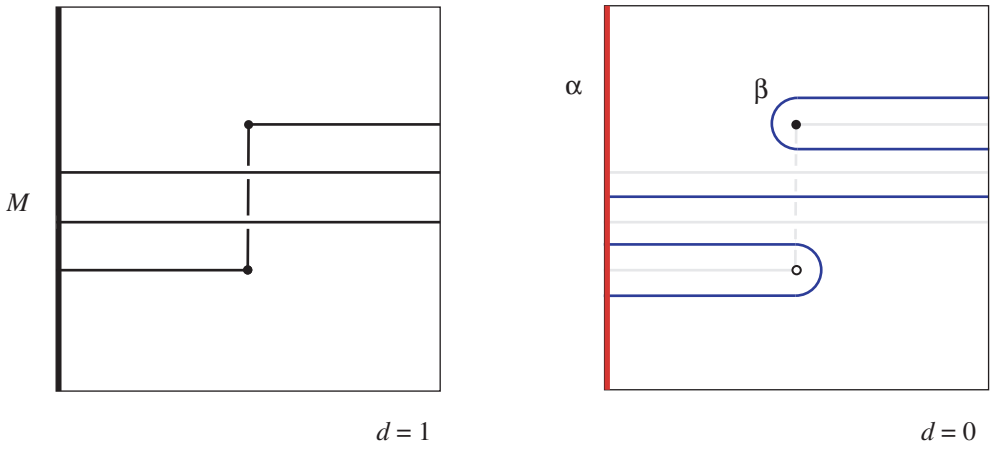

Figure 2.8: The right-handed trefoil. On the left, $(1,1)$ normal form $\mathfrak{d}(0,-2,0,1)$, and Heegaard normal form $\mathfrak{D}(1,-1,0,0)$, on the right.

the 3 intersection points of $\tilde{\alpha} \cap \tilde{\beta}$ shown in Figure 2.9. These yield the following

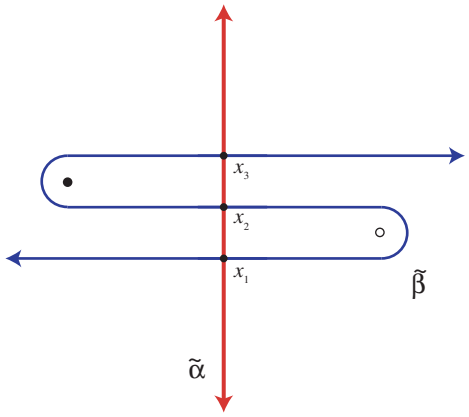

Figure 2.9: A lift of the Heegaard knot diagram of the trefoil. The open and closed circles are respectively w and z.

differentials:

$$\begin{aligned}
\partial[x_1, i, i] &= 0 \\
\partial[x_2, i, i] &= [x_1, i-1, i] + [x_3, i, i-1] \\
\partial[x_3, i, i] &= 0
\end{aligned}$$

Notice the Heegaard knot diagram in figure 2.9 is transformed to the Heegaard knot diagram of the unknot under an isotopy of $\tilde{\beta}$ which cancels the proper Whitney disk from x_2 to x_3. Such an isotopy is clearly a w-pointed Heegaard move, and it follows that the generator x_1 has absolute homological grading zero. Arranging the generators according to homological and filtration gradings in the columns and rows respectively, the following table is obtained:

	-2	-1	0
1			x_1
0		x_2	
-1	x_3		

Thus, the knot Floer homology groups of the right-handed trefoil are:

$$\widehat{HFK}(\mathfrak{b}(3,-1),i) \cong \begin{cases} \mathbb{Z}_{(0)} & \text{if } i = 1 \\ \mathbb{Z}_{(-1)} & \text{if } i = 0 \\ \mathbb{Z}_{(-2)} & \text{if } i = -1 \\ 0 & \text{else} \end{cases}$$

Chapter 3

Cat's Cradle Algorithm

Given a genus one Heegaard knot diagram $(\Sigma, \alpha, \beta, w, z)$, a diagram of a compatible $(1,1)$ knot can be drawn by simply joining the basepoints w, z by a trivial arc t_α in the α-handlebody and a trivial arc t_β in the β-handlebody, making sure to avoid intersection with the meridian disks defined by α resp. β. This chapter addresses the converse problem: producing a genus one Heegaard knot diagram for a given $(1,1)$ knot.

Theorem 3.5 proves an algorithm for constructing a genus one Heegaard knot diagram $(\Sigma, \alpha, \beta, w, z)$ from a $(1,1)$ normal form $\mathfrak{d}(a,b,c,d)$. The algorithm starts with a Heegaard diagram for the unknot and ends with the Heegaard diagram for the $(1,1)$ knot represented by $\mathfrak{d}(a,b,c,d)$. Each step in the algorithm involves a simple isotopy of the β attaching circle to accommodate a translation of the basepoint z. This simple process of looping a loop and the complicated diagrams produced by it are somewhat reminiscent of the string patterns in the child's game of cat's cradle. If z crosses α under this shift, then the number of intersection points in $\alpha \cap \beta$ may increase (by an even number). Else, the number of points of intersection is unchanged; and in particular, the knot Floer homology is preserved.

Thus, the algorithm can be seen as inductively building up the homology in steps of monotonically increasing complexity.

The uniformity in this construction depends on $(1,1)$ normal form. This can be made especially clear by using a particularly symmetric modification of normal form that will be called *standard position*. Standard position for $(1,1)$ knots is defined in the first section of this chapter. Section 3.2 presents the algorithm for constructing a Heegaard knot diagram from a standard position of a $(1,1)$ knot. Lemmas 3.3 and 3.4 obtain the Heegaard normal form from the algorithm output. This is important because it allows for the application of Doyle's program to read the Heegaard diagram and calculate its knot Floer homology. At the end of section 3.2 an example of the algorithm is illustrated for a torus knot. The chapter closes with a comparison to the examples of Heegaard knot diagrams constructed in [GMM05].

3.1 Standard position

Let $\mathfrak{d}(a,b,c,d)$ be a $(1,1)$ normal form of a knot K. We may assume $b \geq 0$ (see section 2.3). Let T denote the flat torus with left/right sides M and top/bottom L, where M and L are the standard meridian and longitude. In particular, the flat torus T shows the meridional twisting, unlike the $(1,1)$ normal form diagram. Let $w, z \in T$ denote respectively the lower and upper endpoint of the trivial arcs. To obtain $(1,1)$ standard position, translate the fundamental domain so that its corners coincide with w. Then, remove the subarc $\overline{xz} \subset t_\beta$ which extends from z to a point $x \in M \cup L$, by an isotopy sliding z to x along $\overline{xz}$ and fixing K elsewhere. The resulting diagram is called $(1,1)$ *standard position for* $\mathfrak{d}(a,b,c,d)$, and it takes one of two forms $\epsilon = \pm 1$ depending on the twist parameter d. See figure 3.1.

In $(1,1)$ standard position, t_β consists of at most five different classes of parallel

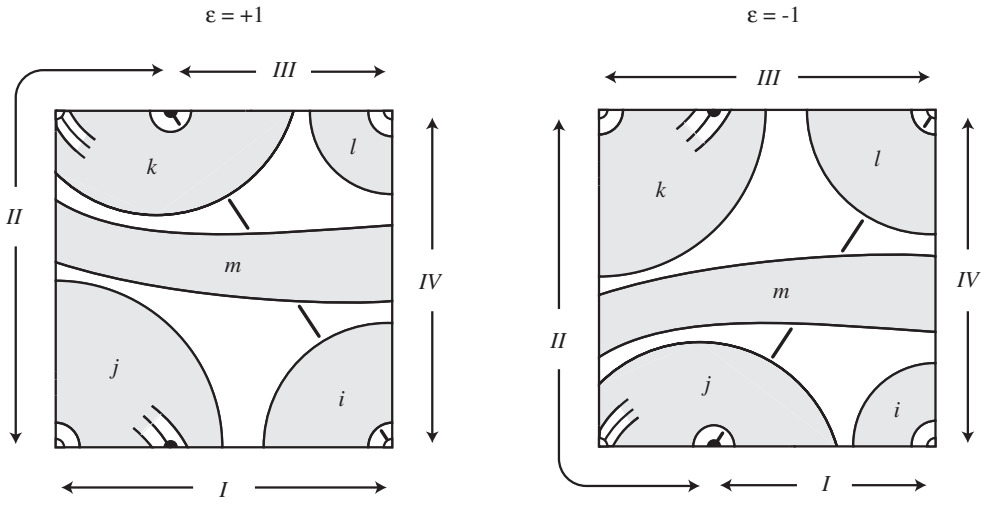

Figure 3.1: $(1,1)$ standard form $\mathfrak{r}(i,j,k,l,m)_\epsilon$ for $\epsilon = +1$ on the left and $\epsilon = -1$ on the right. The parameters i,j,k,l,m count the number of arcs of t_β in each of the five parallel classes connecting regions I, II, III, IV in the torus fundamental domain perimeter.

arcs. The endpoints of an arc determine which parallel class it belongs to. The basepoints w, z separate the perimeter of the flat torus into six segments which we number clockwise, starting at the bottom right corner. An end of a parallel class lies in one of four regions I, II, III, IV defined as follows:

ϵ=+1	ϵ=−1
I=1 ∪ 2	I=1
II=3 ∪ 4	II=2 ∪ 3
III=5	III=4 ∪ 5
IV=6	IV=6

Let $\mathfrak{r}(i,j,k,l,m)_\epsilon$ denote the $(1,1)$ standard position consisting of i,j,k,l,m arcs in the parallel class joining region IV to I, I to II, II to III, III to IV, II to IV, respectively. See figure 3.1 The parameters of the $(1,1)$ standard position are determined by the $(1,1)$ normal form:

Lemma 3.1. *Let K be a $(1,1)$ knot and $\mathfrak{d}(a,b,c,d)$ a $(1,1)$ normal form for K with $b \geq 0$. Then, K admits the $(1,1)$ standard position $\mathfrak{r}(i,j,k,l,m)_\epsilon$ where*

$$\mathfrak{r}(i,j,k,l,m)_\epsilon = \begin{cases} \mathfrak{r}(a, d-a-1, a, a+c, b)_+ & \text{if } d > a \\ \mathfrak{r}(a+b, a, a-d, a, c)_- & \text{if } d \leq a \end{cases}$$

Proof. In each case, begin by vertically shifting the fundamental domain of the torus until the longitude L intersects w. Depending on the twist parameter d, the resulting diagram may admit some simplification. The proof follows easily from inspecting the flat torus diagrams in each case. In the diagrams that follow, the twisting is isolated to the left in a box containing $2a+b+c+d$ strands.

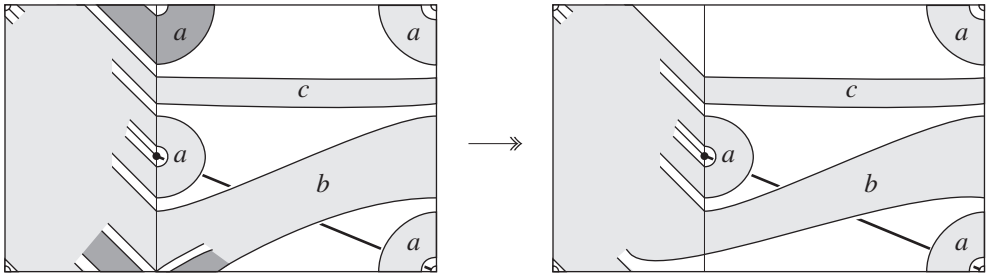

Figure 3.2: The flat torus diagrams for Case 1: $d > a$. The darker shading on the left indicates arcs with non-essential intersection. The diagram to the right is the result of canceling these intersections.

Case 1: $d > a$. It is immediate from the diagram that $k = a$. The diagram can be simplified by canceling the arcs which, with a subarc of the top horizontal edge of the diagram, bound a disk disjoint from w and z. After isotoping these disks away, an $\epsilon = +1$ standard position is obtained; it appears on the right side of figure 3.2. With the arcs removed, the c strands are clearly parallel to the a strands in the upper-right, hence $l = a + c$. The b strands no longer meet the

bottom edge of the diagram but pass clear across. Since these are the only arcs to connect II and IV, it follows that $m = b$. This leaves only the a strands (in the lower right) between I and IV, hence $i = a$. The remaining parameter j is just the total number of arcs in the twist rectangle less the number of arcs counted by the other parameters:

$$j = (2a + b + c + d) - ((2a + 1) - b - c - a) = d - a - 1$$

Case 2a: $0 < d \leq a$. Here (figure 3.3) there are d non-essential arcs bounding disks at the bottom horizontal of the diagram. Removing them leaves a diagram in $\epsilon = -1$ normal form, as shown on the right side of figure 3.3. The parameters are immediate from the diagram.

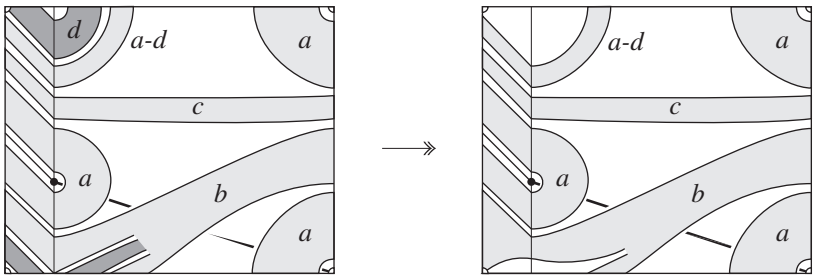

Figure 3.3: The flat torus diagram in Case 2a: $0 < d \leq a$. There are d non-essential arcs on the left. Removing them leaves the diagram to the right.

Case 2b: $d \leq 0$. Here (figure 3.4) the diagram does not require any simplification and we can read off the parameters of its $\epsilon = -1$ normal form immediately. □

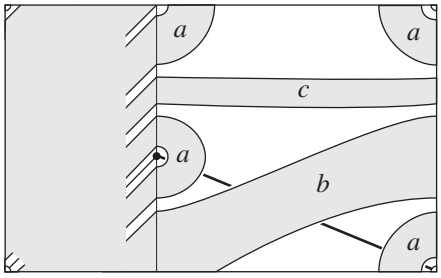

Figure 3.4: The flat torus diagram in Case 2b: $d \leq 0$.

3.2 Heegaard knot diagram construction

The overpass t_β of a $(1,1)$ knot in standard position $\mathfrak{r}(i,j,k,l,m)_\epsilon$ appears as a collection of $N = i+j+k+l+m$ segments. Label each segment c_i, $i = 1,\ldots,N$ according to its order, moving along t_β in the torus, starting from w and ending at z. Consider the sequence of partial arcs $\{t^i_\beta = c_1 \cup \cdots \cup c_i\}$, $i = 1,\ldots,N$. Given an attaching circle β_i which is disjoint from t^i_β, it is not difficult to accommodate the addition of a single segment c_{i+1}. The following definition will be used to present the isotopy that realizes this induction step in the algorithm.

Definition 3. Let t be an embedded arc in the torus T with meridian M and longitude L. A *branch sequence* b is a sequence $b^1,\ldots,b^n$ of subarcs $b^j \subset (M \cup L) - t$ such that b^j and b^k are in the boundary of the same connected component of $T - (M \cup L \cup t)$, where $k \equiv j+1 \mod n$ and $j = 1,\ldots,n$.

To each branch sequence b there corresponds a closed curve γ in $T - t$. The curve γ can be constructed inductively by joining, end to end, a path between b^{j-1}, b^j to a path between b^j, b^{j+1}. (Mixing metaphors, a path between branches b^j and b^{j+1} will be referred to as a *strand* of the branch.) The closed curve γ is unique (up to isotopy) since each component of $T - (M \cup L \cup t)$ is homeomorphic to a disk. Conversely, given a closed curve γ in $T - \{w,z\}$ that intersects M, L

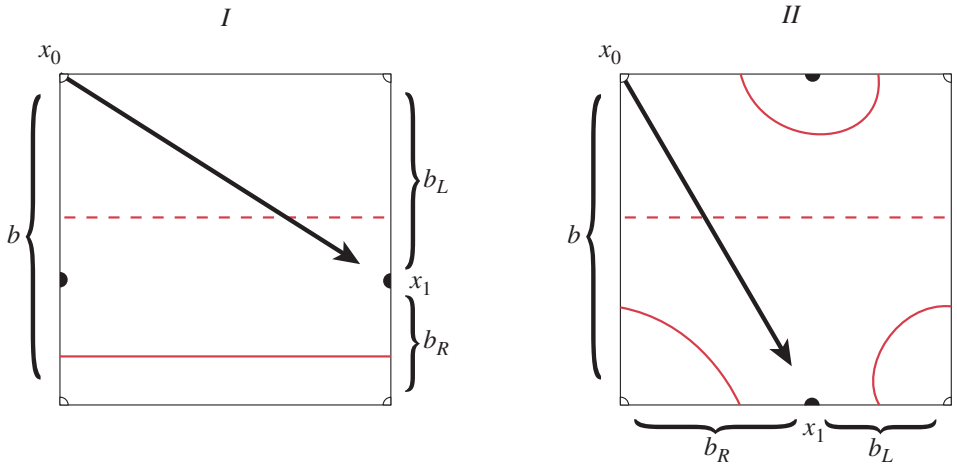

Figure 3.5: Strand isotopies I and II. The solid black arrow marks the cut c_{i+1}, the dashed red line across the middle represents a strand of β_i, and the result of the isotopy is in solid red. If we orient β_i from left to right, then isotopy I (above left) replaces $\{b\}$ with $\{b_R\}$, and isotopy II (above right) replaces $\{b\}$ with $\{b, b_R, b_L\}$ in the branch sequence.

transversely, a branch sequence can be written down as the sequence of intervals that γ crosses in the course of one cycle.

In particular, the attaching circle β_i in $T - t^i_\beta$ is represented by some branch sequence $b_i = b^1_i, \ldots, b^n_i$. The isotopy involved in the induction step of the algorithm will act on consecutive pairs of branches b^j_i, b^{j+1}_i or strands of the branch sequence b_i in the region of the "cut" c_{i+1}. Define this region P_i to be the closure of the connected component of $T - (M \cup L \cup t^i_\beta)$ that contains c_{i+1}. Label the endpoints of the the cut $\partial c_{i+1} = \{x_i, x_{i+1}\}$ according to the orientation of t_β given above. Now is the time to take advantage of standard position: assuming t_β is in standard position, c_{i+1} separates P_i, for all i. Let P_L, P_R denote the two halves, where P_L lies to the left of c_{i+1} as we move from x_i to x_{i+1}. Similarly, label the halves b_L, b_R of the interval separated by x_{i+1}. See figure 3.5.

The isotopy defining the induction step consists of two parts: The first part

moves ends of β_i strands (or, more precisely, strands of the branch sequence representing β_i) into the new branches b_L, b_R, and the second adds branches to go around essential intersections with c_{i+1}. Let s be a strand of β_i.

(I) If s lies in the cut region P_i, and goes between a branch b_i^j containing x_{i+1} and a branch contained in P_L (P_R), then replace b_j^i by b_L (b_R) in the branch sequence for β_i. Else do nothing.

(II) If s starts in a branch b_i^j in P_L (P_R) and crosses c_{i+1} to end in a branch b_i^{j+1} in P_R (P_L), then replace b_i^j in the branch sequence by the ordered triple $\{b_i^j, b_L, b_R\}$ ($\{b_i^j, b_R, b_L\}$). Else do nothing.

Theorem 3.2. *Let t be an arc with endpoints $\partial t = \{w, z\}$ which is embedded in standard position in a torus T with meridian M and longitude L. Suppose M and L cut t into N subarcs. Then the following algorithm produces a branch sequence $b = b_N$ whose corresponding closed curve is isotopic to L in T, and admits an embedding disjoint from t.*

1. *Define initial branch sequence $b_0 = \{M - w\}$.*
2. *Loop*
   - *Replace b_i by the result of applying isotopy I to each of its branches.*
   - *Replace b_i by the result of applying isotopy II to each of its branches.*
   - *If $i < N$ replace i by $i + 1$, else return b_N.*

Proof. As mentioned above, to every branch sequence there corresponds a closed curve in T. Define the closed curve β_0 corresponding to b_0 to be a parallel copy of L which is disjoint w. Each step in the algorithm can be realized by an isotopy of a closed curve β_i, corresponding to b_i, which does not introduce any intersection

with t. If β_{i-1} is isotopic to L and disjoint t, this implies that β_{i+1}, the result of the ith isotopy, is also isotopic L and disjoint t, and the induction step is complete. □

The attaching curve β associated to the branch sequence produced by the algorithm of theorem 3.2 can be drawn in the flat torus as a collection of arcs similar to the standard position of the arc t_β. Count the strands of β with a signed 5-tuple $\mathfrak{R}(i,j,k,l,m)_\epsilon$ almost exactly as was defined for $\mathfrak{r}(i,j,k,l,m)_\epsilon$. The only difference here is that should $m = 0$, β may have vertical strands with endpoints in L. (See Figure 3.11 for an example.) In such case, m is defined to be *negative* the number of vertical strands.

Finally, we want to put the standard position for β produced by the algorithm of theorem 3.2 into Heegaard normal form. To begin, slide the point w along L and move z to the middle of the flat torus diagram. This results in a diagram $\mathfrak{D}^*(A,B,C,D)$ of the type illustrated by figure 3.6, and it is characterized by the four integers A, B, C, D. We refer to this as *semi-normal form*. The parameter A

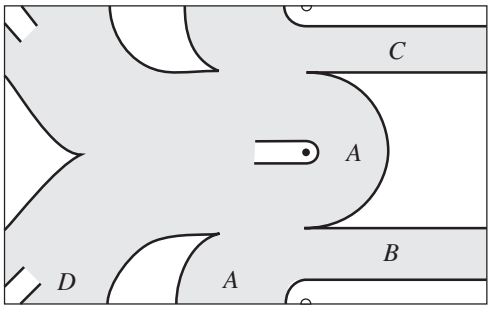

Figure 3.6: Semi-normal form $\mathfrak{D}^*(A,B,C,D)$ for an attaching curve in the twice punctured torus.

represents the number of strands in each of the rainbows passing around w and z. The parameter B (C) counts the strands passing below (above) z and ending on the right side of the diagram. And D is defined exactly as the parameter d was

defined in the Heegaard normal form.

Lemma 3.3. *Let $\mathfrak{R}(i,j,k,l,m)_\epsilon$ be standard position for an attaching curve β. Then β has semi-normal form*

$$\mathfrak{D}^*(A,B,C,D) = \begin{cases} \mathfrak{D}^*(i, i+m, l, j) & \text{if } m \geq 0, \epsilon = +1 \\ \mathfrak{D}^*(l, i, l+m, k) & \text{if } m \geq 0, \epsilon = -1 \\ \mathfrak{D}^*(i-m, i, l, j) & \text{if } m < 0, \epsilon = +1 \\ \mathfrak{D}^*(l-m, i, l, k) & \text{if } m < 0, \epsilon = -1 \end{cases}$$

Proof. Consider the case $m \geq 0$, $\epsilon = +1$. This takes one of two semi-normal forms depending on the sign of $l - i$. See figure 3.7.

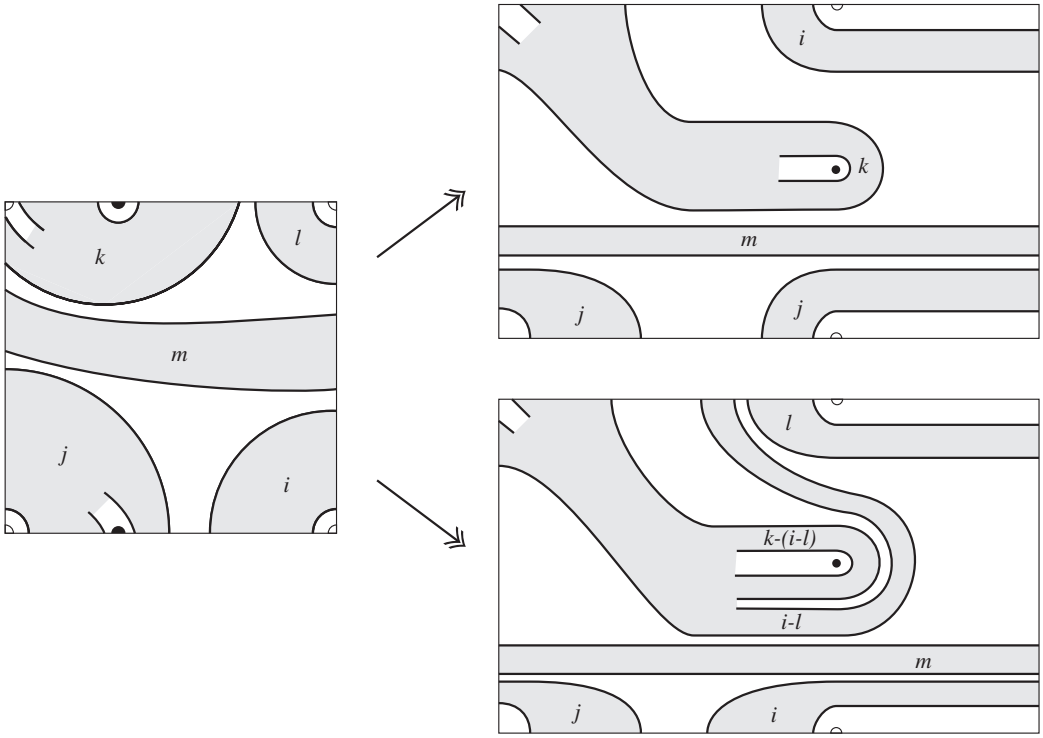

Figure 3.7: From Heegaard standard position (left) with $m \geq 0$, $\epsilon = +1$ to Heegaard semi-normal form (right). Case $l - i \geq 0$ on top. Case $l - i < 0$ on bottom.

If $m < 0$ the attaching curve passes vertically in the flat torus. Consider the case $\epsilon = -1$. See figure 3.8.

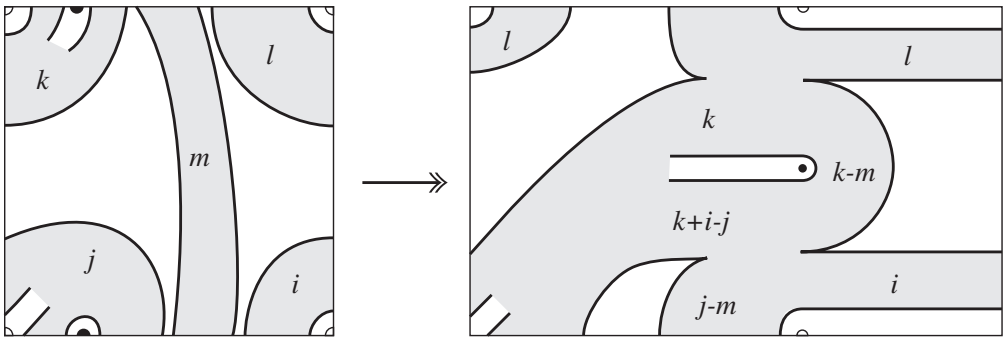

Figure 3.8: From Heegaard standard position (left) with $m < 0$, $\epsilon = -1$ to Heegaard semi-normal form (right).

The remaining cases follow from similar diagrams. These shall be omitted. □

Lemma 3.4. *An attaching curve in semi-normal form* $\mathfrak{D}^*(A, B, C, D)$ *has Heegaard normal form*

$$\mathfrak{D}(a,b,c,d) = \begin{cases} \mathfrak{D}(A, B-A, C-A, D+A) & \text{if } A \le B, A \le C \\ \mathfrak{D}(C, A-C, B-A, D-A) & \text{if } C < A \le B \\ \mathfrak{D}(C, B-C, 0, D-(A-C)(B+C)+C) & \text{if } C < B < A \\ \mathfrak{D}(B, C-A, A-B, D+A+2B) & \text{if } B < A \le C \\ \mathfrak{D}(B, 0, C-B, D+(A-B)(B+C)+B) & \text{if } B < C < A \end{cases}$$

The case $B = C < A$ does not appear in the lemma because this implies that the curve has multiple link components which contradicts the assumption that it is an attaching curve.

Proof. To transform an attaching curve from semi-normal form to normal form, shift w toward the middle of the flat torus diagram. For the case $A \le B, A \le C$,

this is the only isotopy that needs to be carried out. In the remaining cases, it

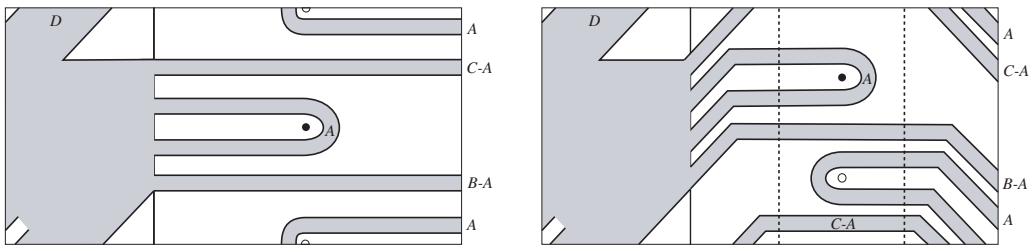

Figure 3.9: From semi-normal (left) to normal form (right): Case $A \leq B, A \leq C$.

is necessary to remove "S"-strands which have non-minimizal intersection with the torus meridian containing w and z. This is accomplished by one or more applications of an isotopy of the torus that exchanges w and z, before shifting w to the interior of the flat torus. In the case $C < A \leq B$, shown in figure 3.10, a single clockwise rotation of a disk neighborhood of the points removes the "S"-strands. The case $C < B < A$ is treated in the same way as the last case except that

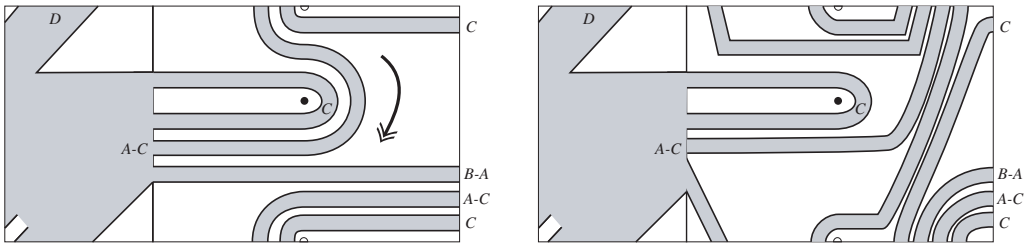

Figure 3.10: From semi-normal to normal form: Case $C < A \leq B$

exchange isotopy must be applied a total of $(A - C)$ times. The case $B < A \leq C$ differs from the case $C < A \leq B$ above only in that the exchange isotopy must go counter-clockwise. The last case $B < C < A$ is obtained by repeating the counter-clockwise exchange isotopy a total of $(A - B)$ times before shifting w to the interior of the flat torus diagram. □

The following theorem defines the cat's cradle algorithm which uses all the results so far obtained in the chapter to construct a genus one Heegaard knot diagram in normal form from a $(1,1)$ normal form of a given $(1,1)$ knot.

Theorem 3.5. *Let $\mathfrak{d}(a,b,c,d)$ be the $(1,1)$ normal form of a knot K with $(1,1)$ decomposition $(H_\alpha, t_\alpha) \cup (H_\beta, t_\beta)$, and define $T = \partial H_\alpha = \partial H_\beta$. Then the following algorithm produces the Heegaard normal form of a genus one Heegaard knot diagram for K.*

1. *Transform $\mathfrak{d}(a,b,c,d)$ into $(1,1)$ standard position.*
2. *Construct an attaching circle β isotopic to the standard longitude in T, and disjoint from the projection $p(t_\beta) \subset T$.*
3. *Determine the Heegaard normal form of the attaching curve β.*

Proof. Step 1 is given by lemma 3.1. Step 2 is completed using the algorithm in theorem 3.2. Step 3 is given by lemmas 3.3 and 3.4. □

3.3 A torus knot example

Example 3.3.1. The torus knot $\mathfrak{t}(5,3)$ has (1,1) normal form $\mathfrak{d}(0,0,2,5)$. Here is what happens in each step of the algorithm defined in theorem 3.5.

Step 1. The normal form falls into the case $a < d$, and according to lemma 3.1 it is represented by the standard position $\mathfrak{r}(0,4,0,2,0)_{+1}$. See figure 3.11.

Step 2. Apply the algorithm in theorem 3.2. It takes six steps, one for each "cut" along the six strands of t_β in standard position. Number the endpoints $t_\beta \cap (M \cup L)$ around the perimeter of the flat torus diagram starting at zero at the bottom right corner and continuing clockwise. A branch is indicated by an integer pair bounding the interval in the diagram that represents the branch.

Since intervals on opposite sides of the diagram represent the same branch, we choose the following convention: Orient the initial branch sequence from left to right and represent branch b by the interval corresponding to the latter side of the branch. For example, the branch sequence algorithm starts with the branch sequence $b_0 = \{(5,8)\}$. To obtain the next sequence, apply isotopy II. This results in the addition of two branches b_L, b_R which is emphasized with a double underline; $b_1 = \{(5,8), \underline{\underline{(8,11),(0,2)}}\}$. In step two, both isotopy I and II are used. The result of isotopy I is indicated by a single underline. The remaining steps follow in a similar pattern. The six steps of the branch sequence algorithm are listed below and figure 3.11 illustrates the process.

$$
\begin{aligned}
b_0 &= \{(5,8)\} \\
b_1 &= \{(5,8), \underline{\underline{(8,11),(0,2)}}\} \\
b_2 &= \{\underline{(5,6)}, (8,11), \underline{(5,6),(13,15)}, (0,2)\} \\
b_3 &= \{(5,6), \underline{(8,9)}, (5,6), \underline{\underline{(8,9),(2,4)}}, (13,15), (0,2)\} \\
b_4 &= \{(5,6), (8,9), \underline{\underline{(11,12),(0,1)}}, (5,6), (8,9), \underline{\underline{(11,12),(0,1)}}, \\
&\quad (2,4), (13,15), \underline{(0,1)}\} \\
b_5 &= \{(5,6), (8,9), (11,12), \underline{\underline{(6,7),(13,14)}}, (0,1), (5,6), (8,9), \\
&\quad (11,12), \underline{\underline{(6,7),(13,14)}}, (0,1), (2,4), \underline{(13,14)}, (0,1)\} \\
b_6 &= \{(5,6), (8,9), (11,12), (6,7), \underline{\underline{(9,10),(2,3)}}, (13,14), (0,1), \\
&\quad (5,6), (8,9), (11,12), (6,7), \underline{\underline{(9,10),(2,3)}}, (13,14), (0,1), \\
&\quad \underline{(2,3)}, (13,14), (0,1)\}
\end{aligned}
$$

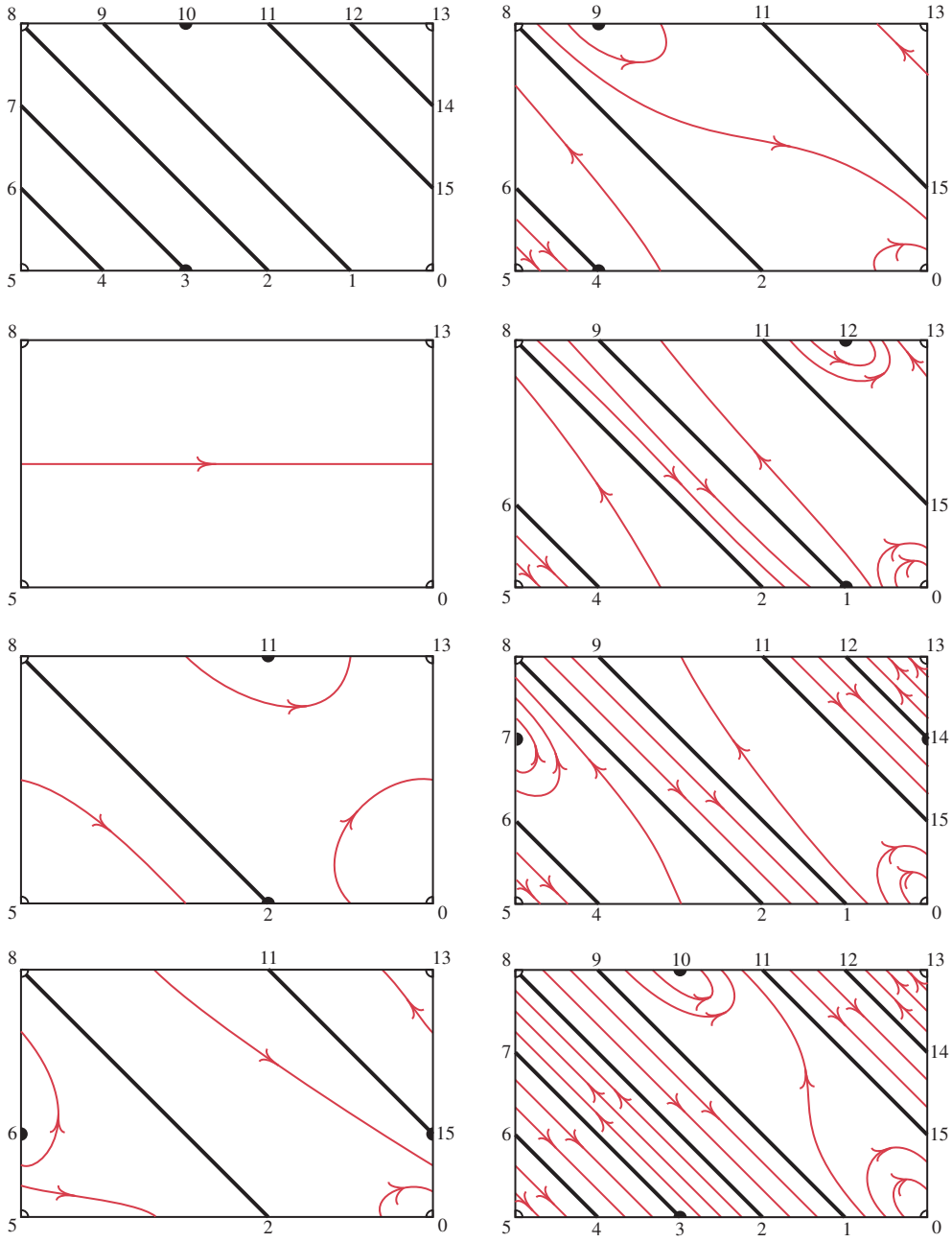

Figure 3.11: The algorithm in theorem 3.5 applied to torus knot $\mathfrak{t}(5,3)$. Standard position for the knot appears in top left. The algorithm proceeds down the left, then down the right column. The β attaching circle appears in red. Throughout the isotopy, w (open circle) remains fixed in the corners of the diagram, while z (closed circle) crosses the diagram at every step.

Step 3. Counting the strands of the attaching curve corresponding to the final branch sequence b_N we have $\mathfrak{R}(i,j,k,l,m) = (2,9,2,5,-1)_+1$. The sign ϵ in the Heegaard standard position coincides with the sign of the $(1,1)$ knot standard position for all attaching curves constructed by the branch sequence algorithm. The standard position $\mathfrak{R}(2,9,2,5,-1)_{+1}$ takes, in turn, the semi-normal form $\mathfrak{D}^*(3,2,5,9)$ and Heegaard normal form $\mathfrak{D}(2,2,1,2)$ as shown in figure 3.12.

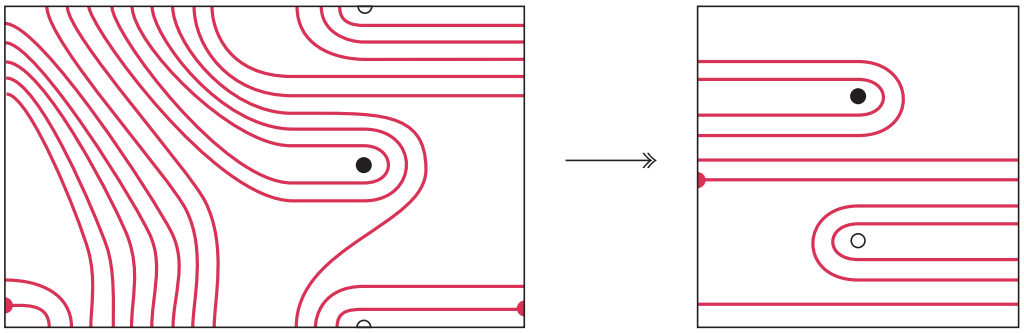

Figure 3.12: A Heegaard knot diagram for the torus knot $\mathfrak{t}(5,3)$: from seminormal form $\mathfrak{D}^*(3,2,5,9)$ (left) to normal form $\mathfrak{D}(2,2,1,2)$ (right). The intersection corresponding to the unknot at the start of the algorithm is emphasized by the red dots.

Chapter 4

Satellite $(1,1)$ Knots

In this chapter, the algorithm for constructing genus one Heegaard knot diagrams from theorem 3.5 is applied to several satellite $(1,1)$ knots and their knot Floer homology groups are calculated.

4.1 Definition and normal form

As was discussed in section 2.2, $(1,1)$ knots admit an unknotting tunnel. Morimoto and Sakuma completely determined which satellite knots admit unknotting tunnels in [MS91]. Each is a certain satellite of a $\mathfrak{t}(p,q)$ torus knots constructed via a 2-bridge link $\mathfrak{b}(\alpha,\beta)$, and they are all $(1,1)$ knots. The knots are denoted by the symbol $K(\alpha,\beta;p,q)$.

Definition 4. Let K_0 be a torus knot $\mathfrak{t}(p,q)$ and $K_1 \cup K_2$ a nontrivial 2-bridge link $\mathfrak{b}(\alpha,\beta)$ other than the hopf link. Let r and s be integers such that $ps-qr=1$. Then $E(K_0)$ is a Seifert fibred space $D(-r/p, s/q)$ whose base orbifold is a disk with two cone points, and the Seifert invariants of the singular fibers are $-r/p$ and s/q. Since K_2 is a trivial knot, there is an orientation-preserving homeomorphism $f : E(K_2) \to N(K_0)$ which takes the meridian $m \subset \partial E(K_2)$ of K_2 to a regular

fiber $h \subset \partial N(K_0)$ of the Seifert fibration of $E(K_0)$. We let $K(\alpha, \beta; p, q)$ denote the knot $f(K_1) \subset \partial N(K_0) \subset S^3$.

A pair of satellite $(1,1)$ knots $K(\alpha, \beta; p, q)$, $K(\alpha', \beta'; p', q')$ have the same knot type if and only if their torus knot and 2-bridge knot constituents have the same knot type. The $(1,1)$ normal form is helpful for visualizing this satellite construction. Before presenting a $(1,1)$ normal form of an arbitrary $K(\alpha, \beta; p, q)$ knot, consider the following example:

Example 4.1.1. $K(8,3;3,2)$. Here we have $K_0 = \mathfrak{t}(3,2)$ and $K_1 \cup K_2 = \mathfrak{b}(8,3)$. The 2-bridge link is represented by $(1,1)$ normal form $\mathfrak{d}(2,3,0,-1)$. Identify K_1 with the component of the 2-bridge link that contains the bridge and K_2 with the one embedded in the torus T of the $(1,1)$ decomposition of $K_1 \cup K_2$, as shown in figure 4.1.1. By isotoping K_2 in S^3, it is clear that T bounds a tubular neighborhood of K_2 there, and $K_1 \cap T$ is contained in an annular neighborhood $A \subset T$ of a meridian $m \subset \partial E(K_2)$. Let M, L be a meridian-longitude pair for $\partial N(\mathfrak{t}(3,2))$. Then a regular fiber of the exterior of the trefoil is $h = L + 3 \cdot 2M$. Under f, the annulus A is glued once along the length of the trefoil with 6 twists. This is exactly like gluing A into an annular neighborhood of the trefoil embedded in a torus. The gluing is illustrated in figure 4.1.1, and the resulting diagram is in $(1,1)$ normal form $\mathfrak{d}(1,1,4,12)$.

The knot $K(\alpha, \beta; p, q)$ is a satellite knot with $\mathfrak{t}(p,q)$ torus knot companion. The pattern is obtained by putting pq right-handed full twists in one component K_1 of the 2-bridge link $K_1 \cup K_2 = \mathfrak{b}(\alpha, \beta)$ where it passes through the other (trivial) component K_2. In fact, the pattern is represented by $K(\alpha, \beta; pq, 1)$. In the original definition of $K(\alpha, \beta; p, q)$ found in [MS91], the torus knot K_0 is required to be non-trivial. However, the construction is still well-defined for $p, q = 1$, and, for convenience, these degenerate cases are included in our definition of $K(\alpha, \beta; p, q)$.

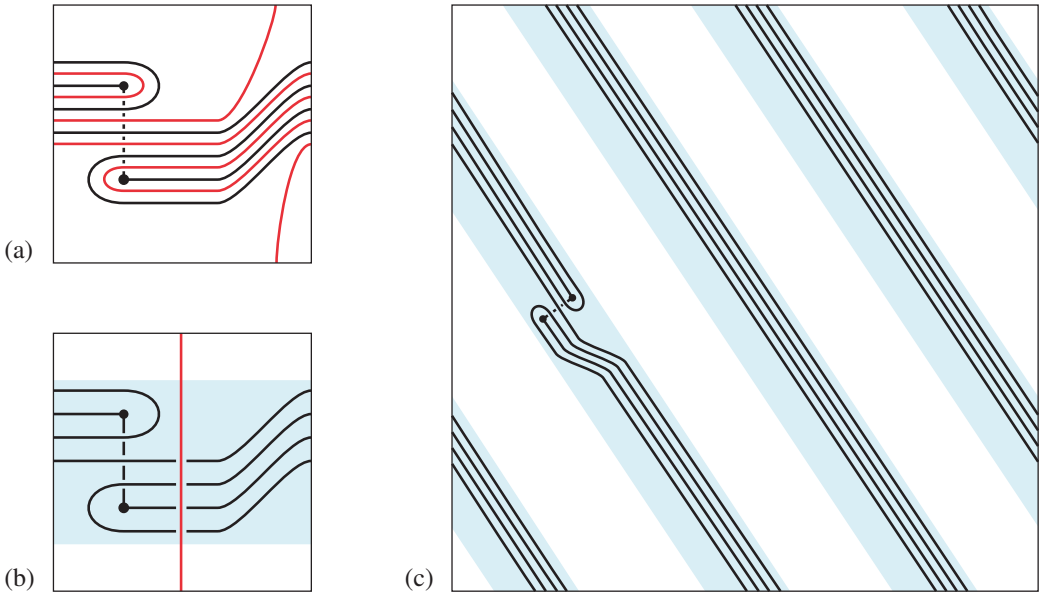

Figure 4.1: Satellite $(1,1)$ knot $K(8,3;3,2)$. (a) $(1,1)$ normal form for the 2-bridge link $K_1 \cup K_2$, with K_1 in black and K_2 in red. (b) K_2 isotoped to a meridian. (c) $(1,1)$ normal form for the satellite knot $f(K_1)$. The blue stripes form an annular neighborhood of the companion K_0.

In particular, a formula providing a $(1,1)$ normal simultaneously for the satellite $(1,1)$ knot and its pattern can be stated as follows.

Lemma 4.1. *Let $\alpha, \beta, \epsilon, p, q, \in \mathbb{Z}$ be integers where $\alpha \geq 4$ is even, $0 < \beta < \alpha/2$, $\epsilon = \pm 1$, $p \neq 0$, $q > 0$, and $\gcd(\alpha, \beta) = 1 = \gcd(p, q)$. Then $K(\alpha, \epsilon\beta; p, q)$ is a $(1,1)$ knot with normal form*

$$\mathfrak{d}(\frac{\beta-1}{2}, \frac{\epsilon(\alpha-2\beta)}{2}, \frac{\alpha(q-1)}{2}, \frac{\alpha p}{2})$$

It should be noted that the case $p, q > 0$ appears as a remark without proof in [CK03].

Proof. The 2-bridge link $K_1 \cup K_2 = \mathfrak{b}(\alpha, \epsilon\beta)$ has (1,1) normal form $\mathfrak{d}(\beta - 1, \epsilon(\alpha - 2\beta + 1), 0, -\epsilon)$. Let K_1 be the link component in the (1,1) normal form that is not embedded in the (1,1) decomposition torus T. Since K_2 is isotopic to a meridian of T let us assume $\partial E(K_2) = -T$. By itself, K_1 has (1,1) normal form $\mathfrak{d}((\beta-1)/2, \epsilon(\alpha - 2\beta)/2, 0, 0)$, and it is contained in an annular neighborhood $A \subset T$ of a meridian m of $\partial E(K_2)$.

If (M, L) is a meridian longitude pair for $\partial N(K_0)$, then $h = L + pqM$ is a regular fiber of the torus knot exterior. Consider an annular neighborhood $A' \subset T'$ of $\mathfrak{t}(p, q)$ embedded in a torus T'. Then, the effect of $f : E(K_2) \to N(K_0)$ on K_1 can be realized by an orientation preserving map of A into A'. The image of K_1 under f is now in $(1,1)$ normal form relative to T', and it remains only to count strands. The first two parameters in the normal form of $K(\alpha, \beta; p, q)$ are the same as those for K_1; that is, $a = (\beta - 1)/2$ and $b = \epsilon(\alpha - 2\beta)/2$. Each crossing of M, L by the companion $\mathfrak{t}(p, q)$ means $\alpha/2$ crossings of M, L respectively by the satellite knot. Hence, $K(\alpha, \beta; p, q)$ crosses the meridian $q\alpha/2$ times and the longitude $p\alpha/2$ times in T'. This implies $c = \alpha(q-1)/2$ and $d = p\alpha/2$. □

The lemma provides a $(1,1)$ normal form for $K(\alpha,\beta;p,q)$ which helps to visualize their construction. More importantly, this lemma allows for the application of the algorithm in theorem 3.5 to produce genus one Heegaard knot diagrams for satellite $(1,1)$ knots.

To determine parameters α,β,p,q which represent a satellite $(1,1)$ knot whose companion and Heegaard diagram is already known, it is useful to recall (see [Lic97], for example) the correspondence between Schubert normal form and Conway's rational tangles. This states that the $\mathfrak{b}(\alpha,\beta)$ is equivalent to the rational tangle $C(a_1,\ldots,a_n)$, where a_i is the ith coefficient in the continued fraction expansion

$$\frac{\beta}{\alpha} = \cfrac{1}{a_1 + \cfrac{1}{a_2 + \ldots \cfrac{1}{a_{n-1} + \cfrac{1}{a_n}}}}$$

For example, the 2-bridge link $\mathfrak{b}(8,3)$ depicted in figure 2.5 is equivalent to the rational tangle $C(2,1,2)$ since $\frac{1}{2+\frac{1}{1+\frac{1}{2}}} = 3/8$. That this link is the Whitehead link is, perhaps, more apparent from the tangle diagram than the Schubert normal form. See figure 4.2. Thus, the satellite $(1,1)$ knot $K(8,3;3,2)$ is exactly the 6-twisted Whitehead double of the trefoil that was discussed in section 2.2.

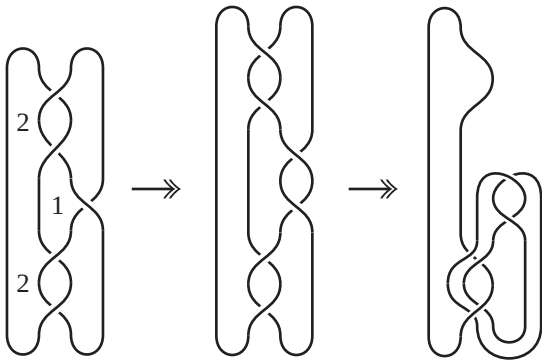

Figure 4.2: The Whitehead link. An isotopy taking the rational tangle $C(2,1,2)$ to a more common projection of the Whitehead link.

4.2 A Whitehead double example

In this section, an explicit calculation of the knot Floer homology groups of the satellite $(1,1)$-knot $K(8,3;3,2)$ is shown.

Having just identified $K(8,3;3,2)$ as the Whitehead double described in section 2.2, there is no need to construct its Heegaard knot diagram; it appears in figure 2.4. Figure 4.2 shows the Heegaard knot diagram in the flat torus. Figure 4.2

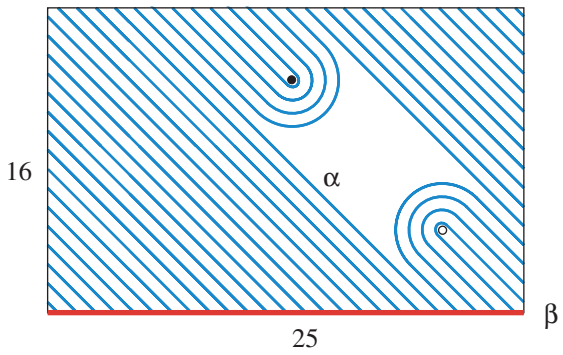

Figure 4.3: Heegaard knot diagram of the 6-twisted Whitehead double of the right-handed trefoil in the flat torus.

shows lifts of α, β attaching circles in the universal cover. There are 36 proper

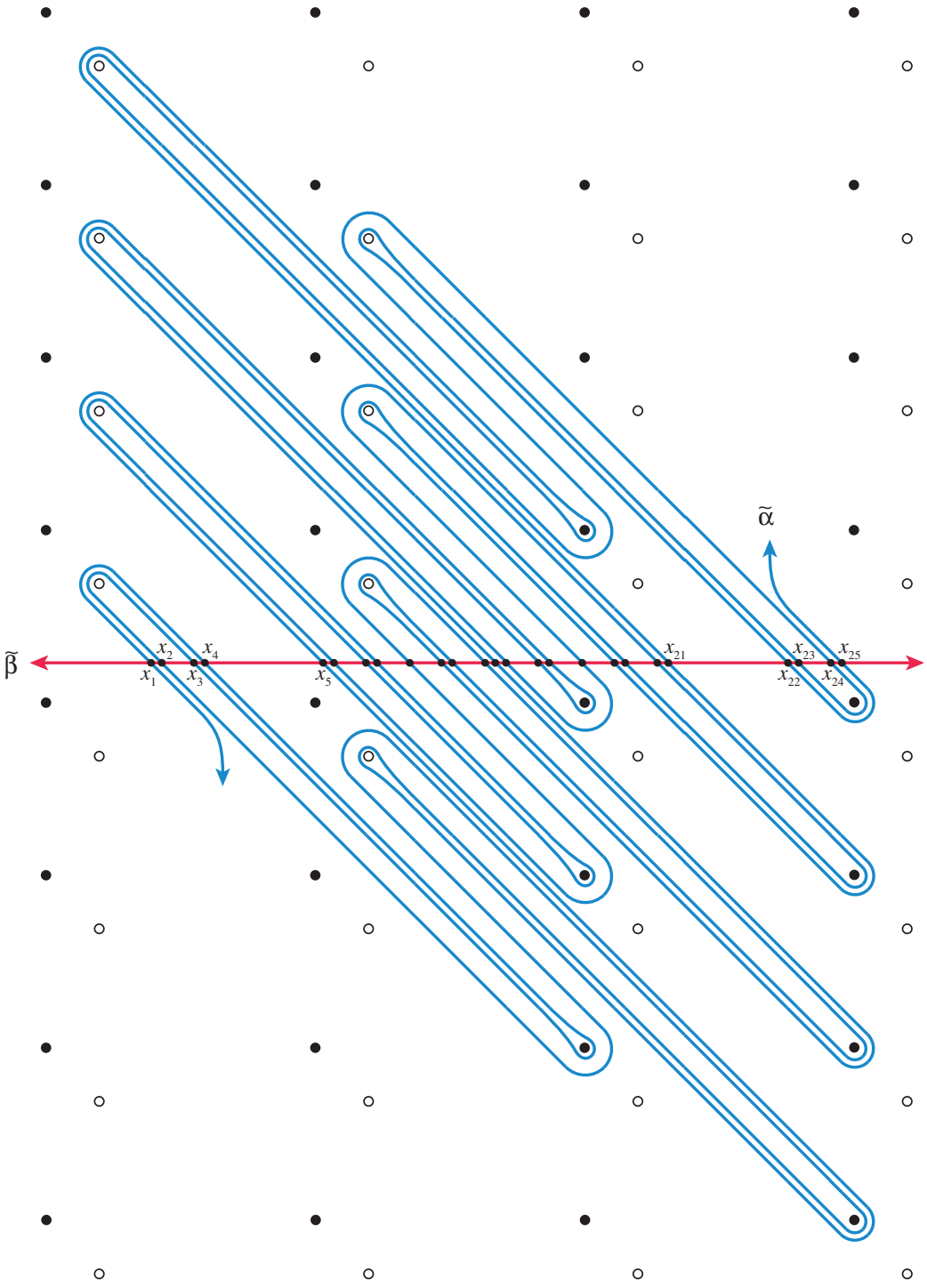

Figure 4.4: The Heegaard knot diagram in figure 4.2, lifted to the universal cover. The curves $\tilde{\alpha}$ and $\tilde{\beta}$ represent a particular lift of of the attaching circles α and β. The open circles denote lifts of the basepoint w while the black circles denote lifts of z.

Whitney disks connecting the 25 intersections of the attaching circles in this diagram. They yield the following differentials.

$$
\begin{aligned}
\partial[x_1,i,i] &= 0\\
\partial[x_2,i,i+1] &= [x_1,i,i]+[x_5,i-1,i-1]\\
\partial[x_3,i,i] &= [x_2,i-1,i]+[x_4,i,i-1]\\
\partial[x_4,i,i-1] &= [x_1,i-1,i-1]+[x_5,i-2,i-2]\\
\partial[x_5,i,i] &= 0\\
\partial[x_6,i,i+1] &= [x_5,i,i]+[x_9,i,i]\\
\partial[x_7,i,i] &= [x_6,i-1,i]+[x_8,i,i-1]\\
\partial[x_8,i,i-1] &= [x_5,i-1,i-1]+[x_9,i-1,i-1]\\
\partial[x_9,i,i] &= 0\\
\partial[x_{10},i,i+1] &= [x_9,i,i]+[x_{13},i,i]\\
\partial[x_{11},i,i] &= [x_{10},i-1,i]+[x_{12},i,i-1]\\
\partial[x_{12},i,i-1] &= [x_9,i-1,i-1]+[x_{13},i-1,i-1]\\
\partial[x_{13},i,i] &= 0\\
\partial[x_{14},i,i+1] &= [x_{13},i,i]+[x_{17},i,i]\\
\partial[x_{15},i,i] &= [x_{14},i-1,i]+[x_{16},i,i-1]\\
\partial[x_{16},i,i-1] &= [x_{13},i-1,i-1]+[x_{17},i-1,i-1]\\
\partial[x_{17},i,i] &= 0\\
\partial[x_{18},i,i+1] &= [x_{17},i,i]+[x_{21},i,i]\\
\partial[x_{19},i,i] &= [x_{18},i-1,i]+[x_{20},i,i-1]\\
\partial[x_{20},i,i-1] &= [x_{17},i-1,i-1]+[x_{21},i-1,i-1]\\
\partial[x_{21},i,i] &= 0\\
\partial[x_{22},i,i+1] &= [x_{25},i,i]+[x_{21},i-1,i-1]\\
\partial[x_{23},i,i] &= [x_{22},i-1,i]+[x_{24},i,i-1]\\
\partial[x_{24},i,i-1] &= [x_{25},i-1,i-1]+[x_{21},i-2,i-2]\\
\partial[x_{25},i,i] &= 0.
\end{aligned}
$$

	-3	-2	-1	0	1
1			x_2, x_{22}		x_6, x_{10}, x_{14}, x_{18}
0		x_1, x_3, x_{23}, x_{25}		$x_5, x_7, x_9, x_{11}, x_{13}$, $x_{15}, x_{17}, x_{19}, x_{21}$	
-1	x_4, x_{24}		x_8, x_{12}, x_{16}, x_{20}		

Table 4.1: Generators of knot Floer homology of the satellite $(1,1)$ knot $K(8,3;3,2)$ arranged horizontally (vertically) according to Maslov grading (filtration level).

Based on the table of differentials, it is easy to separate the generators of the chain complex into their respective filtration and homological gradings. In the table below the vertical (horizontal) direction indicates the filtration (homological) grading:

Here are the knot Floer homology groups.

$$\widehat{HFK}_*(K(8,3;3,2),i) \cong \begin{cases} \mathbb{Z}^4_{(1)} \oplus \mathbb{Z}^2_{(-1)} & \text{for } i = 1 \\ \mathbb{Z}^9_{(0)} \oplus \mathbb{Z}^4_{(-2)} & \text{for } i = 0 \\ \mathbb{Z}^4_{(-1)} \oplus \mathbb{Z}^2_{(-3)} & \text{for } i = -1 \\ 0 & \text{else} \end{cases}$$

In [OS03b] Ozsváth and Szabó defined a smooth concordance invariant, denoted $\tau(K)$, whose value for the (p,q) torus knot provided a new proof of Milnor's famous conjecture on the unknotting number of torus knots. Rasmussen independently discovered this invariant in his thesis, [Ras03]. Milnor's conjecture has a long history in gauge theory, and its original proof is due to Kronheimer and Mrowka, [KM93]. Recently, however, Rasmussen [Rasa] discovered another smooth concordance invariant whose value for torus knots proves the conjecture. Denoted $s(K)$, the invariant is defined using a refinement, due to Lee [Lee], of the purely

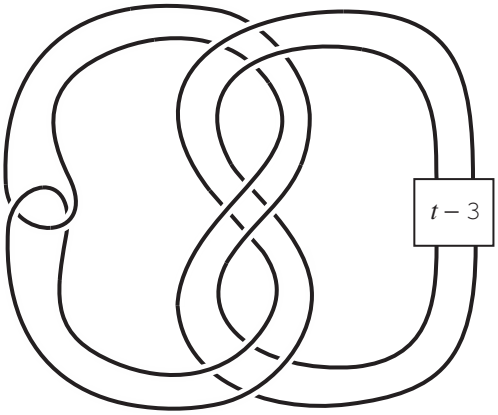

Figure 4.5: $D_+(\mathfrak{t}(3,2),t)$, the t-twisted positive Whitehead double of the right-handed trefoil. The box indicates the number of full right-handed twists to insert.

combinatorial knot (co)homology theory introduced by Khovanov [Kho00]. Rasmussen's proof of the Milnor conjecture using s is the first proof which avoids the analytical machinery of gauge theory. It was noted immediately that the two invariants share several formal properties (e.g. an inequality relating the invariants of knots which differ by a crossing change) which in turn imply that they agree (or more precisely, that $s(K)$ and $2\tau(K)$ agree) for many knots.

Indeed, it was conjectured that the two invariants always coincide:

Conjecture 1 ([Rasa])**.** $s(K) = 2\tau(K)$ for all knots, K.

There are counterexamples, however, and the first to be announced [HO] was found by Hedden and the author using the above Heegaard knot diagram and knot Floer homology of $K(8,3;3,2)$.

Theorem 4.2 ([HO])**.** *Let $D_+(\mathfrak{t}(3,2),2)$ denote the 2-twisted positive Whitehead double of the right-handed trefoil knot.*
Then $\tau(D_+(\mathfrak{t}(3,2),2) = 0$ while $s(D_+(\mathfrak{t}(3,2),2)) = 2$.

In the proof, τ is determined by combining the above calculation of $\widehat{HFK}$ of

$K(8,3;3,2)$ (which is the same knot as $\widehat{HFK}(D_+(\mathfrak{t}(3,2),6))$), results of Eftekhary [Eft05] for the 0-twisted Whitehead double of $\mathfrak{t}(2,2n+1)$, and properties of the skein exact sequence for knot Floer homology. The calculation of s is deduced from the computation of the Khovanov homology performed by Bar-Natan and Shumakovitch's programs [BN06, Shu06].

4.3 On the Floer homology data

Constructing Heegaard knot diagrams is complicated. Even with the results of theorem 3.5 — let alone by an unknotting $(1,1)$ tunnel — it is tedious and prone to error. To implement the algorithm of theorem 3.5 for constructing Heegaard knot diagrams the software system *Mathematica* [Wol05] was used. (See appendix A for the *Mathematica* code.)

The calculation of $\widehat{HFK}$, up to relative homological grading, for a given Heegaard knot diagram can be performed by Gabriel Doyle's program solve11knot [Doy05]. As discussed in chapter 2, the absolute homological grading is determined by the generator corresponding to the intersection of a Heegaard knot diagram of the unknot. The *Mathematica* program keeps track of this intersection, and Doyle's program can easily be modified to incorporate this information so as to produce knot Floer homology groups with absolute grading defined.

These programs were applied to a the following set of $(1,1)$ satellites of the right-handed trefoil:

$$K(\alpha,\beta;3,2) \qquad \text{for} \qquad \alpha \leq 30, \qquad 0 < \beta < \alpha/2$$

This set comprises 43 distinct satellite knots. Appendix B is a catalogue of the knot Floer homology groups for each of these satellite $(1,1)$ knots and their patterns. In each entry, an array of shaded boxes represents the knot Floer homology data.

A non-trivial knot Floer homology group $\widehat{HFK}_d(K,i)$, $i,d \in \mathbb{Z}$ of the knot K is represented by a gray box in the row and column labelled respectively i and d. The shade of the box indicates the rank n of the $\mathbb{Z}$ summand, according to the key provided. It is not necessary to record the generators in every non-trivial filtration level; there is a symmetry in the knot Floer homology groups [OS04c] which indicates that negative filtration levels mirror those above zero:

$$\widehat{HFK}_*(K,i) \cong \widehat{HFK}_{*-2i}(K,-i)$$

(This is a generalization of the symmetry in the Alexander polynomial under the involution $t \mapsto t^{-1}$.) For this reason, the Floer homology data corresponding to $\widehat{HFK}_*(K, i < 0)$ is supressed. The data in table 4.1 for the satellite $\widehat{HFK}(K(8,3;3,2))$, for example, is represented by the plot in figure 4.6. Doyle's program does provide enough information to compute the differentials in the knot Floer homology. However, that data is not included in the appendices, but will be presented in a subsequent work.

I conclude with a few observations about the data. Let K_S denote a satellite $(1,1)$ knot $K(\alpha,\beta;3,2)$ and P its pattern $K(\alpha,\beta;6,1)$ of K, where $0 < \alpha \leq 30$ and $0 < \beta < \alpha/2$.

Remark 3. The total rank of the knot Floer homology of the satellite K_S equals the total rank of its pattern P:

$$\sum\nolimits_{i\in\mathbb{Z}} \text{rk } \widehat{HFK}(K_S,i) = \sum\nolimits_{i\in\mathbb{Z}} \text{rk } \widehat{HFK}(P,i)$$

Remark 4. The degree of the knot Floer homology of a satellite exceeds the degree of the knot Floer homology of its pattern by the absolute value of the linking number of the 2-bridge link from which the pattern is defined:

$$\deg \widehat{HFK}(K(\alpha,\beta;3,2)) = \deg \widehat{HFK}(K(\alpha,\beta;6,1)) + |\text{lk}(\mathfrak{b}(\alpha,\beta))|$$

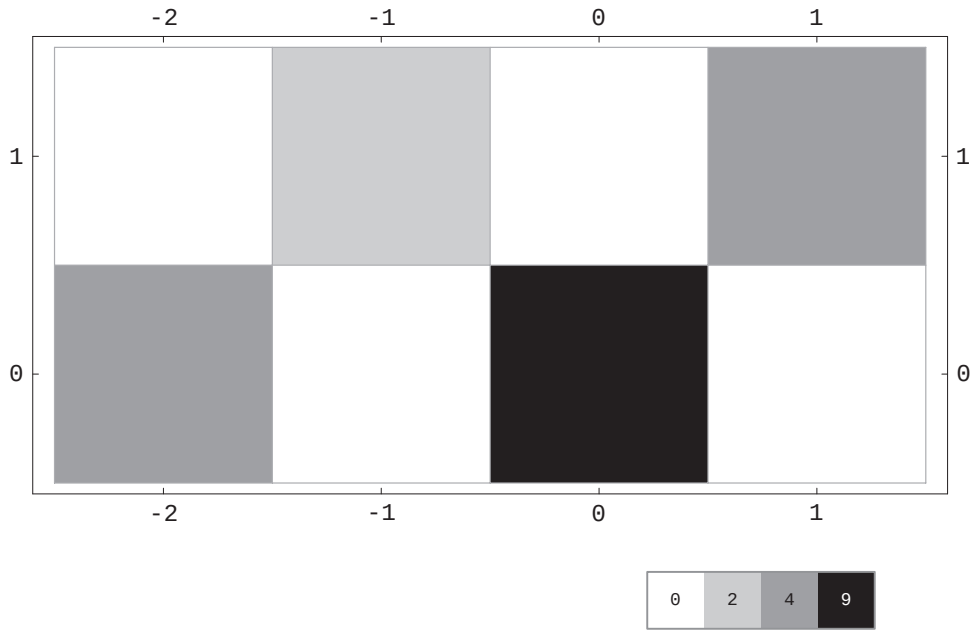

Figure 4.6: Distribution of generators of knot Floer homology groups $\widehat{HFK}_d(K(8,3;3,2),i)$ for $i \geq 0$, and arranged vertically by filtration level i and horizontally by homological grading d. The shade of each box indicates the number of generators there, as defined by the key to the right.

Remark 5. The satellite $K(\alpha,1;p,q)$ is the $(3\frac{\alpha}{2}+1,\frac{\alpha}{2})$ cable of the $\mathfrak{t}(p,q)$ torus knot. In particular, the first 14 satellites in the data set $K(2\frac{\alpha}{2},1;3,2)$, $\frac{\alpha}{2} = 2,3,\ldots,15$ are respectively the $(3\frac{\alpha}{2}+1,2)$ cables of the trefoil. The pattern of an (r,s) cable knot is the $\mathfrak{t}(r,s)$ torus knot. The knot Floer homology of torus knots was determined in [OS05]. The knot Floer homology groups of the $\mathfrak{t}(3\frac{\alpha}{2}+1,\frac{\alpha}{2})$ torus knot patterns for the above cables appearing in appendix B were calculated using the methods described in this thesis. The results agree with the results of [OS05]. Hedden proved [Hed05] that for sufficiently large $|i| \leq \deg \widehat{HFK}(K_S)$, the knot Floer homology groups $\widehat{HFK}(K_S,i)$ of $(kn+1,k)$ cables of the alternating torus knots stabilize for large n. The data agree with these results, too. Hedden

does not provide a minimum for $|i|$. For the data calculated in this thesis, $|i| \geq \deg \widehat{HFK}(K_S) - 3\alpha$.

Remark 6. Let $\delta \in Z$ denote a *diagonal* of knot Floer homology groups; that is, the groups $\widehat{HFK}_d(K, i)$ where $i - d = \delta$. There are at most finitely many non-trivial diagonals $\delta_1, \ldots, \delta_n$ for any given knot. Assume the diagonals are ordered $\delta_i < \delta_i + 1$, and define the *width* of K to be the number $\omega(K) := \delta_n - \delta_1$. Alternating knots have width $\omega = 1$ [OS03a]. Width 1 knots have also been studied by Rasmussen [Rasb], who refers to them as δ-thin. For the cases computed, the width of the satellite knot exceeds the width of its pattern by 2:

$$\omega(K(\alpha, \beta; 3, 2)) - \omega(K(\alpha, \beta; 6, 1) = 2$$

Preliminary data for the satellite $(1, 1)$ knots with torus knot companion $\mathfrak{t}(5, 2)$ and torus knot companion $\mathfrak{t}(7, 2)$ suggest a more general relation, for $k = 1, 2, \ldots$:

$$\omega(K(\alpha, \beta; 2k + 1, 2)) - \omega(K(\alpha, \beta; 4k + 2, 1) = 2k$$

Appendix A

Mathematica Code

The algorithm in theorem 3.5 produces a Heegaard knot diagram for a $(1,1)$ knot. This appendix provides *Mathematica* [Wol05] functions to implement the algorithm. After evaluating the entire code in *Mathematica*, a Heegaard diagram may be obtained by entering the command `CC[a,b,c,d]`, where $\mathfrak{d}(\mathtt{a},\mathtt{b},\mathtt{c},\mathtt{d})$ is $(1,1)$ normal form for a $(1,1)$ knot. Output is of the form `{{p,q,r,s},x}` and represents the Heegaard knot diagram for $K(\mathtt{p},\mathtt{q},\mathtt{r},\mathtt{s})$, as defined in [Rasb]. The corresponding Heegaard normal form is $\mathfrak{D}(\mathtt{q},\mathtt{r},\mathtt{p}-2\mathtt{q}-\mathtt{r},\mathtt{s})$. The number `x` indicates the order, counting down from the top left, of the intersection point in the Heegaard diagram which persists after removing basepoint z. This can be used to fix the absolute Maslov grading in a subsequent knot Floer homology calculation.

```
f[x_]:=RotateLeft[Flatten[Which[
          m>=0,Mod[{
                Reverse[Range[2*i+1]],
                Reverse[Range[2*j+1]+2*i+1],
                Reverse[Range[m]+2(i+j+k+l)+m+4],
                Reverse[Range[2*k+1]+2(i+j)+m+2],
                Reverse[Range[2*l+1]+2(i+j+k)+m+3],
                Reverse[Range[m]+2(i+j)+2]
                }-i-1,2(i+j+k+l+m)+4],
          m<0,Mod[{
                Reverse[Range[2*i+1]],
                Reverse[Range[-m]+2(i+j+k)+-m+3],
                Reverse[Range[2*j+1]+2*i-m+1],
                Reverse[Range[2*k+1]+2(i+j)-m+2],
                Reverse[Range[-m]+2*i+1],
                Reverse[Range[2*l+1]+2(i+j+k-m)+3]
                }-i-1,2(i+j+k+l-m)+4]
          ]],i][[x+1]]
g[x_]:=Which[
    MemberQ[{0,width,width+height,2*width+height},x],x,
    0<x<width||width+height<x<2*width+height,2*width+height-x,
    width<x<width+height||2*width+height<x<2(width+height),
    3*width+2*height-x
    ]
CatsCradle[X_]:=PostIsotopy[Isotope[PreIsotopy[X]]]
PreIsotopy[X_]:=Composition[
      SetCutPieces,
      KnotPath
      ][X]
KnotPath[X_]:=Insert[X,Unevaluated[Sequence@@{
          f[x[X]],
          g[f[x[X]]]
          }],{3,2}]
SetCutPieces[X_]:=Composition[
      PickupRightPiece,
      PickupLeftPiece,
      SortPreCutPieceVertices,
      PreCut,
      FindPieceToCut
      ][X]
FindPieceToCut[X_]:=Insert[X,P[y[X],X],{4,1}]
PreCut[X_]:=Insert[X,
```

```
    Sort[Append[Complement[P[y[X],X],{VX[y[X],X]}],
        Unevaluated[
          Sequence@@{{First[VX[y[X],X]],y[X]},{y[X],
          Last[VX[y[X],X]]}}]]],{4,
      2}]
SortPreCutPieceVertices[X_]:=
  Insert[X,RotateLeft[PreCutPiece[X],
      Position[PreCutPiece[X],VP[x[X]-0.5,PreCutPiece[X]]]
      [[1,1]]],{4,3}]
PickupLeftPiece[X_]:=ReplacePart[X,
    Sort[Select[SortedPreCutPiece[X],
        Position[SortedPreCutPiece[X],#][[1,1]]<=
            Position[SortedPreCutPiece[X],
                VP[y[X]-0.5,SortedPreCutPiece[X]]][[1,1]]&]],
    {4,2}]
PickupRightPiece[X_]:=
  ReplacePart[X,Sort[Complement[SortedPreCutPiece[X],
  LeftPiece[X]]],{4,3}]
TheIntersections[X_]:=X[[1]]
AnteriorIntersection[i_,intxs_]:=If[i\[Equal]1,intxs[[-1]],
intxs[[i-1]]]
PosteriorIntersection[i_,intxs_]:=
  If[i\[Equal]Length[intxs],intxs[[1]],intxs[[i+1]]]
NewIntersections[X_]:=X[[2]]
Isotope[X_]:=NestWhile[Insert[#1,
        IsotopeIntersection[
          AnteriorIntersection[Length[NewIntersections[#1]]+1,
            TheIntersections[X]],
          TheIntersections[X][[Length[NewIntersections[#1]]+1]],
          PosteriorIntersection[Length[NewIntersections[#1]]+1,
            TheIntersections[X]],
          X]
        ,{2,-1}]&,X,Length[NewIntersections[#1]]<Length
        [TheIntersections[X]]&]\
IsotopeIntersection[antew_,w_,postw_,X_]:=

  If[PieceMemberQ[w,CutPiece[X]]||PieceMemberQ[g[w],CutPiece[X]],
    Composition[
        IsotopeObstructing,
        IsotopeParallel
        ][antew,w,postw,X],
    w]
```

```
IsotopeParallel[antew_,w_,postw_,X_]:=Which[
    VX[w,X]\[Equal]VX[y[X],X],Which[
      PieceMemberQ[g[postw],LeftPiece[X]],
      {antew,y[X]-0.5,postw,X},
      PieceMemberQ[g[postw],RightPiece[X]],
      {antew,y[X]+0.5,postw,X}],
    VX[g[w],X]\[Equal]VX[y[X],X],Which[
      PieceMemberQ[antew,LeftPiece[X]],
      {antew,g[y[X]]+0.5,postw,X},
      PieceMemberQ[antew,RightPiece[X]],
      {antew,g[y[X]]-0.5,postw,X}],
    True,{antew,w,postw,X}
    ]
IsotopeObstructing[{antew_,w_,postw_,X_}]:=Which[
    VX[g[postw],X]\[Equal]VX[y[X],X],w,
    PieceMemberQ[w,LeftPiece[X]]&&PieceMemberQ[g[postw],
    RightPiece[X]],{w,
      z[X]+0.5,y[X]+0.5},
    PieceMemberQ[g[postw],LeftPiece[X]]&&PieceMemberQ[w,
    RightPiece[X]],{w,
      z[X]-0.5,y[X]-0.5},
    True,w]
PostIsotopy[X_]:=Composition[
      FinalOutput,
      RemoveCutInfo,
      UpdateKnotStart,
      AddNextCutStart,
      UpdatePieces,
      UpdateIntersections
      ][X]
UpdateIntersections[X_]:=ReplacePart[ReplacePart[X,
Flatten[X[[2]]],1],{},2]
UpdatePieces[X_]:=
  ReplacePart[X,
    Append[Complement[Pieces[X],{CutPiece[X]}],
      Unevaluated[Sequence@@{LeftPiece[X],RightPiece[X]}]],5]
AddNextCutStart[X_]:=ReplacePart[X,
    Sort[Append[Complement[Pieces[X],{P[z[X],X]}],
        Sort[Append[Complement[P[z[X],X],{VX[z[X],X]}],
            Unevaluated[
              Sequence@@{{First[VX[z[X],X]],z[X]},{z[X],
                    Last[VX[z[X],X]]}}]]]],#1[[1,1]]
```

```
                    <#2[[1,1]]&],5]
UpdateKnotStart[X_]:=ReplacePart[X,{z[X]},3]
RemoveCutInfo[X_]:=ReplacePart[X,{},4]
DoneQ[X_]:=x[X]\[Equal]KnotEnd
FinalOutput[X_]:=If[DoneQ[X],
    {
      TheIntersections[X],
      Table[{TheIntersections[X][[icount]],
          g[PosteriorIntersection[icount,TheIntersections[X]]]},
          {icount,1,
          Length[TheIntersections[X]]}]
      },X]
iiStrands[X_]:=
  Select[Strands[X],
    Max[#]>2*width+height&&Mean[{#[[1]],#[[2]]}]==width+height&]
ii[X_]:=Length[iiStrands[X]]
jjStrands[X_]:=Which[
    KnotStart==width,
    Select[Strands[X],Mean[{#[[1]],#[[2]]}]\[Equal]KnotEnd&],
    KnotStart\[Equal]width+height,
    Select[Strands[X],Mean[{#[[1]],#[[2]]}]\[Equal]width&]
    ]
jj[X_]:=Length[jjStrands[X]]
kkStrands[X_]:=Which[
    KnotStart==width,
    Select[Strands[X],
      Mean[{#[[1]],#[[2]]}]\[Equal]width+height&&Min[#]
      >KnotEnd&],
    KnotStart\[Equal]width+height,
    Select[Strands[X],Mean[{#[[1]],#[[2]]}]\[Equal]KnotEnd&]
    ]
kk[X_]:=Length[kkStrands[X]]
llStrands[X_]:=
  Select[Strands[X],
    Max[#]>2*width+height&&Mean[{#[[1]],#[[2]]}]\[Equal]
    2*width+height&]
ll[X_]:=Length[llStrands[X]]
mmStrands[X_]:=
  Select[Strands[
      X],!MemberQ[
          Join[iiStrands[X],jjStrands[X],kkStrands[X],
          llStrands[X]],#]&]
```

```
mm[X_]:=Which[
    Length[mmStrands[X]]\[Equal]0,0,
    Max[mmStrands[X][[1]]]>2*width+height,Length[mmStrands[X]],
    Max[mmStrands[X][[1]]]<2*width+height,-Length[mmStrands[X]]
    ]
ff[x_]:=RotateLeft[Flatten[Which[
          m>=0,Mod[{
                Reverse[Range[2*i]],
                Reverse[Range[2*j]+2*i],
                Reverse[Range[m]+2(i+j+k+l)+m],
                Reverse[Range[2*k]+2(i+j)+m],
                Reverse[Range[2*l]+2(i+j+k)+m],
                Reverse[Range[m]+2(i+j)]
                }-i-1,2(i+j+k+l+m)],
          m<0,Mod[{
                Reverse[Range[2*i]],
                Reverse[Range[-m]+2(i+j+k)+-m],
                Reverse[Range[2*j]+2*i-m],
                Reverse[Range[2*k]+2(i+j)-m],
                Reverse[Range[-m]+2*i],
                Reverse[Range[2*l]+2(i+j+k-m)]
                }-i-1,2(i+j+k+l-m)]
          ]],i][[x+1]]
HDwidth[X_]:=Length[Select[Strands[X],Min[#]<width&]]
HDheight[X_]:=Length[Select[Strands[X],Max[#]>2*width+height&]]
gg[x_]:=Which[
    0<=x<width||width+height<=x<2*width+height,2*width+height-x-1,
    width<=x<width+height||2*width+height<=x<2(width+height),
    3*width+2*height-x-1
    ]
x[X_]:=X[[3,1]]
y[X_]:=X[[3,2]]
z[X_]:=X[[3,3]]
V[X_]:=X[[3,4]]
CutPiece[X_]:=X[[4,1]]
PreCutPiece[X_]:=X[[4,2]]
SortedPreCutPiece[X_]:=X[[4,3]]
LeftPiece[X_]:=X[[4,2]]
RightPiece[X_]:=X[[4,3]]
Pieces[X_]:=X[[5]]
Strands[X_]:=X[[2]]
VX[x_,X_]:=Select[Flatten[Pieces[X],1],VertexMemberQ[x,#]&][[1]]
```

```
VP[x_,p_]:=Select[p,VertexMemberQ[x,#]&][[1]]
P[x_,X_]:=Select[Pieces[X],PieceMemberQ[x,#]&][[1]]
PieceMemberQ[x_,p_]:=MemberQ[p,v_?(VertexMemberQ[x,#]&)]
VertexMemberQ[x_,v_]:=x>v[[1]]&&(x<v[[2]]||v[[2]]\[Equal]0)
CC[ai_,bi_,ci_,di_]:=Do[
    {
      If[bi<=0,{a,b,c,d}={ai,ci,-bi,di+2*ai+1},{a,b,c,d}=
      {ai,bi,ci,di} ],
      width=Which[
          a<d,d,
          -b<=d<=a,2*a-d+1,
          -a-b<=d<-b,2(a+b)+d+1,
          d<-a-b,2(a+b)+c+1
          ],
      height=2*a+b+c+1,
      {i,j,k,l,m}=
        Which[
          a<d,{a,-a+d-1,a,a+c,b},
          -b<=d<=a,{a+b,a,a-d,a,c},
          -a-b<=d<-b,{a+b,a+b+d,a+b,a,c},
          d<-a-b,{a+b,a,a-d,a,-c}
          ],
      InitialIntersection=width+0.5,
      KnotStart=Which[
          a<d,width+height,
          -b<d<=a,width,
          -a-b<=d<-b,width+height,
          d<-a-b,width
          ],
      KnotSlope=If[KnotStart\[Equal]width,1,-1],
      KnotEnd=Which[
          d+b>0,width+b+d,
          d+b<0,width+height+d+b],
      InitialPiece={
          {0,width},
          {width,width+height},
          {width+height,2*width+height},
          {2*width+height,0}
          },
      InitialDiagram={
          {InitialIntersection},
          {},
```

```
    {KnotStart},
    {},
    {InitialPiece}
    },
KnotStrandsN=width+height-2,
KnotSequence=
  Append[Flatten[
      Table[{Nest[Composition[g,f],KnotStart,t-1],
          Nest[Composition[f,g],KnotStart,t]},
          {t,1,KnotStrandsN}]],
    KnotEnd],
KnotQ=
  Sort[KnotSequence]\[Equal]
    Sort[Prepend[Complement[Range[2(width+height)]-1,{0,
            width,
            width+height,
            2*width+height}],
        KnotStart]],
If[KnotQ,
  Do[
    {
      If[DoneQ[InitialDiagram],
      Y=FinalOutput[InitialDiagram],
        Y=Nest[CatsCradle,InitialDiagram,width+height-2]]
      }
    ],
  Break[Print["Not a knot"]]
  ],
{i,j,k,l,m}={ii[Y],jj[Y],kk[Y],ll[Y],mm[Y]},
height=HDheight[Y],
width=HDwidth[Y],
rootStrands=Flatten[Position[Sort[Flatten[Y[[2]]]],
First[Y[[1]]]]]-1,
BranchSequenceCast[x_]:=
  Part[Sort[Flatten[Y[[2]]]],
    Table[Nest[Composition[gg,ff],x,t-1],
    {t,1,width+height}]+1],
zeroGrad=
  First[Select[rootStrands,BranchSequenceCast[#]\[Equal]
  Y[[1]]&]],
zeroGradCount=width+height-zeroGrad,
ABCD=Which[
```

```
      m>=0&&KnotSlope\[Equal]-1,{i,i+m,l,j},
      m>=0&&KnotSlope\[Equal]1,{l,i,l+m,-k},
      m<0&&KnotSlope\[Equal]-1,{i-m,i,l,j},
      m<0&&KnotSlope\[Equal]1,{l-m,i,l,-k}
      ],
  {AA,BB,CC,DD}=ABCD,
  aabbccdd=Which[
      AA<=BB&&AA<=CC,{AA,BB-AA,CC-AA,DD+AA},
      CC<AA<=BB,{CC,AA-CC,BB-AA,DD-AA},
      CC<BB<AA,{CC,BB-CC,0,DD-(AA-CC)*(BB+CC)+CC},
      BB<AA<=CC,{BB,CC-AA,AA-BB,DD+AA+2*BB},
      BB<CC<AA,{BB,0,CC-BB,DD+(AA-BB)*(BB+CC)+BB}
      ],
  {aa,bb,cc}=Take[aabbccdd,3],
  dd=Mod[aabbccdd[[4]],2*aa+bb+cc],
  gen=Mod[zeroGradCount-aa-cc+dd,2*aa+bb+cc,1],
  theOutput={{2 aa+bb+cc,aa,bb,dd},gen},
  Clear[a,b,c,d,i,j,k,l,m,Y,width,height,InitialIntersection,
   KnotStart,
    KnotSlope,KnotEnd,InitialPiece,InitialDiagram,KnotStrandsN,
    KnotSequence,KnotQ,rootStrands,BranchSequenceCast,zeroGrad,
    zeroGradCount,ABCD,AA,BB,CC,DD,aabbccdd,gen],
  Break[theOutput]
  }
]
```

Appendix B

Satellite $(1,1)$ Knot Data

This appendix catalogues knot Floer homology groups for 43 distinct satellite $(1,1)$ knots with right-handed trefoil companion:

$$K(\alpha,\beta;3,2) \qquad \text{for} \qquad \alpha \leq 30, \qquad 0 < \beta < \alpha/2$$

and their patterns, where the symbol $K(\alpha,\beta;p,q)$ is as defined in the Morimoto-Sakuma classification of satellite tunnel 1 knots [MS91]. The pattern of $K(\alpha,\beta;p,q)$ is $K(\alpha,\beta;pq,1)$. Example 2.4.2 calculates the knot Floer homology of the right-handed trefoil. The data is ordered by increasing β, then increasing α. If two knots have the same knot type (eg. $K(14,3;3,2)$ and $K(14,5;3,2)$) then only the first $K(\alpha,\beta;3,2)$ representing the knot type is included.

The knot Floer homology data consists of an array of shaded boxes. A non-trivial knot Floer homology group $\widehat{HFK}_d(K,i)$, $i,d \in \mathbb{Z}$ of the knot K is represented by a gray box in the row and column labelled respectively i and d. The shade of the box indicates the rank n of the $\mathbb{Z}$ summand, according to the key provided. Information concerning the differentials is supressed. The various parameters appearing below each plot are defined as follows.

$\mathfrak{d}(a,b,c,d)$	$(1,1)$ normal form
$\mathfrak{D}(a,b,c,d)$	Heegaard normal form
$K(p,q,r,s)$	Rasmussen Heegaard knot diagram parameters [Rasb]
x_0	Order, counting from top left, of intersection point in the Heegaard normal form which persists after removing basepoint z (this determines absolute Maslov grading)
$\mathrm{lk}(\mathfrak{b}(\alpha,\beta))$	Linking number of 2-bridge link $\mathfrak{b}(\alpha,\beta)$ (cf. [BZ03])

$K(4,1;6,1)$

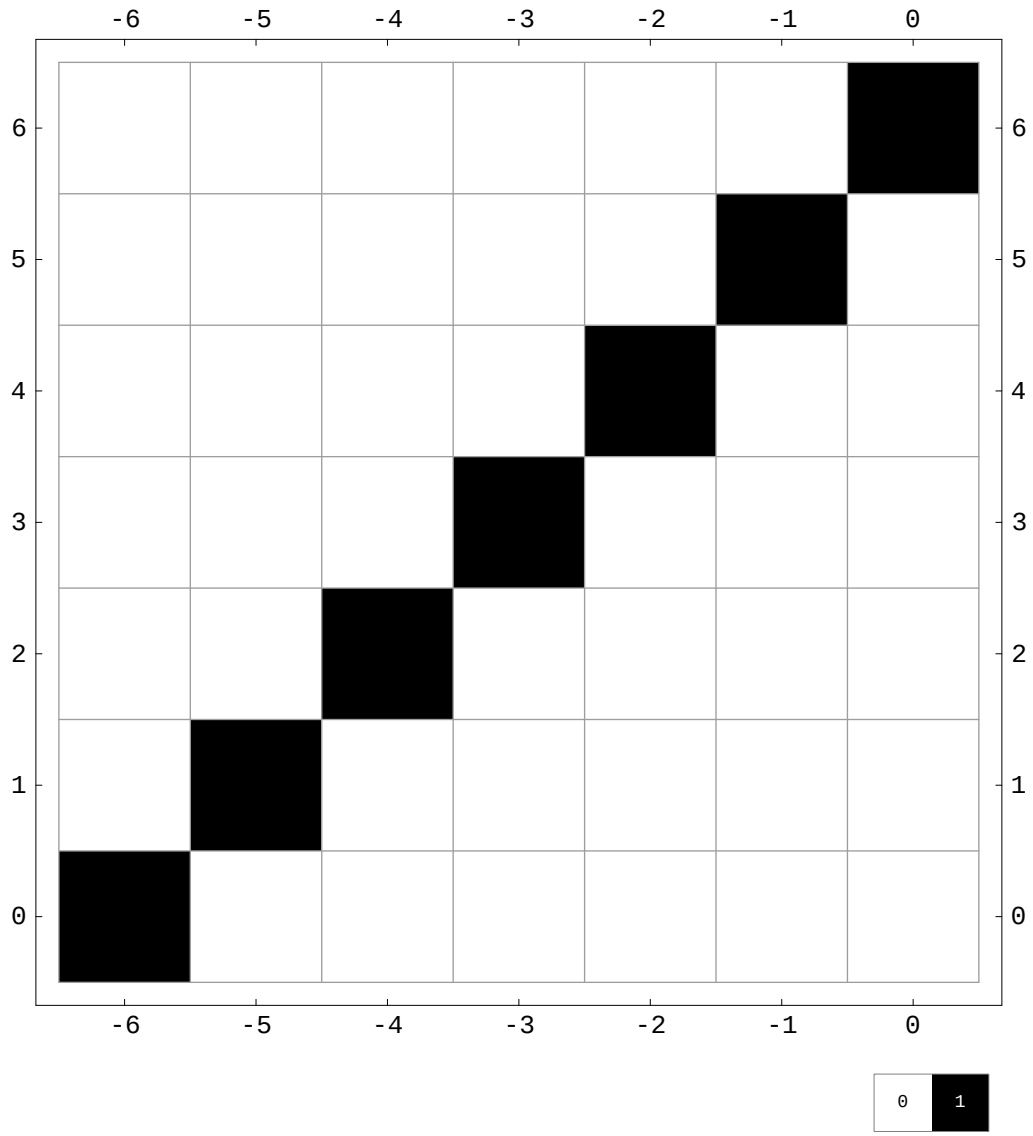

$\mathfrak{d}(0,1,0,12)$

$\mathfrak{D}(6,1,0,6)$

$K(13,6,1,6)$

$x_0 = 13$

$\mathrm{lk}(\mathfrak{b}(4,1)) = 2$

$K(4,1;3,2)$

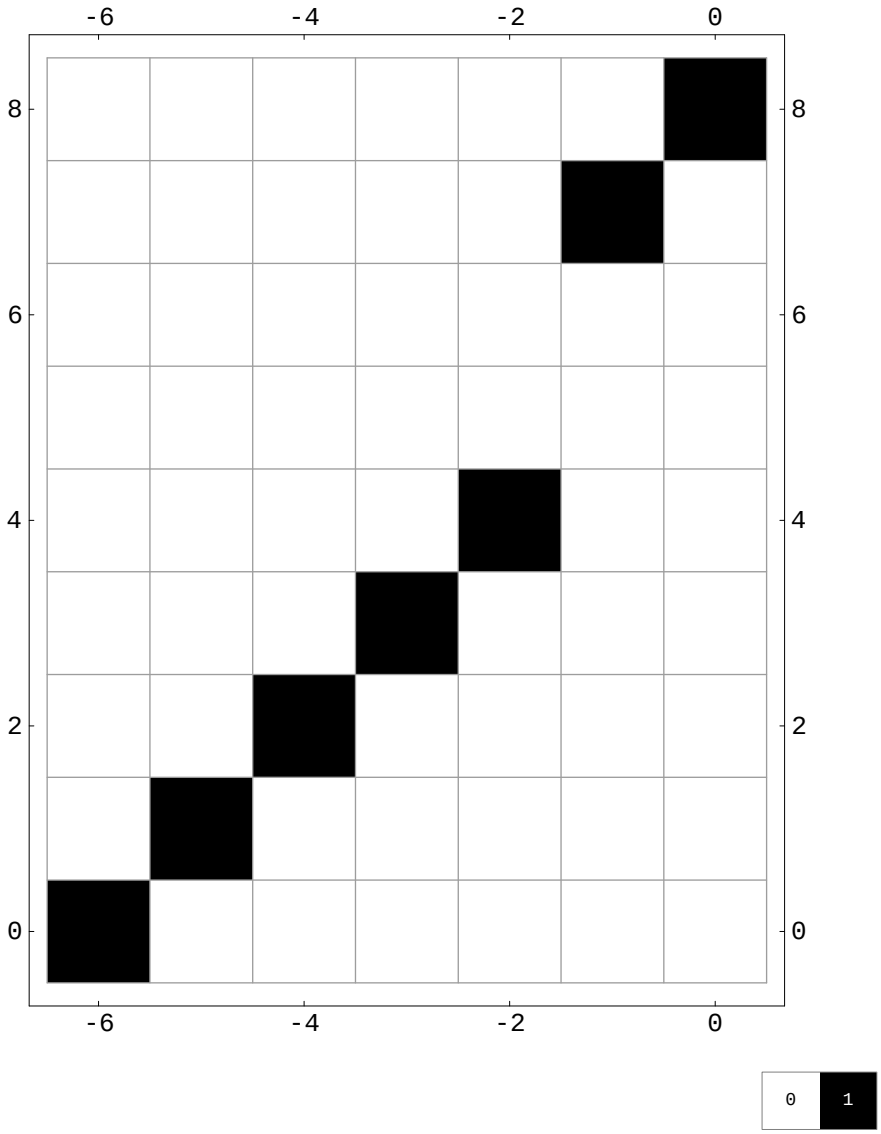

$\mathfrak{d}(0,1,2,6)$

$\mathfrak{D}(3,7,0,11)$

$K(13,3,7,11)$

$x_0 = 8$

$\mathrm{lk}(\mathfrak{b}(4,1)) = 2$

$K(6,1;6,1)$

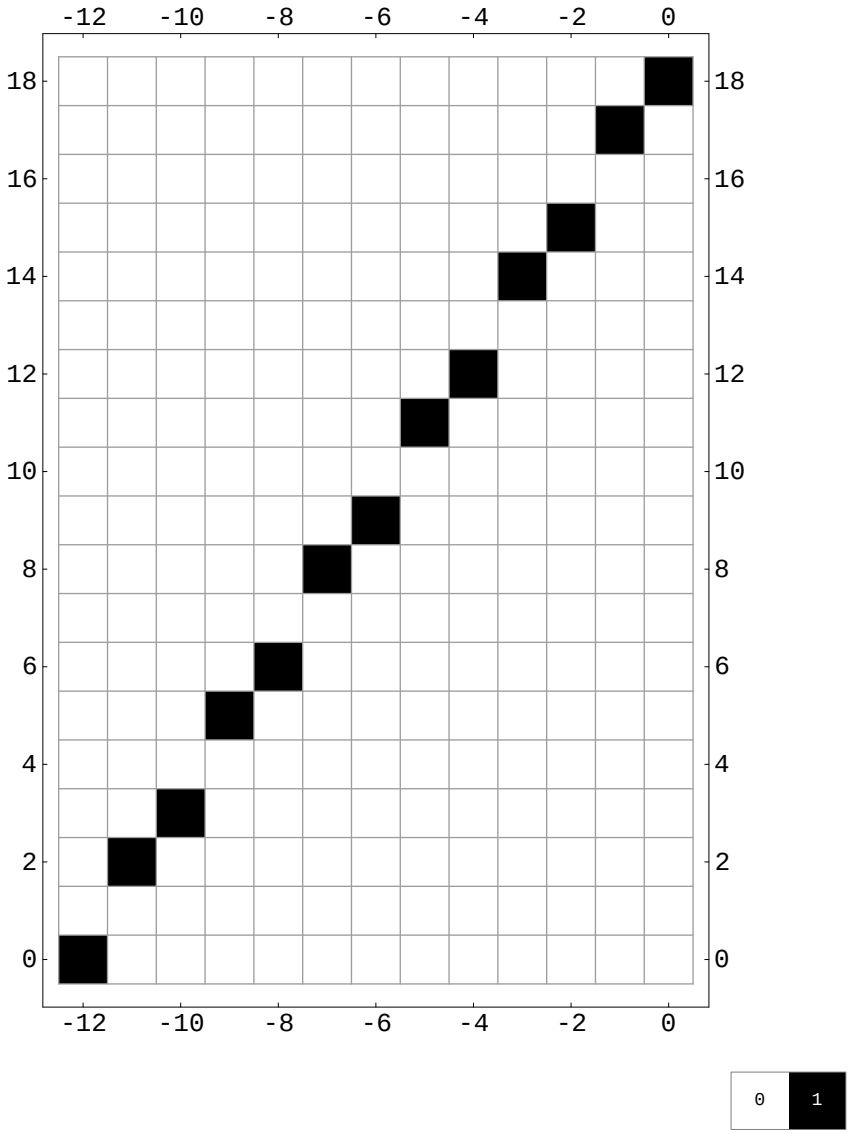

$\mathfrak{d}(0,2,0,18)$

$\mathfrak{D}(6,7,6,6)$

$K(25,6,7,6)$

$x_0 = 19$

$\mathrm{lk}(\mathfrak{b}(6,1)) = 3$

$K(6,1;3,2)$

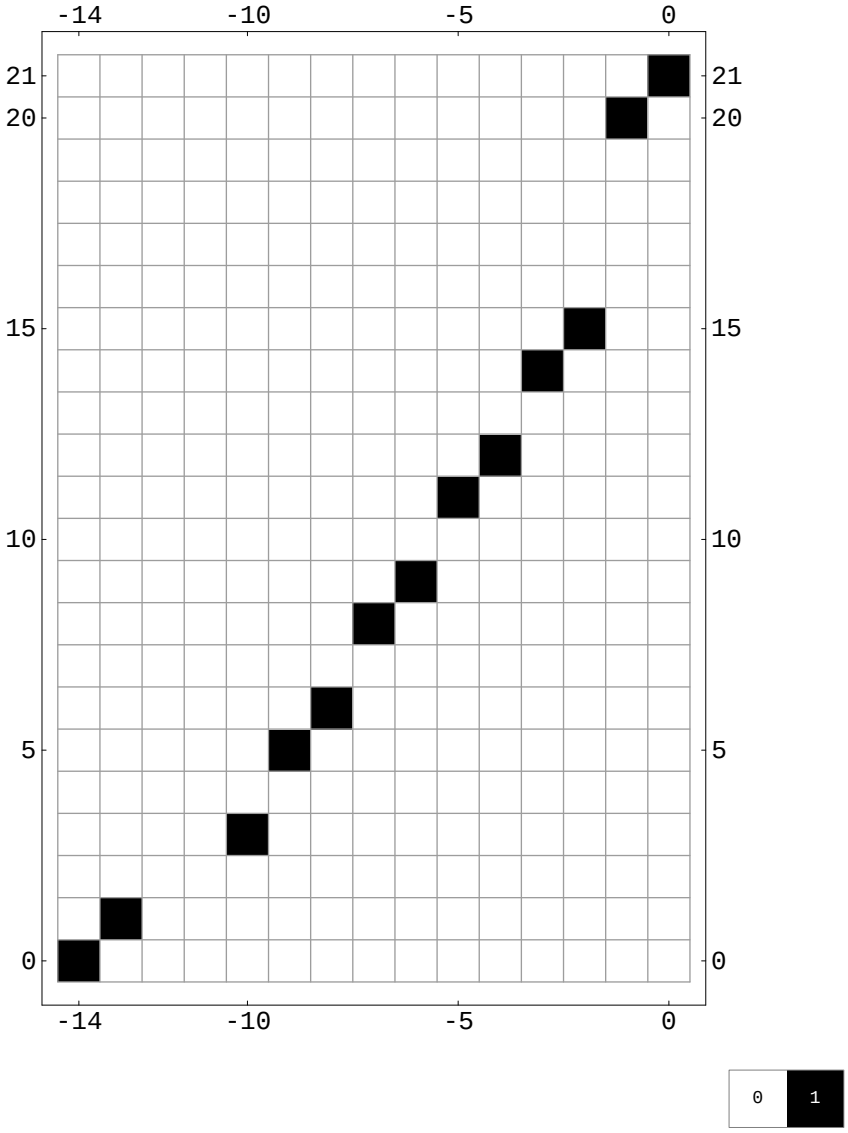

$\mathfrak{d}(0,2,3,9)$

$\mathfrak{D}(3,16,3,17)$

$K(25,3,16,17)$

$x_0 = 11$

$\mathrm{lk}(\mathfrak{b}(6,1)) = 3$

$K(8,1;6,1)$

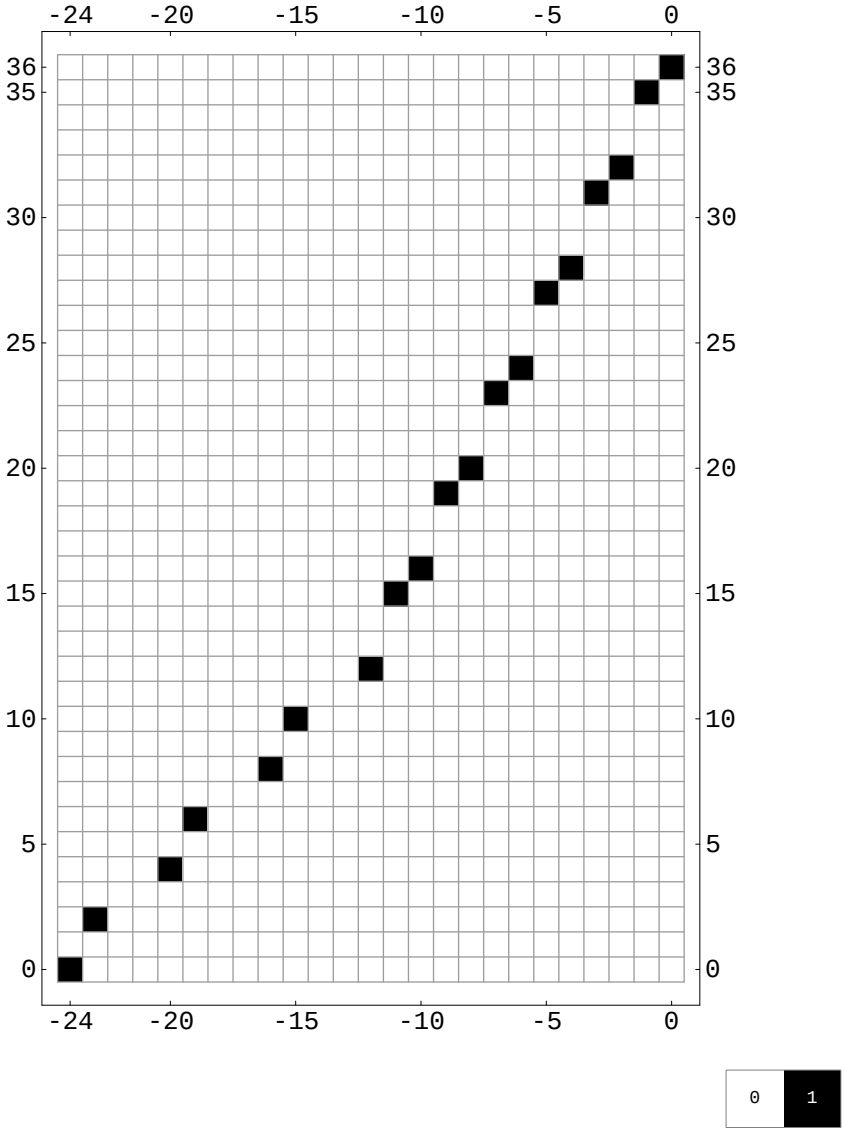

$\mathfrak{d}(0,3,0,24)$

$\mathfrak{D}(6,13,12,6)$

$K(37,6,13,6)$

$x_0 = 25$

$\mathrm{lk}(\mathfrak{b}(8,1)) = 4$

$K(8,1;3,2)$

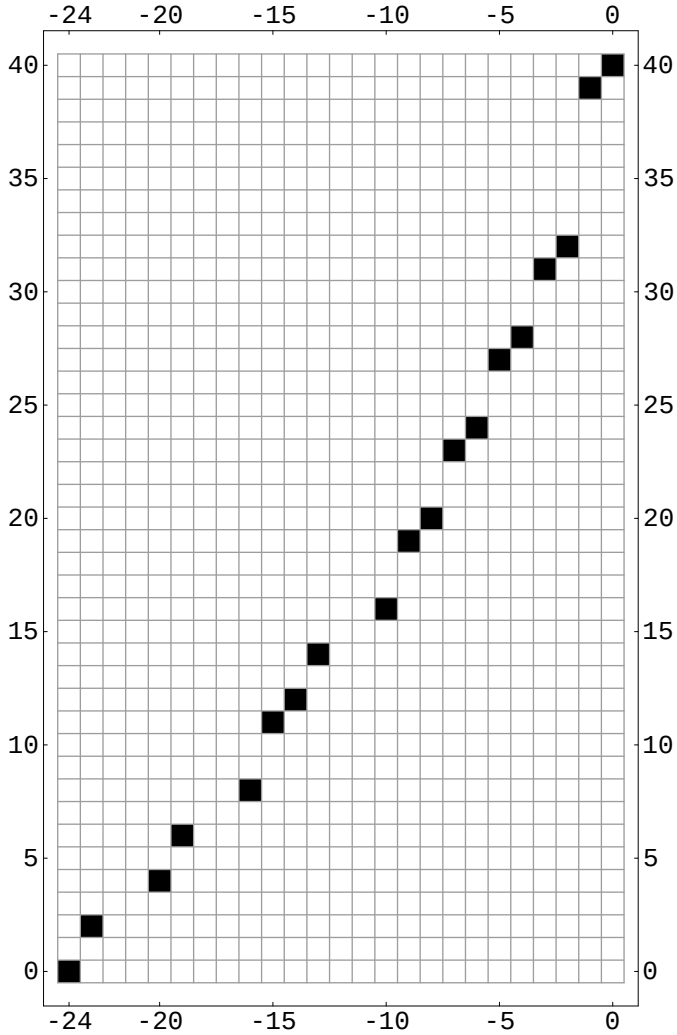

$\mathfrak{d}(0,3,4,12)$

$\mathfrak{D}(3,25,6,23)$

$K(37,3,25,23)$

$x_0 = 14$

$\mathrm{lk}(\mathfrak{b}(8,1)) = 4$

$K(10,1;6,1)$

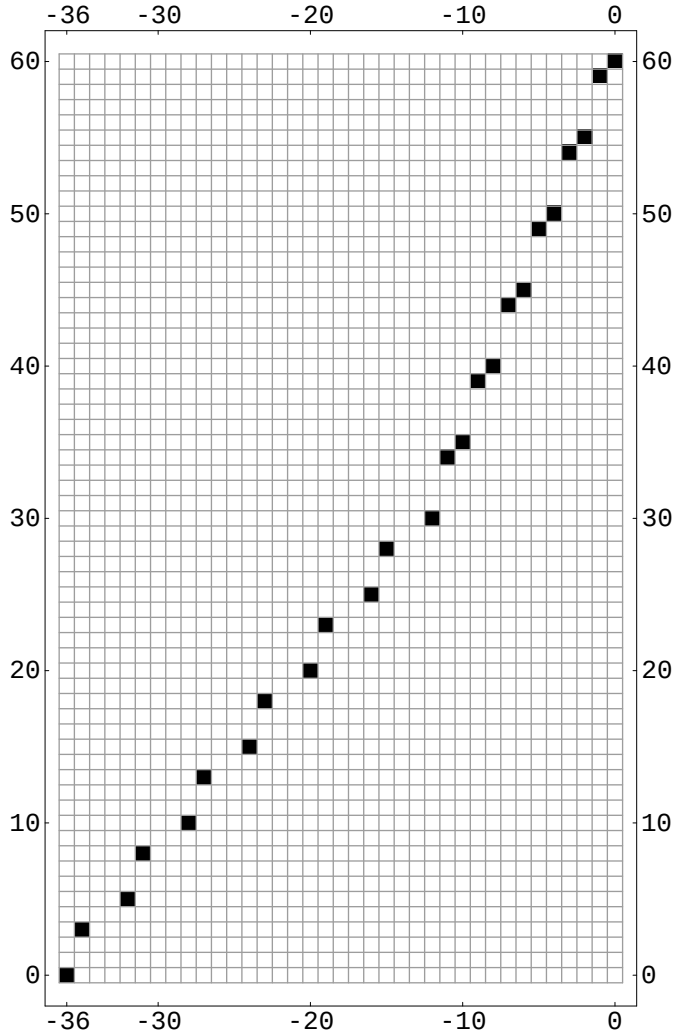

$\mathfrak{d}(0,4,0,30)$

$\mathfrak{D}(6,19,18,6)$

$K(49,6,19,6)$

$x_0 = 31$

$\mathrm{lk}(\mathfrak{b}(10,1)) = 5$

$K(10,1;3,2)$

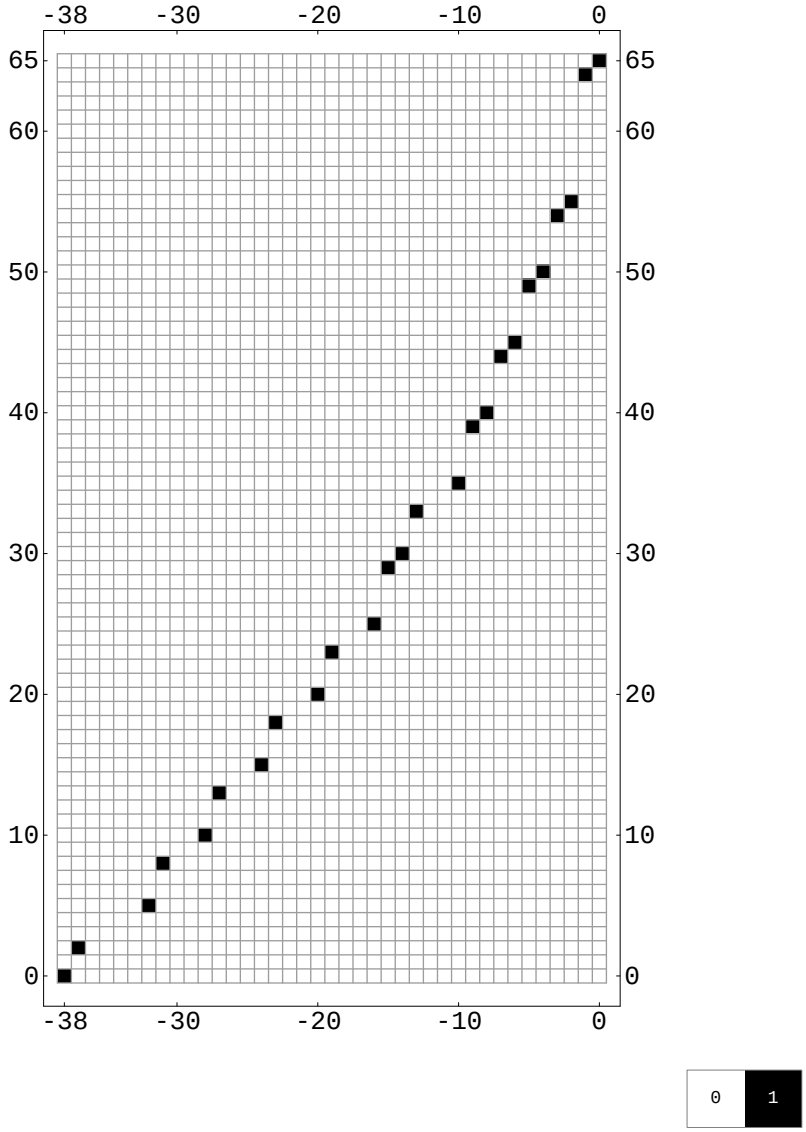

$\mathfrak{d}(0,4,5,15)$

$\mathfrak{D}(3,34,9,29)$

$K(49,3,34,29)$

$x_0 = 17$

$\mathrm{lk}(\mathfrak{b}(10,1)) = 5$

$K(12,1;6,1)$

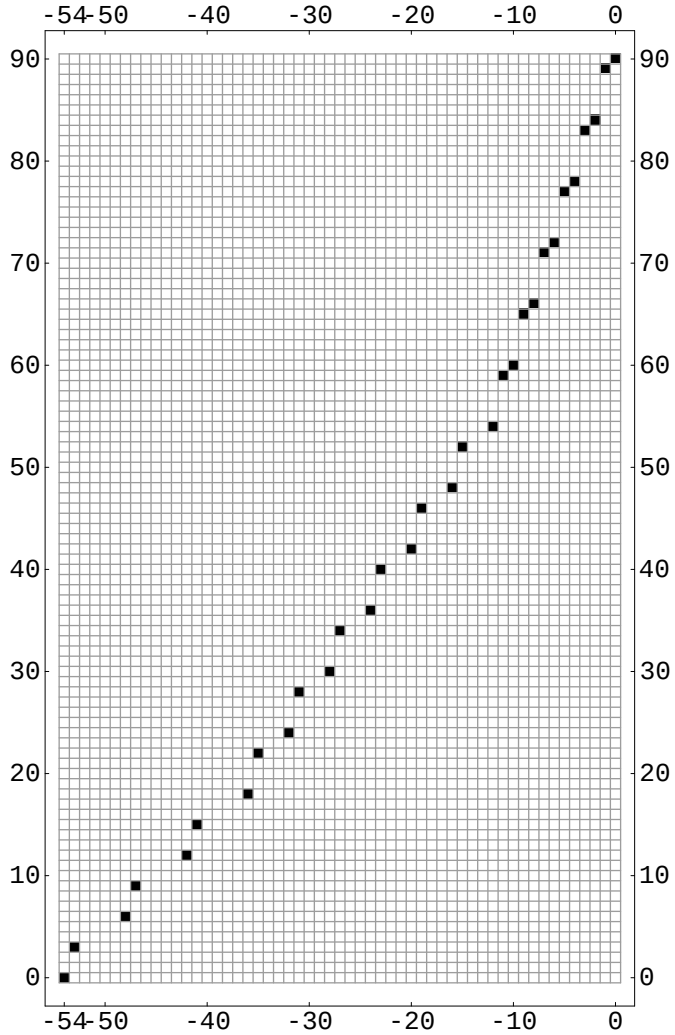

$\mathfrak{d}(0,5,0,36)$

$\mathfrak{D}(6,25,24,6)$

$K(61,6,25,6)$

$x_0 = 37$

$\mathrm{lk}(\mathfrak{b}(12,1)) = 6$

$K(12,1;3,2)$

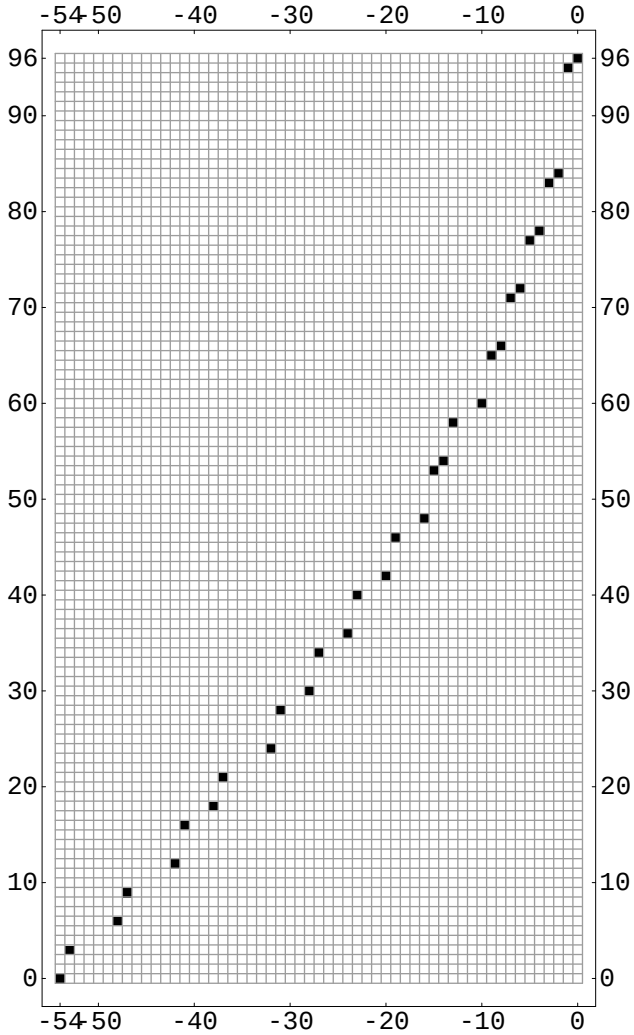

$\mathfrak{d}(0,5,6,18)$

$\mathfrak{D}(3,43,12,35)$

$K(61,3,43,35)$

$x_0 = 20$

$\mathrm{lk}(\mathfrak{b}(12,1)) = 6$

$K(14,1;6,1)$

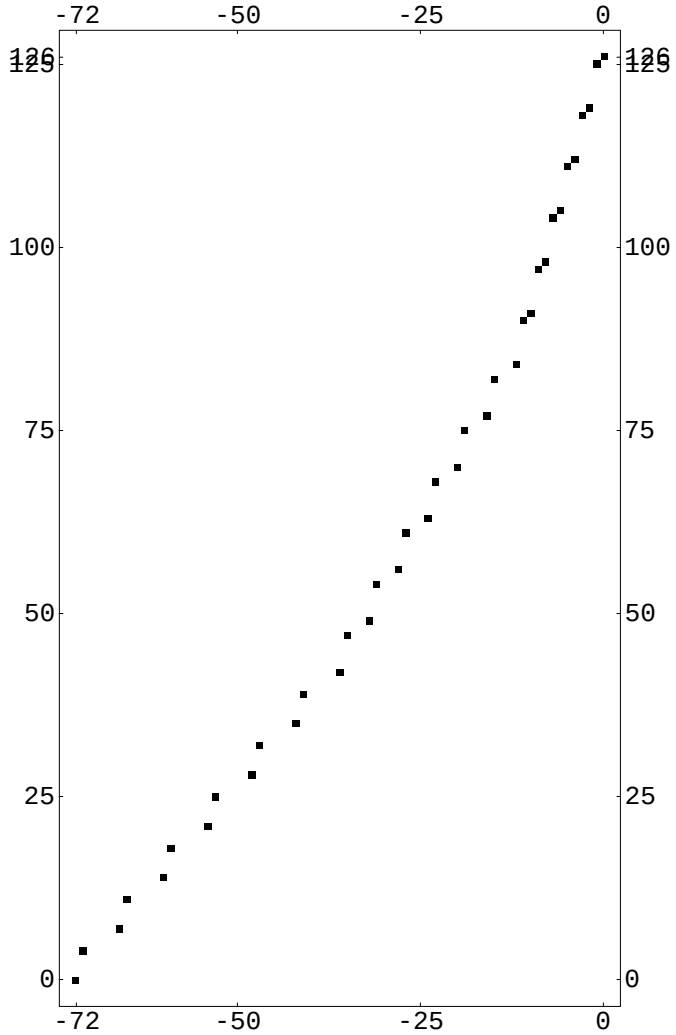

$\mathfrak{d}(0,6,0,42)$

$\mathfrak{D}(6,31,30,6)$

$K(73,6,31,6)$

$x_0 = 43$

$\mathrm{lk}(\mathfrak{b}(14,1)) = 7$

$K(14, 1; 3, 2)$

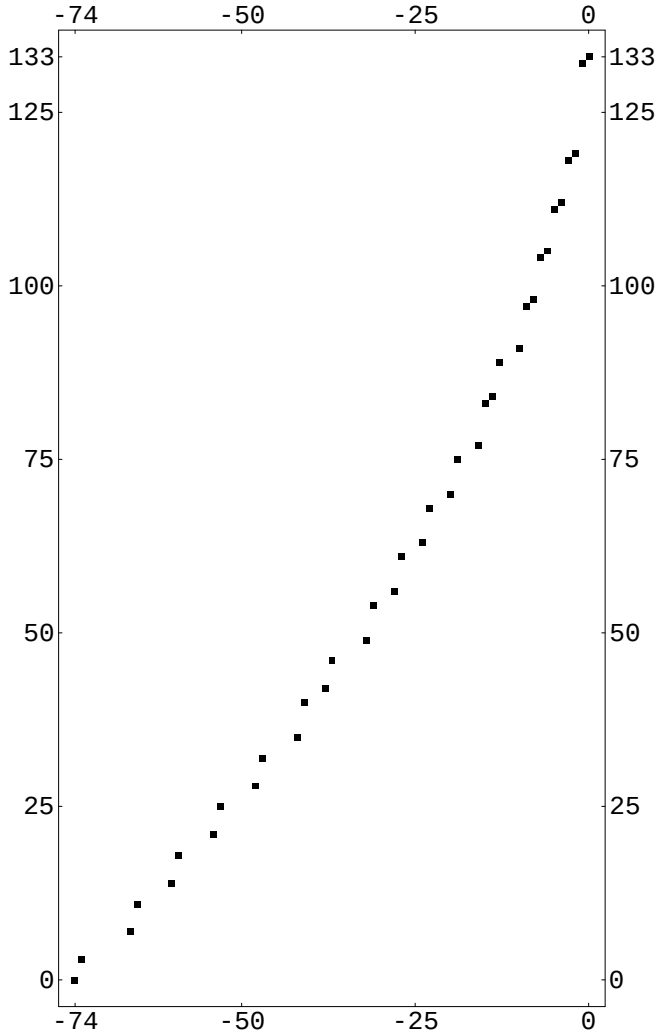

$\mathfrak{d}(0, 6, 7, 21)$

$\mathfrak{D}(3, 52, 15, 41)$

$K(73, 3, 52, 41)$

$x_0 = 23$

$\mathrm{lk}(\mathfrak{b}(14, 1)) = 7$

$K(16, 1; 6, 1)$

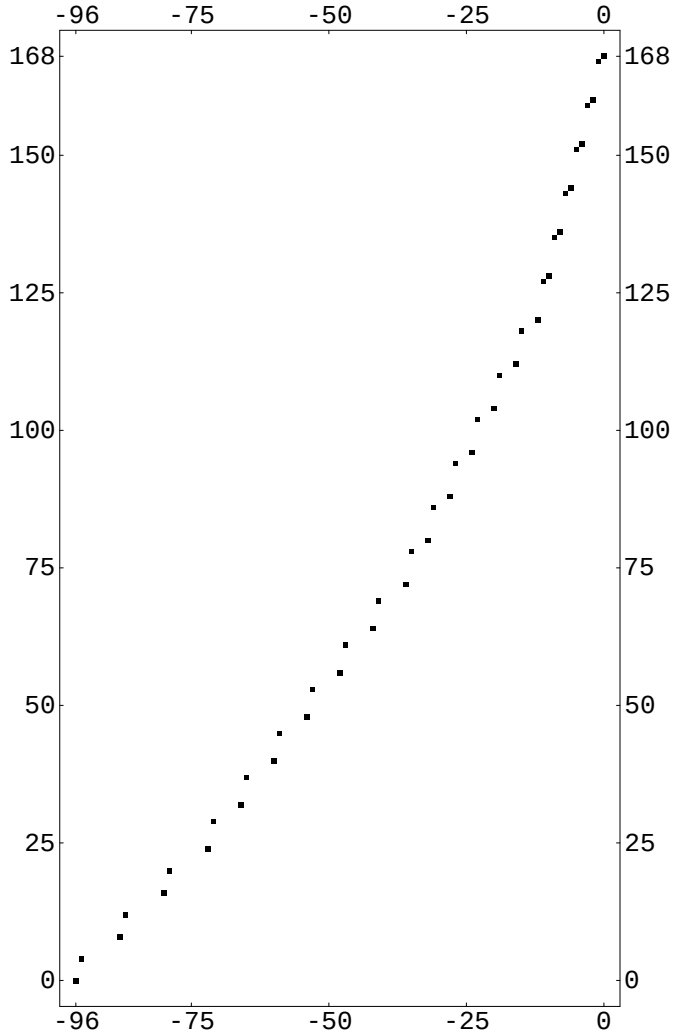

$\mathfrak{d}(0, 7, 0, 48)$

$\mathfrak{D}(6, 37, 36, 6)$

$K(85, 6, 37, 6)$

$x_0 = 49$

$\mathrm{lk}(\mathfrak{b}(16, 1)) = 8$

$K(16,1;3,2)$

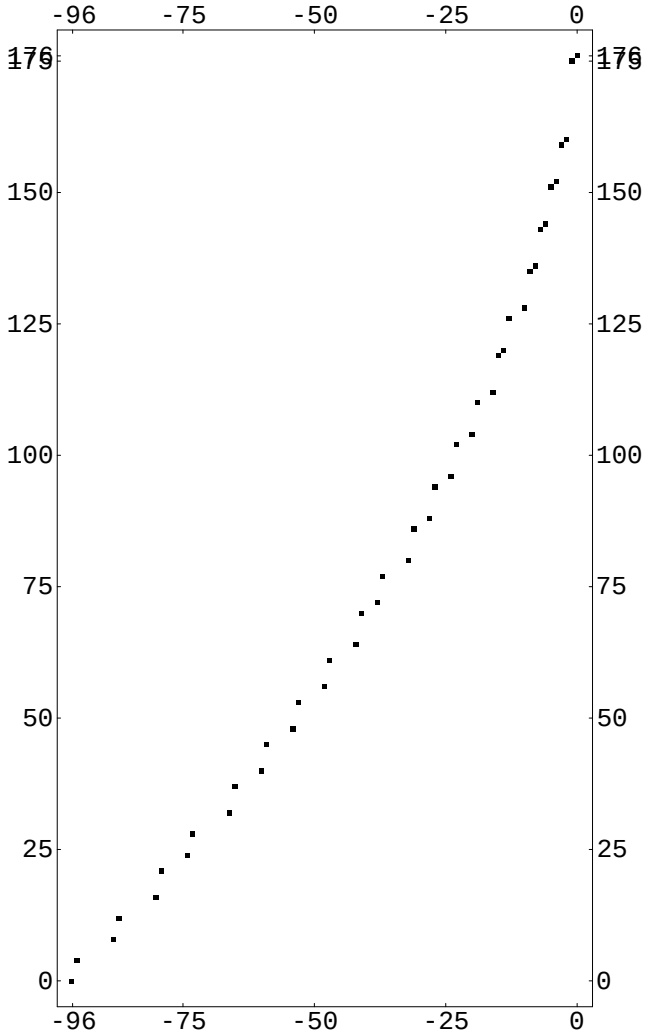

$\mathfrak{d}(0,7,8,24)$

$\mathfrak{D}(3,61,18,47)$

$K(85,3,61,47)$

$x_0 = 26$

$\mathrm{lk}(\mathfrak{b}(16,1)) = 8$

$K(18, 1; 6, 1)$

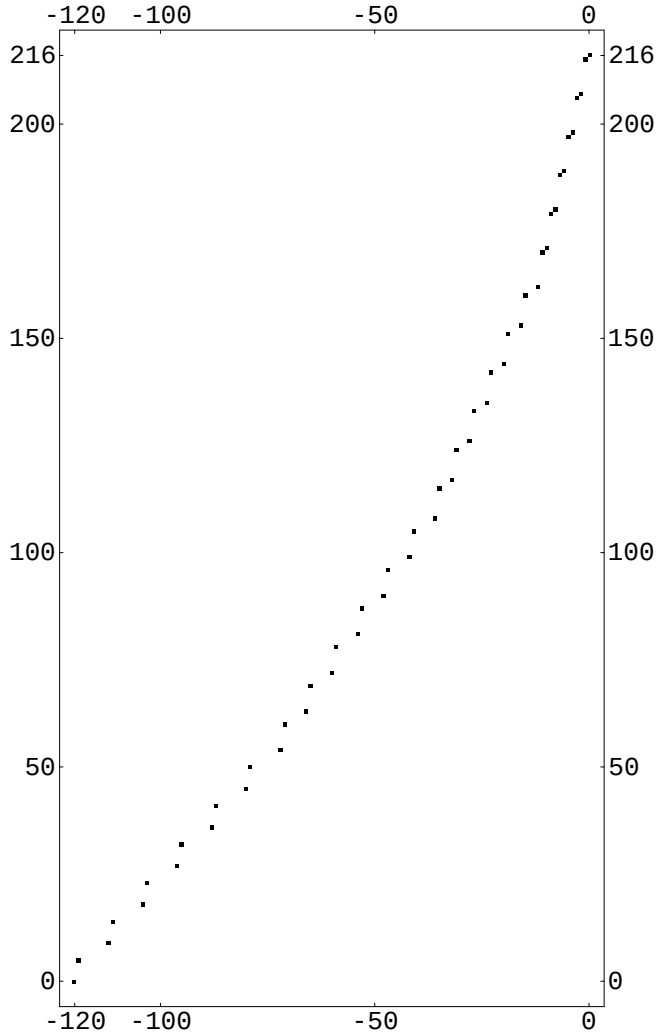

$\mathfrak{d}(0, 8, 0, 54)$

$\mathfrak{D}(6, 43, 42, 6)$

$K(97, 6, 43, 6)$

$x_0 = 55$

$\mathrm{lk}(\mathfrak{b}(18, 1)) = 9$

$K(18, 1; 3, 2)$

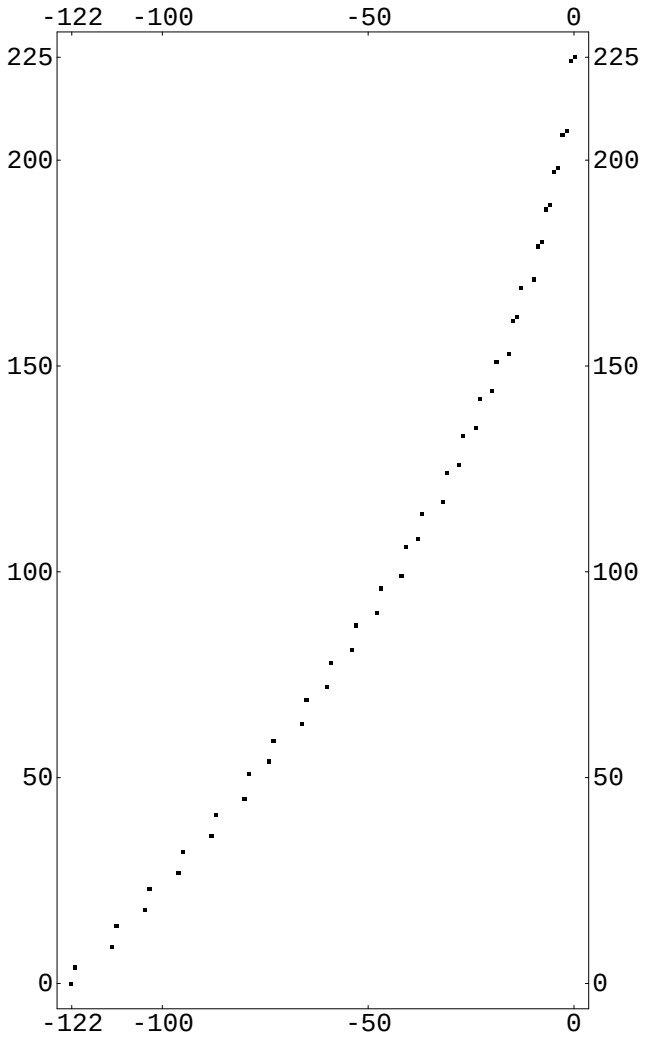

$\mathfrak{d}(0, 8, 9, 27)$

$\mathfrak{D}(3, 70, 21, 53)$

$K(97, 3, 70, 53)$

$x_0 = 29$

$\mathrm{lk}(\mathfrak{b}(18, 1)) = 9$

$K(20,1;6,1)$

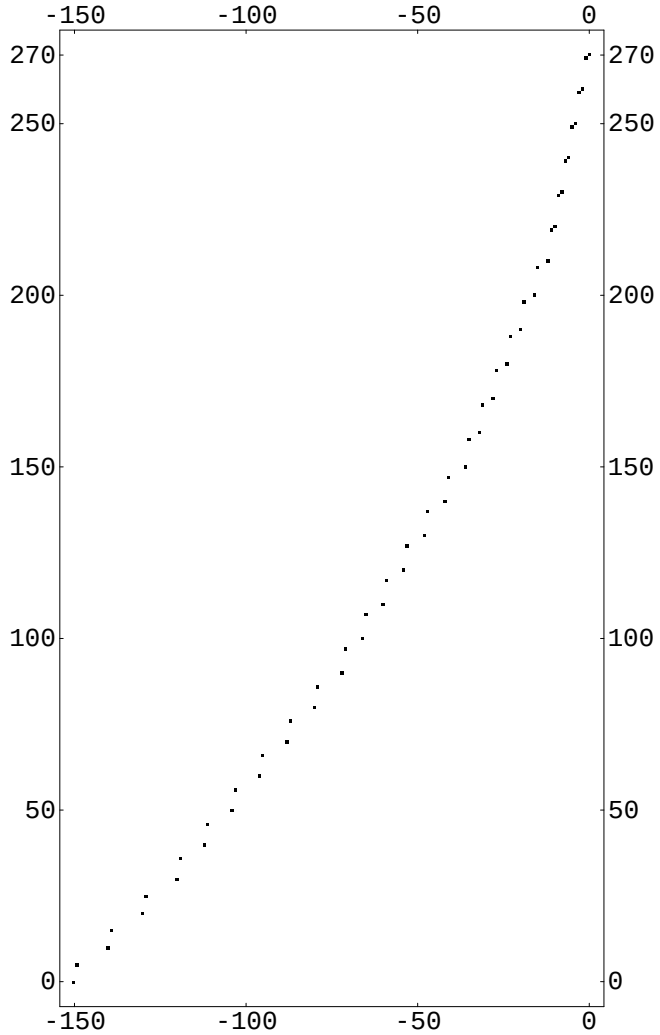

$\mathfrak{d}(0,9,0,60)$

$\mathfrak{D}(6,49,48,6)$

$K(109,6,49,6)$

$x_0 = 61$

$\mathrm{lk}(\mathfrak{b}(20,1)) = 10$

$K(20, 1; 3, 2)$

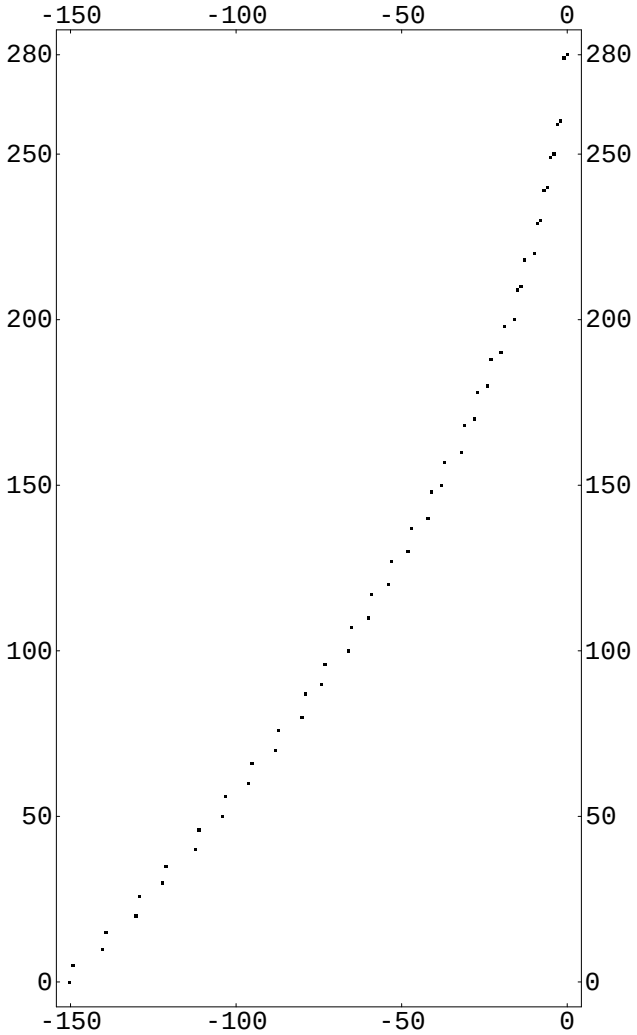

$\mathfrak{d}(0, 9, 10, 30)$

$\mathfrak{D}(3, 79, 24, 59)$

$K(109, 3, 79, 59)$

$x_0 = 32$

$\mathrm{lk}(\mathfrak{b}(20, 1)) = 10$

$K(22, 1; 6, 1)$

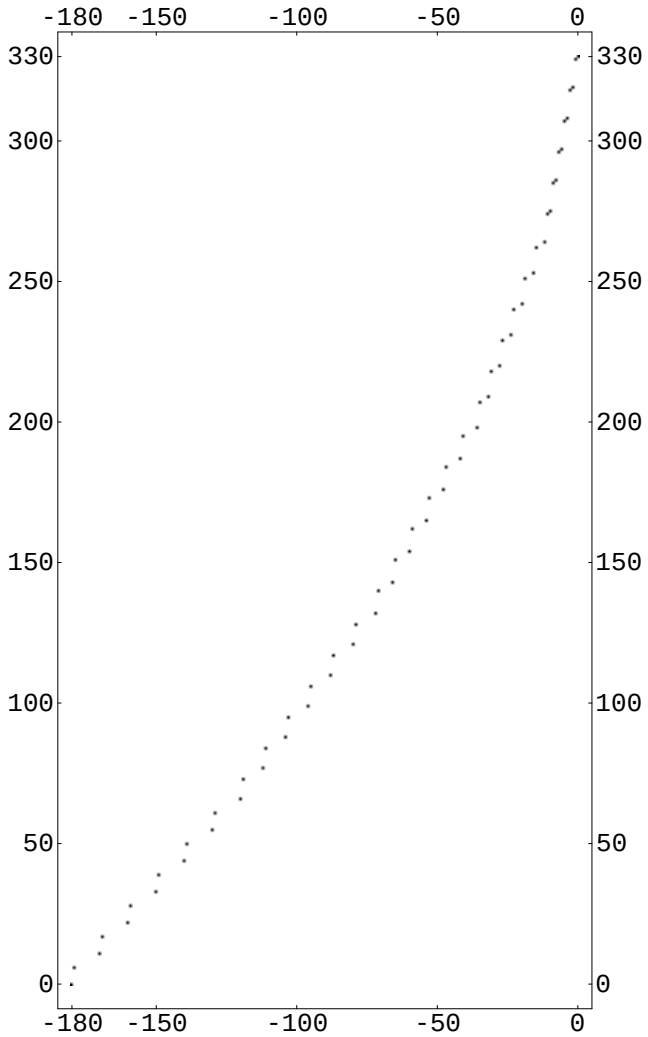

$\mathfrak{d}(0, 10, 0, 66)$

$\mathfrak{D}(6, 55, 54, 6)$

$K(121, 6, 55, 6)$

$x_0 = 67$

$\mathrm{lk}(\mathfrak{b}(22, 1)) = 11$

$K(22, 1; 3, 2)$

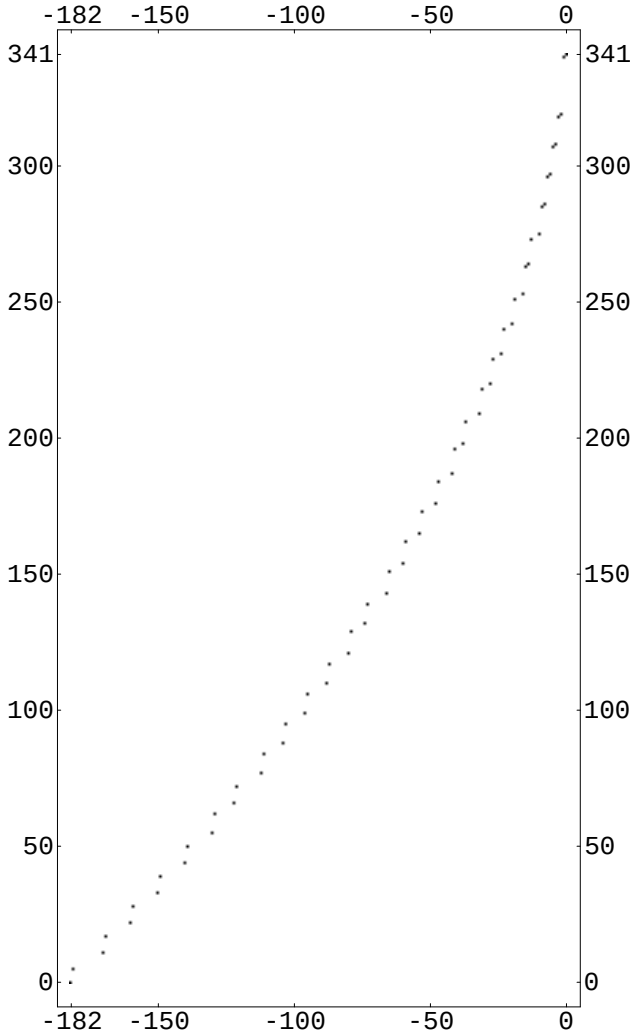

$\mathfrak{d}(0, 10, 11, 33)$

$\mathfrak{D}(3, 88, 27, 65)$

$K(121, 3, 88, 65)$

$x_0 = 35$

$\mathrm{lk}(\mathfrak{b}(22, 1)) = 11$

$K(24, 1; 6, 1)$

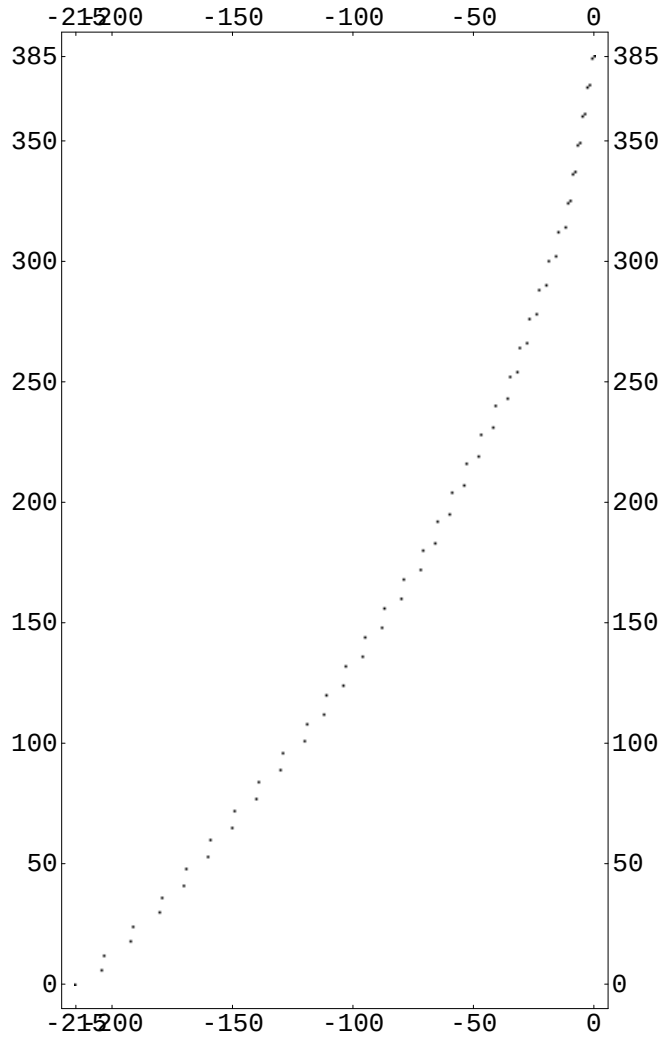

$\mathfrak{d}(0, 11, 0, 72)$

$\mathfrak{D}(6, 60, 59, 6)$

$K(131, 6, 60, 6)$

$x_0 = 72$

$\mathrm{lk}(\mathfrak{b}(24, 1)) = 12$

$K(24, 1; 3, 2)$

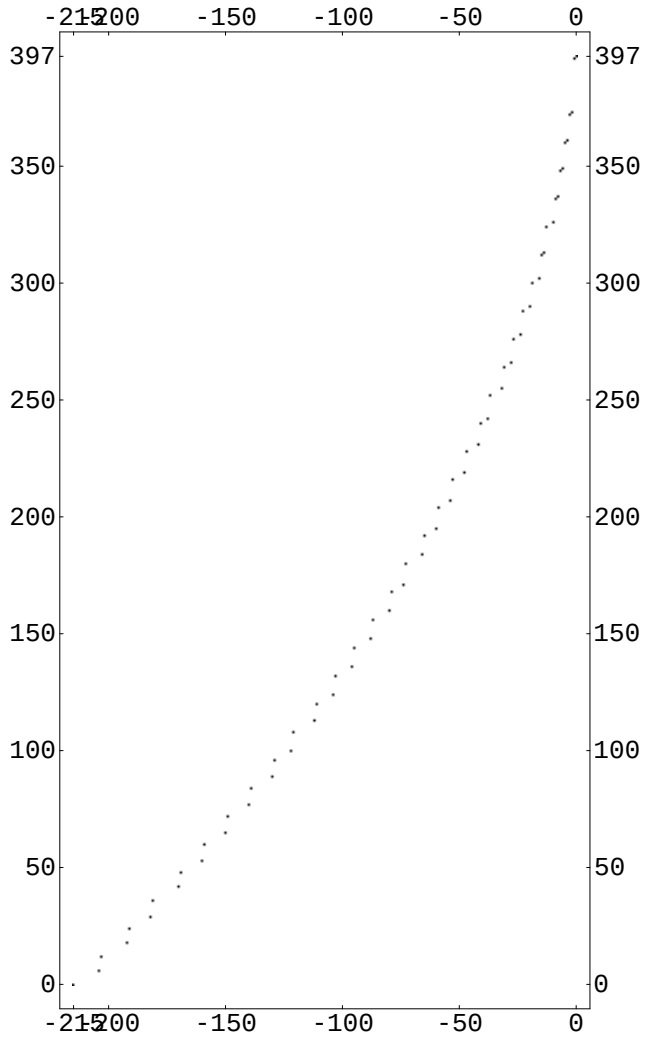

$\mathfrak{d}(0, 11, 12, 36)$

$\mathfrak{D}(3, 30, 95, 67)$

$K(131, 3, 30, 67)$

$x_0 = 100$

$\mathrm{lk}(\mathfrak{b}(24, 1)) = 12$

$K(26, 1; 6, 1)$

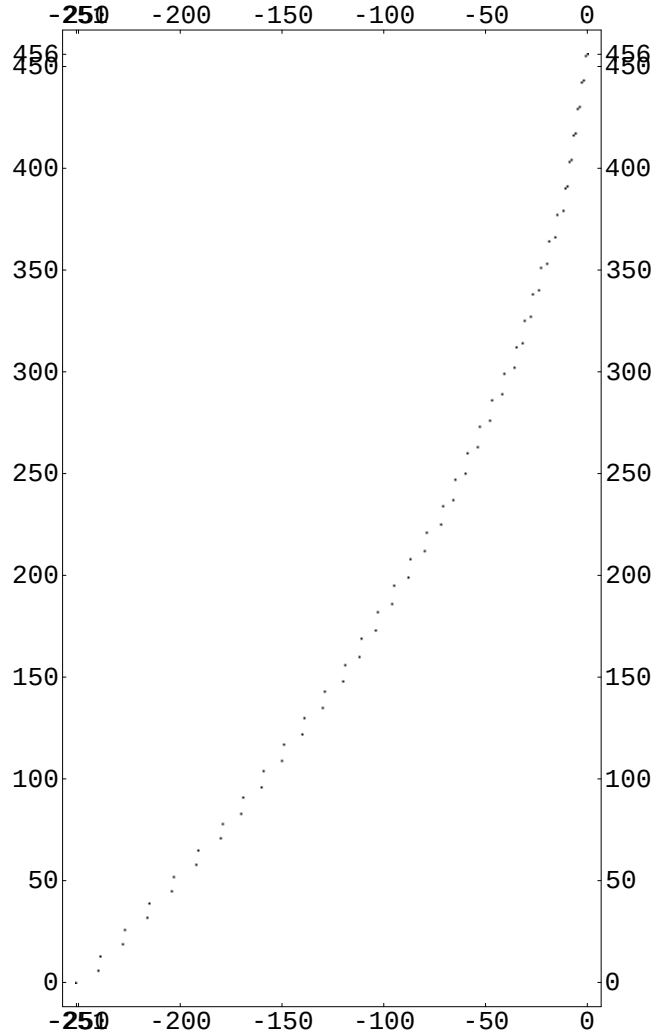

$\mathfrak{d}(0, 12, 0, 78)$

$\mathfrak{D}(6, 66, 65, 6)$

$K(143, 6, 66, 6)$

$x_0 = 78$

$\mathrm{lk}(\mathfrak{b}(26, 1)) = 13$

$K(26, 1; 3, 2)$

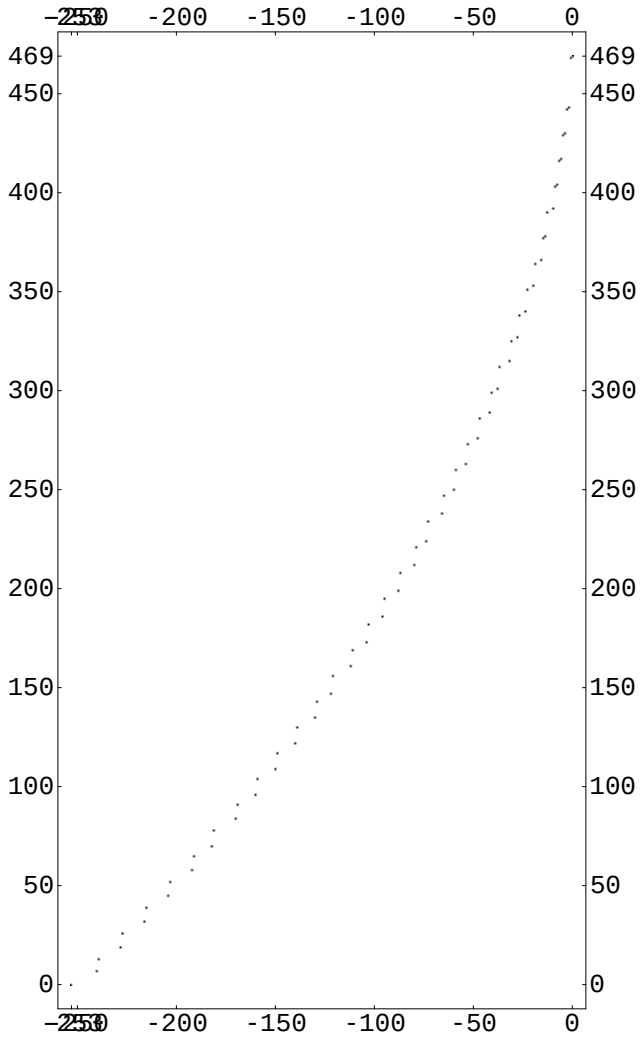

$\mathfrak{d}(0, 12, 13, 39)$

$\mathfrak{D}(3, 33, 104, 73)$

$K(143, 3, 33, 73)$

$x_0 = 109$

$\mathrm{lk}(\mathfrak{b}(26, 1)) = 13$

$K(28, 1; 6, 1)$

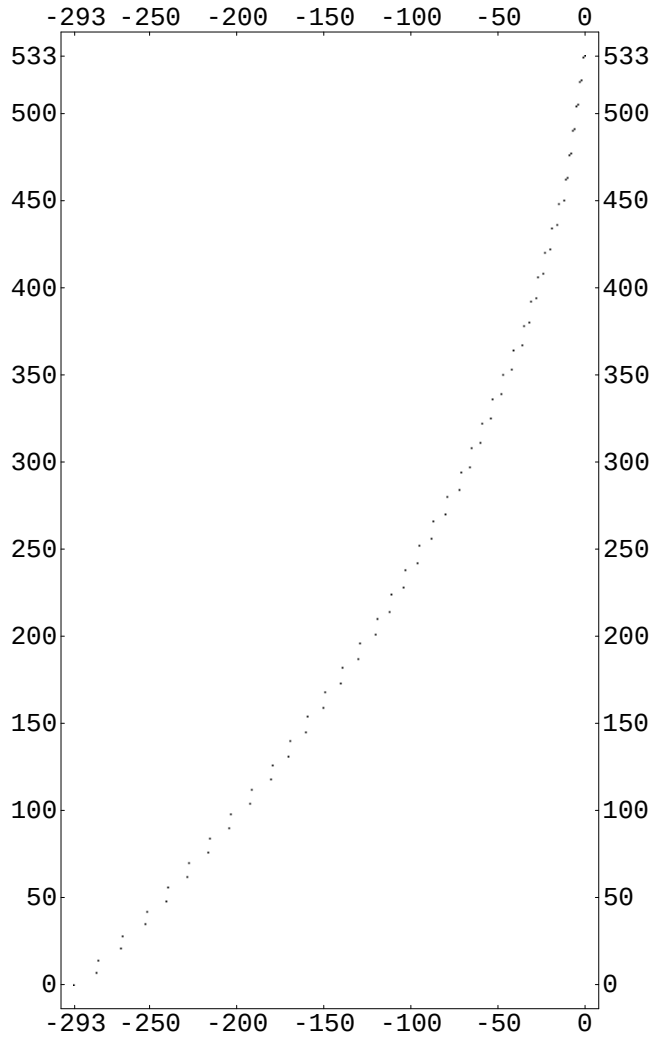

$\mathfrak{d}(0, 13, 0, 84)$

$\mathfrak{D}(6, 72, 71, 6)$

$K(155, 6, 72, 6)$

$x_0 = 84$

$\mathrm{lk}(\mathfrak{b}(28, 1)) = 14$

$K(28, 1; 3, 2)$

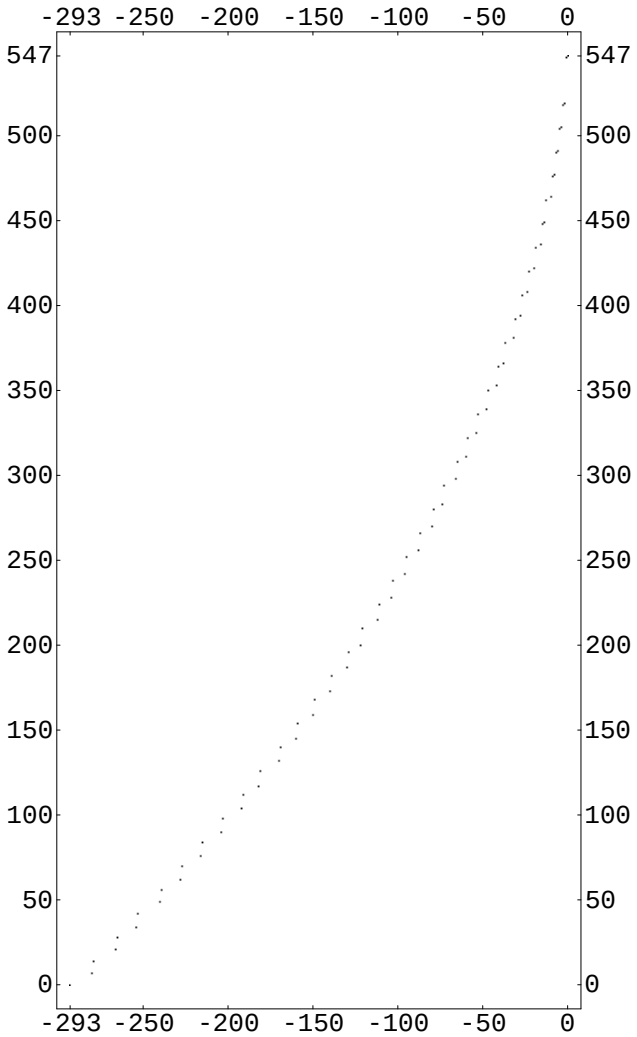

$\mathfrak{d}(0, 13, 14, 42)$

$\mathfrak{D}(3, 36, 113, 79)$

$K(155, 3, 36, 79)$

$x_0 = 118$

$\mathrm{lk}(\mathfrak{b}(28, 1)) = 14$

$K(30, 1; 6, 1)$

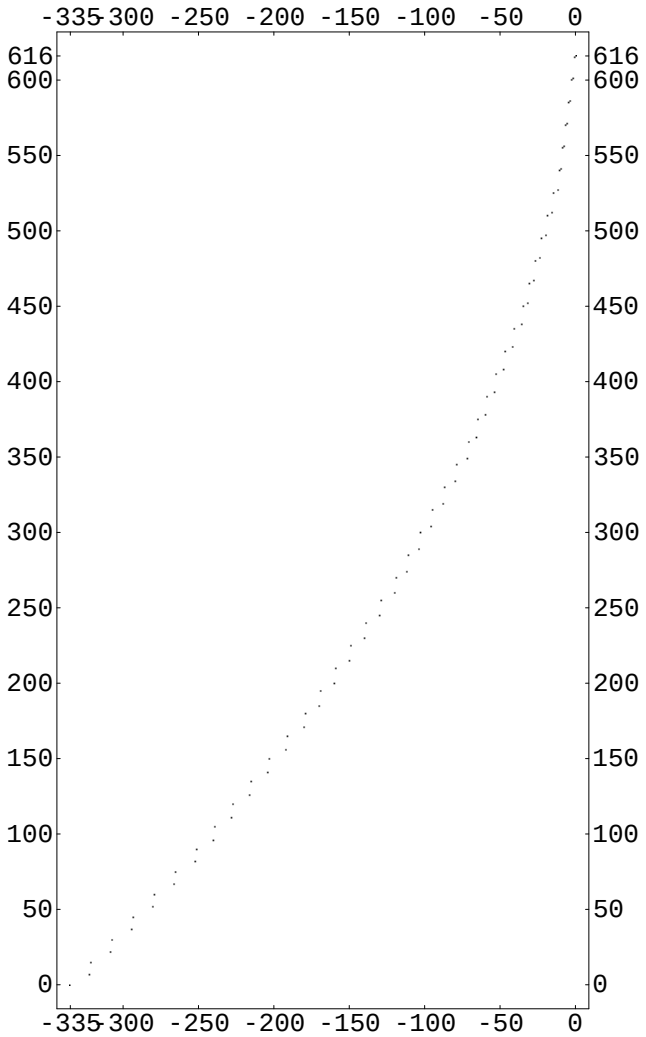

$\mathfrak{d}(0, 14, 0, 90)$

$\mathfrak{D}(6, 78, 77, 6)$

$K(167, 6, 78, 6)$

$x_0 = 90$

$\mathrm{lk}(\mathfrak{b}(30, 1)) = 15$

$K(30, 1; 3, 2)$

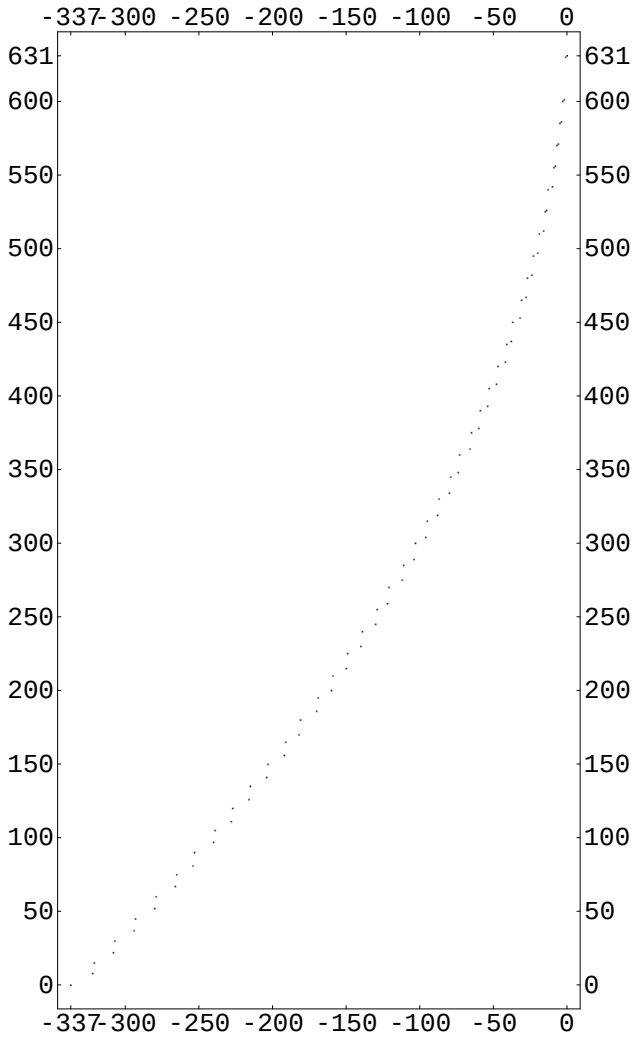

$\mathfrak{d}(0, 14, 15, 45)$

$\mathfrak{D}(3, 39, 122, 85)$

$K(167, 3, 39, 85)$

$x_0 = 127$

$\mathrm{lk}(\mathfrak{b}(30, 1)) = 15$

$K(8,3;6,1)$

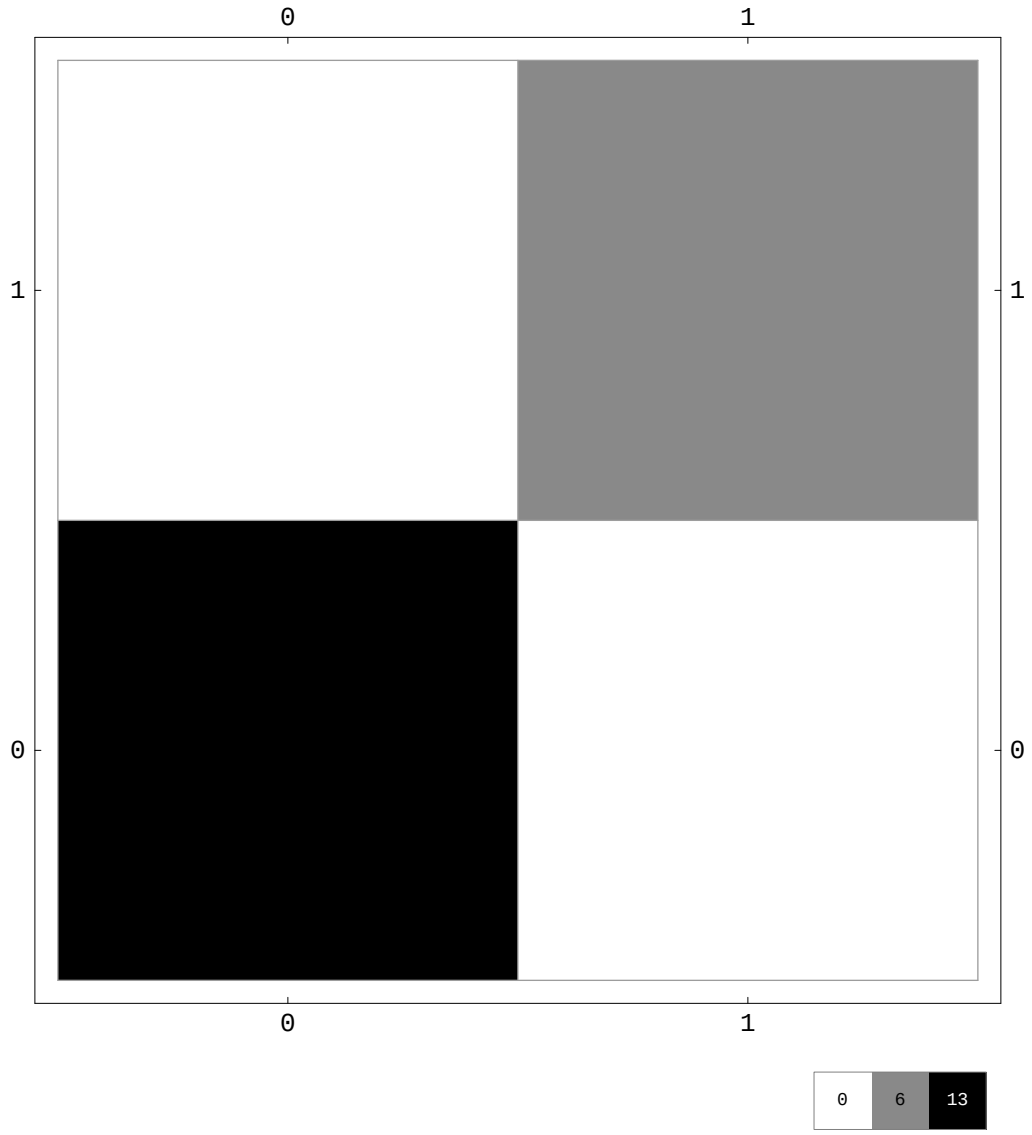

$\mathfrak{d}(1,1,0,24)$

$\mathfrak{D}(12,1,0,18)$

$K(25,12,1,18)$

$x_0 = 19$

$\mathrm{lk}(\mathfrak{b}(8,3)) = 0$

$K(8,3;3,2)$

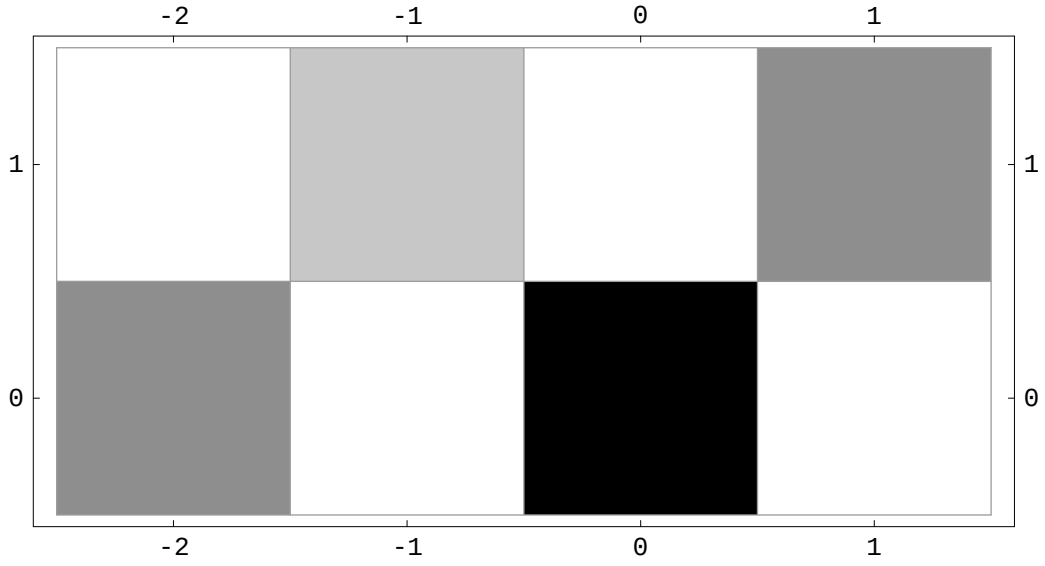

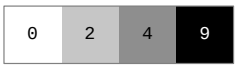

$\mathfrak{d}(1,1,4,12)$

$\mathfrak{D}(6,13,0,23)$

$K(25,6,13,23)$

$x_0 = 11$

$\mathrm{lk}(\mathfrak{b}(8,3)) = 0$

$K(10,3;6,1)$

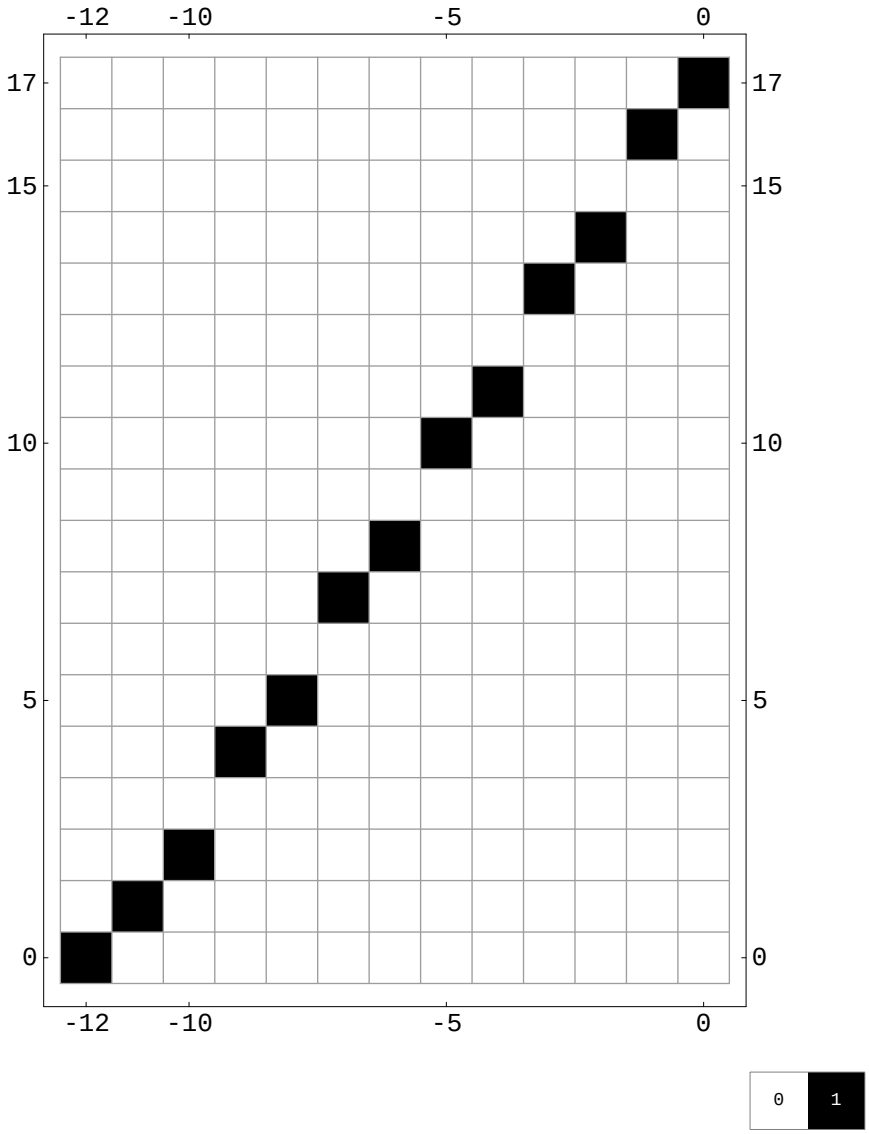

$\mathfrak{d}(1,2,0,30)$

$\mathfrak{D}(7,6,5,7)$

$K(25,7,6,7)$

$x_0 = 20$

$\mathrm{lk}(\mathfrak{b}(10,3)) = 3$

$K(10,3;3,2)$

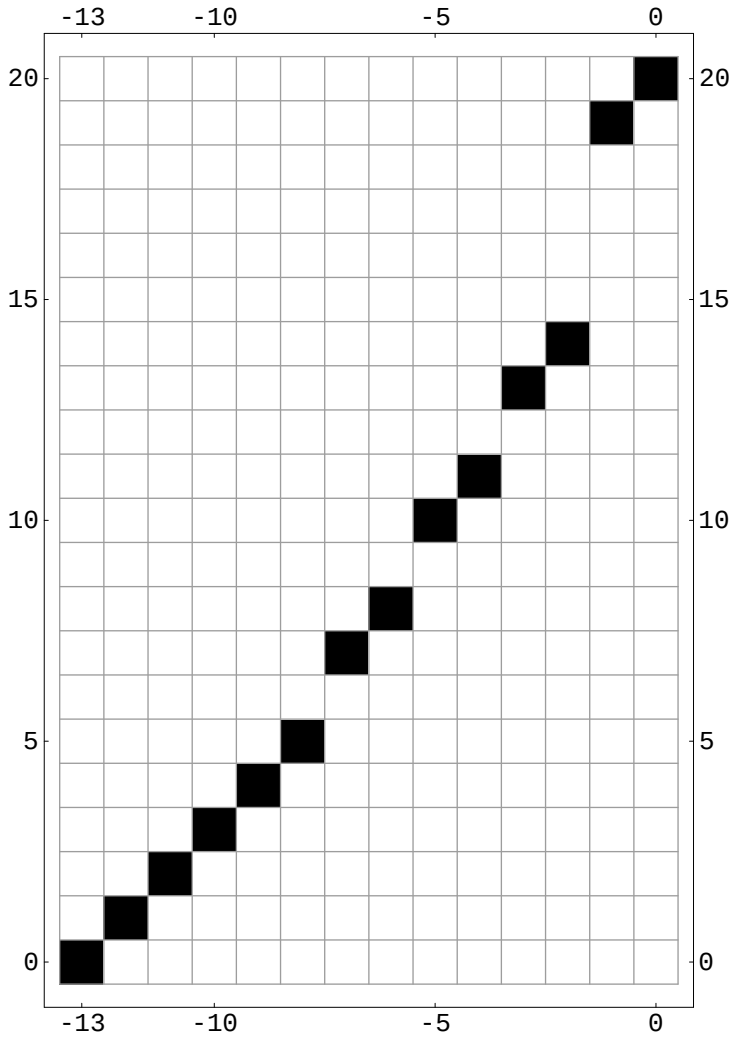

$\mathfrak{d}(1,2,5,15)$

$\mathfrak{D}(5,12,5,23)$

$K(27,5,12,23)$

$x_0 = 13$

$\mathrm{lk}(\mathfrak{b}(10,3)) = 3$

$K(14,3;6,1)$

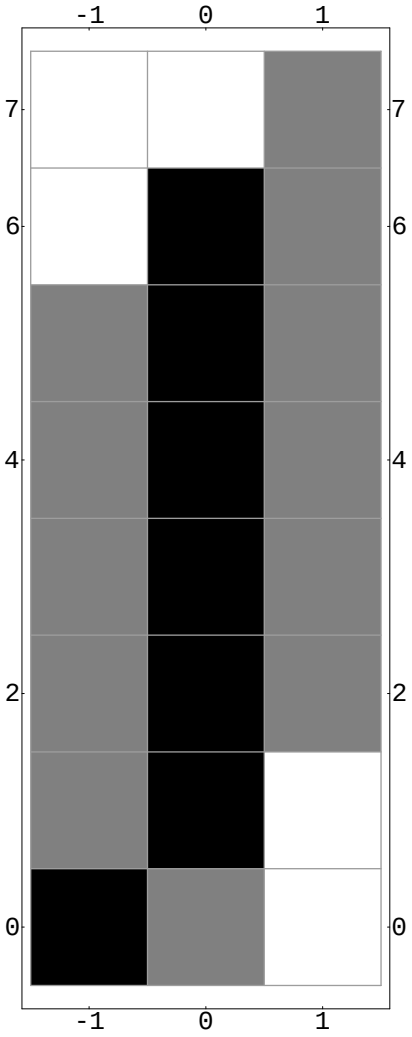

$\mathfrak{d}(1,4,0,42)$

$\mathfrak{D}(12,7,18,18)$

$K(49,12,7,18)$

$x_0 = 25$

$\mathrm{lk}(\mathfrak{b}(14,3)) = 1$

$K(14, 3; 3, 2)$

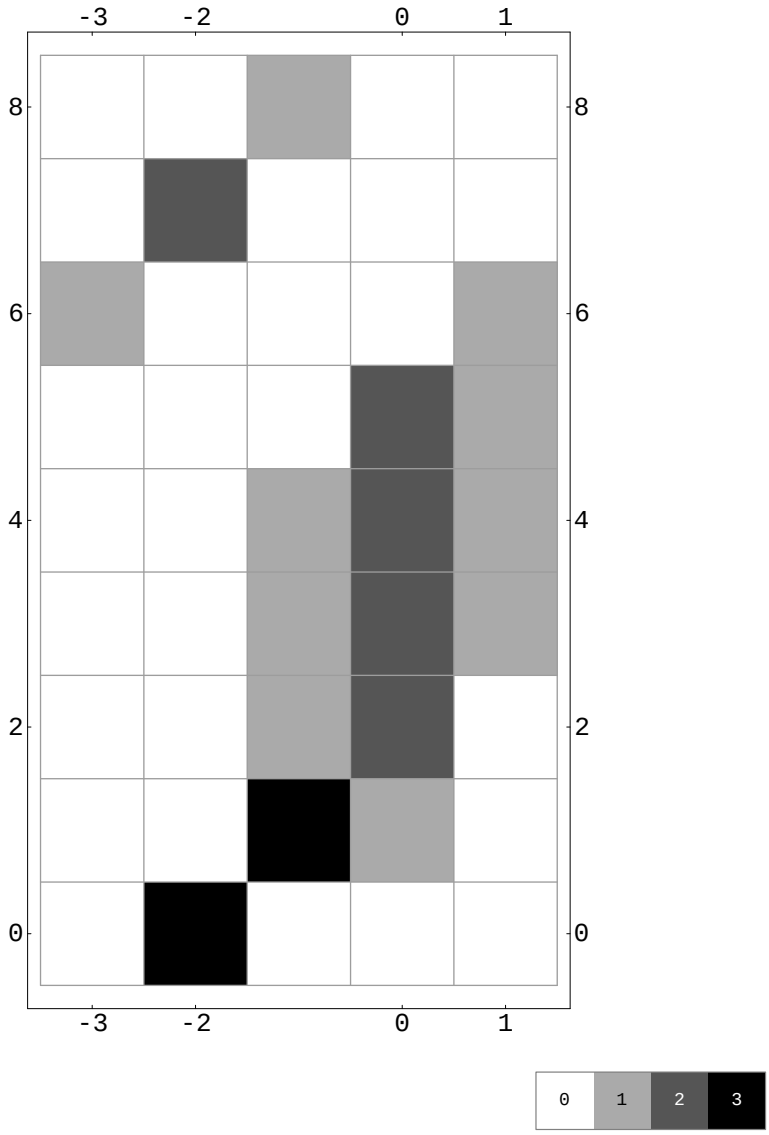

$\mathfrak{d}(1, 4, 7, 21)$

$\mathfrak{D}(6, 28, 9, 35)$

$K(49, 6, 28, 35)$

$x_0 = 14$

$\mathrm{lk}(\mathfrak{b}(14, 3)) = 1$

$K(16,3;6,1)$

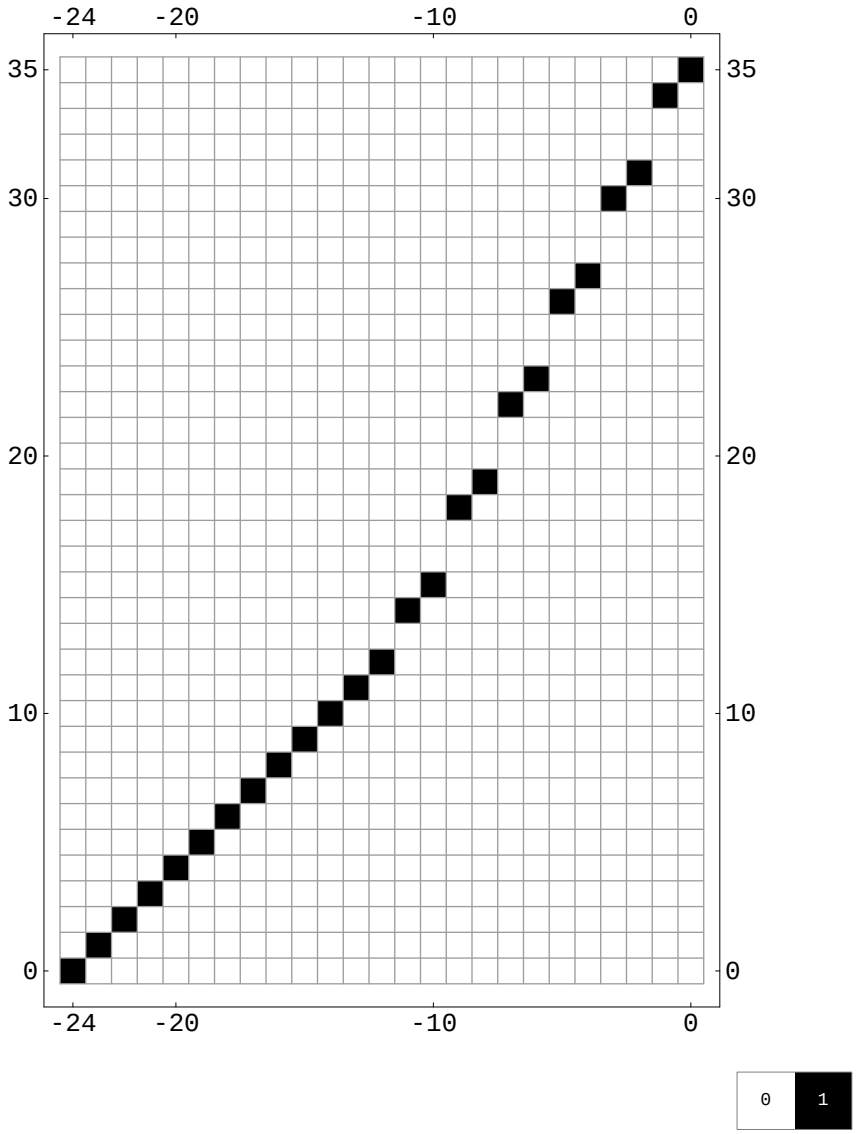

$\mathfrak{d}(1,5,0,48)$

$\mathfrak{D}(12,1,24,18)$

$K(49,12,1,18)$

$x_0 = 31$

$\mathrm{lk}(\mathfrak{b}(16,3)) = 4$

$K(16,3;3,2)$

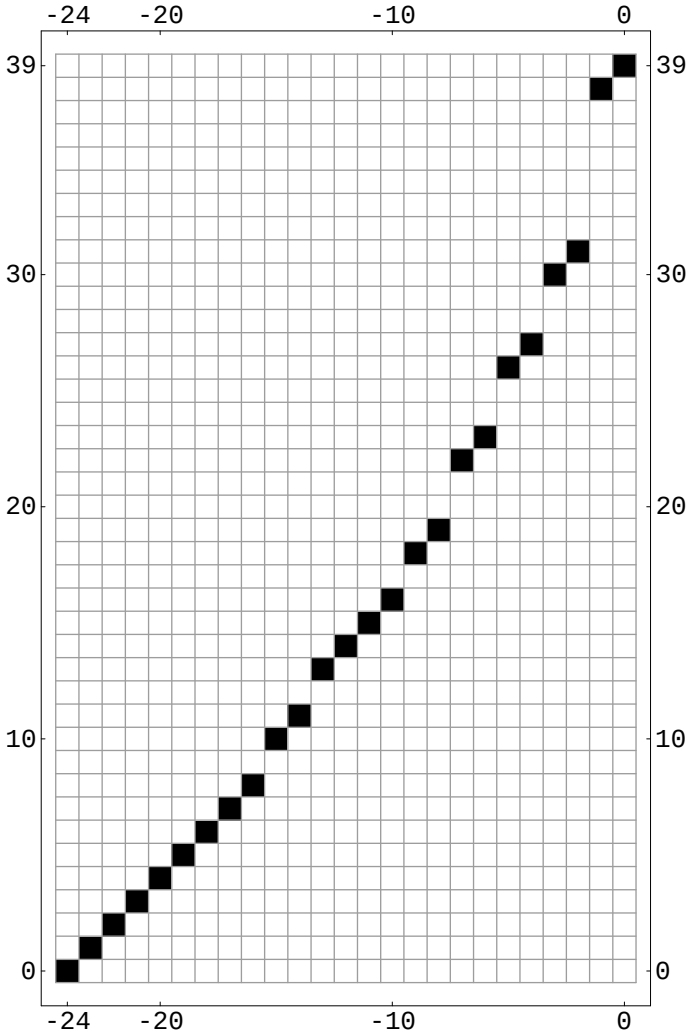

$\mathfrak{d}(1,5,8,24)$

$\mathfrak{D}(6,25,12,35)$

$K(49,6,25,35)$

$x_0 = 17$

$\mathrm{lk}(\mathfrak{b}(16,3)) = 4$

$K(20,3;6,1)$

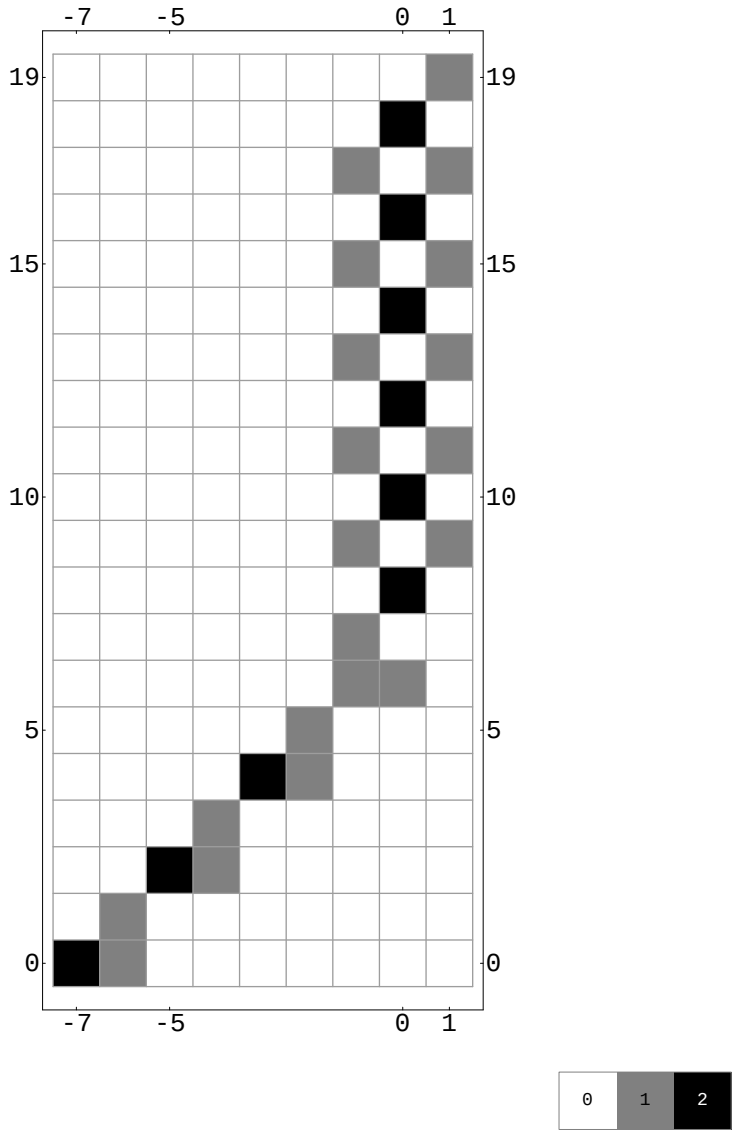

$\mathfrak{d}(1,7,0,60)$

$\mathfrak{D}(12,13,36,18)$

$K(73,12,13,18)$

$x_0 = 31$

$\mathrm{lk}(\mathfrak{b}(20,3)) = 2$

$K(20,3;3,2)$

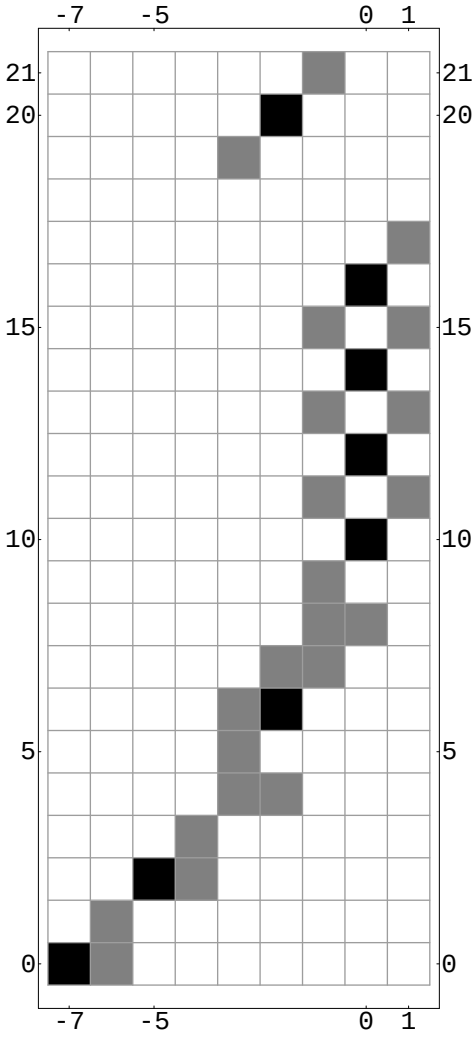

$\mathfrak{d}(1,7,10,30)$

$\mathfrak{D}(6,43,18,47)$

$K(73,6,43,47)$

$x_0 = 17$

$\mathrm{lk}(\mathfrak{b}(20,3)) = 2$

$K(22, 3; 6, 1)$

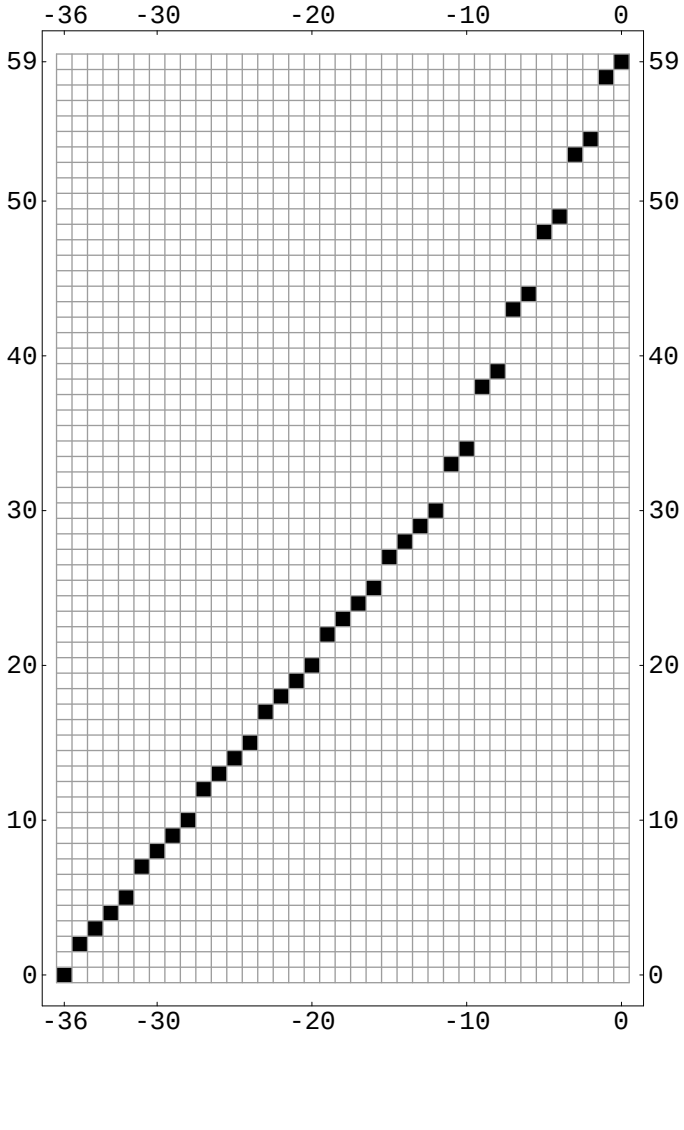

$\mathfrak{d}(1, 8, 0, 66)$

$\mathfrak{D}(12, 7, 42, 18)$

$K(73, 12, 7, 18)$

$x_0 = 37$

$\mathrm{lk}(\mathfrak{b}(22, 3)) = 5$

$K(22, 3; 3, 2)$

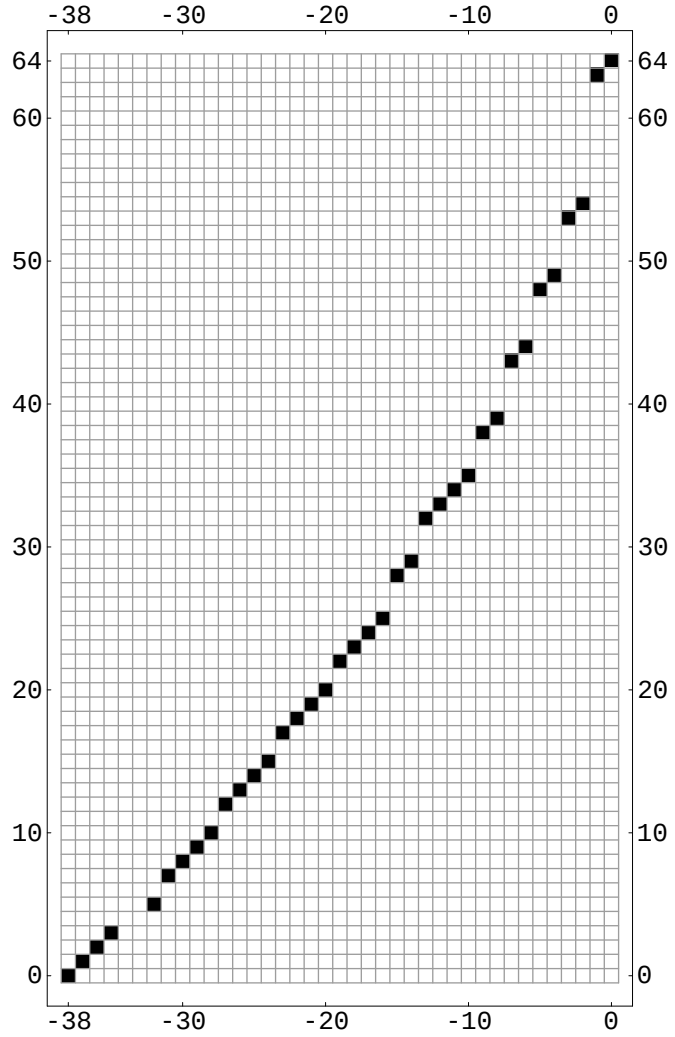

$\mathfrak{d}(1, 8, 11, 33)$

$\mathfrak{D}(6, 40, 21, 47)$

$K(73, 6, 40, 47)$

$x_0 = 20$

$\mathrm{lk}(\mathfrak{b}(22, 3)) = 5$

$K(26,3;6,1)$

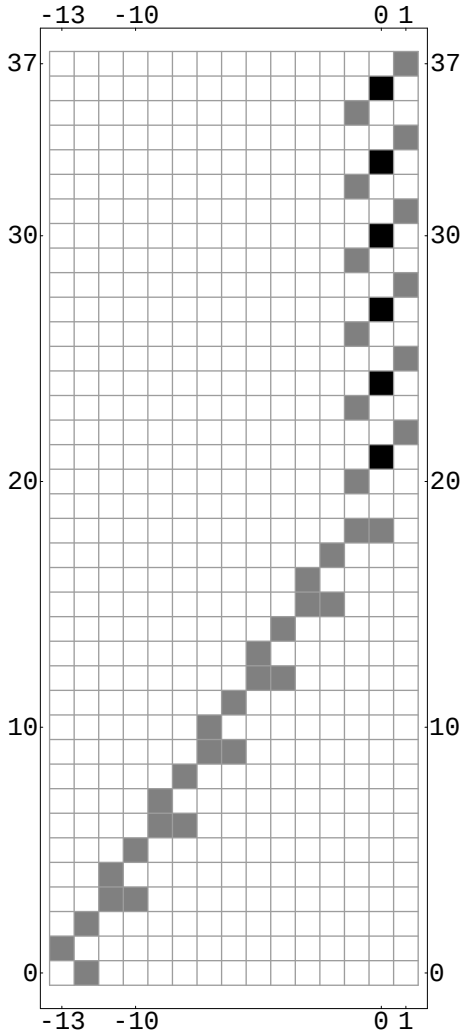

$\mathfrak{d}(1,10,0,78)$

$\mathfrak{D}(12,19,54,18)$

$K(97,12,19,18)$

$x_0 = 37$

$\mathrm{lk}(\mathfrak{b}(26,3)) = 3$

$K(26, 3; 3, 2)$

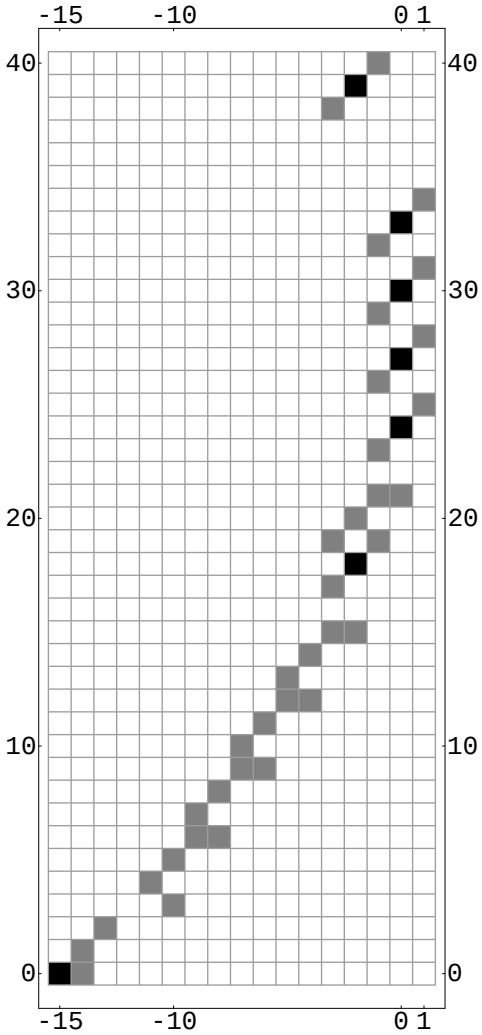

$\mathfrak{d}(1, 10, 13, 39)$

$\mathfrak{D}(6, 58, 27, 59)$

$K(97, 6, 58, 59)$

$x_0 = 20$

$\mathrm{lk}(\mathfrak{b}(26, 3)) = 3$

$K(28, 3; 6, 1)$

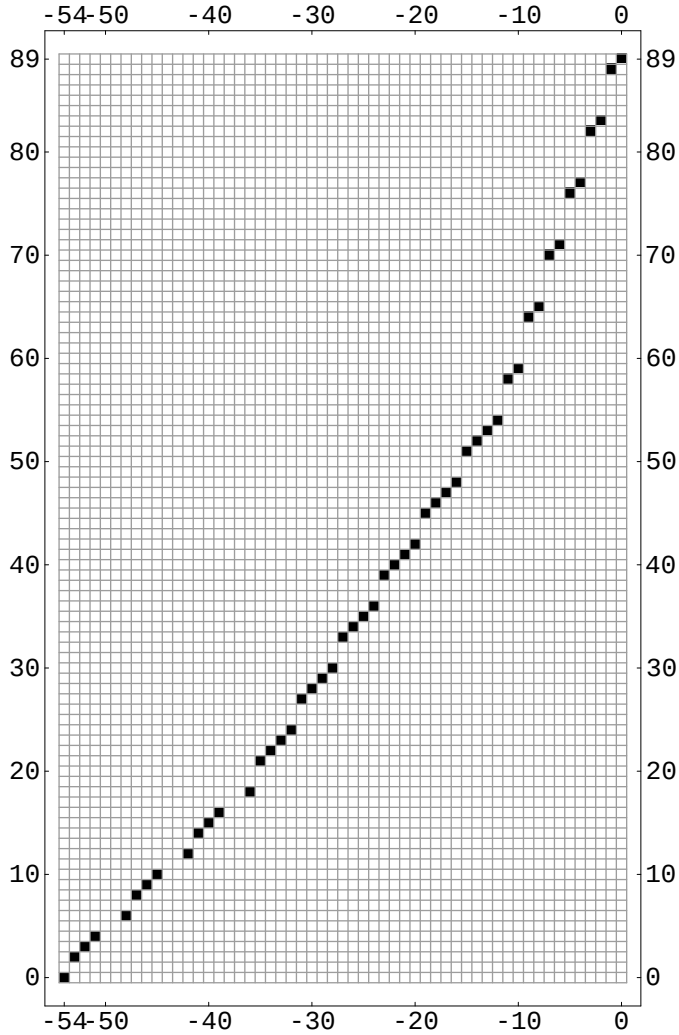

$\mathfrak{d}(1, 11, 0, 84)$

$\mathfrak{D}(12, 13, 60, 18)$

$K(97, 12, 13, 18)$

$x_0 = 43$

$\mathrm{lk}(\mathfrak{b}(28, 3)) = 6$

$K(28,3;3,2)$

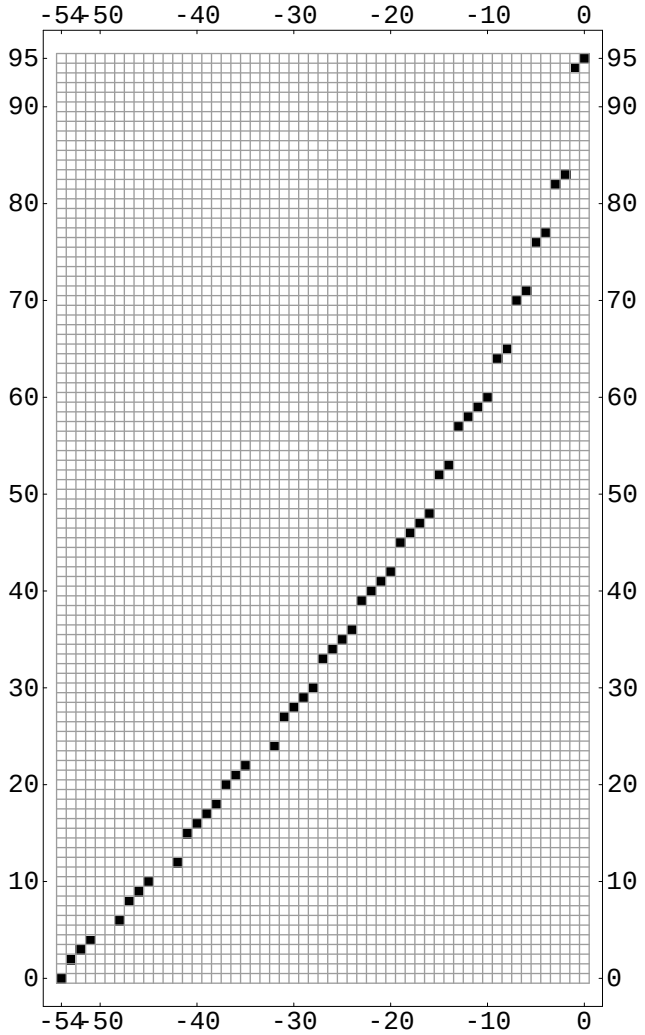

$\mathfrak{d}(1,11,14,42)$

$\mathfrak{D}(6,55,30,59)$

$K(97,6,55,59)$

$x_0 = 23$

$\mathrm{lk}(\mathfrak{b}(28,3)) = 6$

$K(12,5;6,1)$

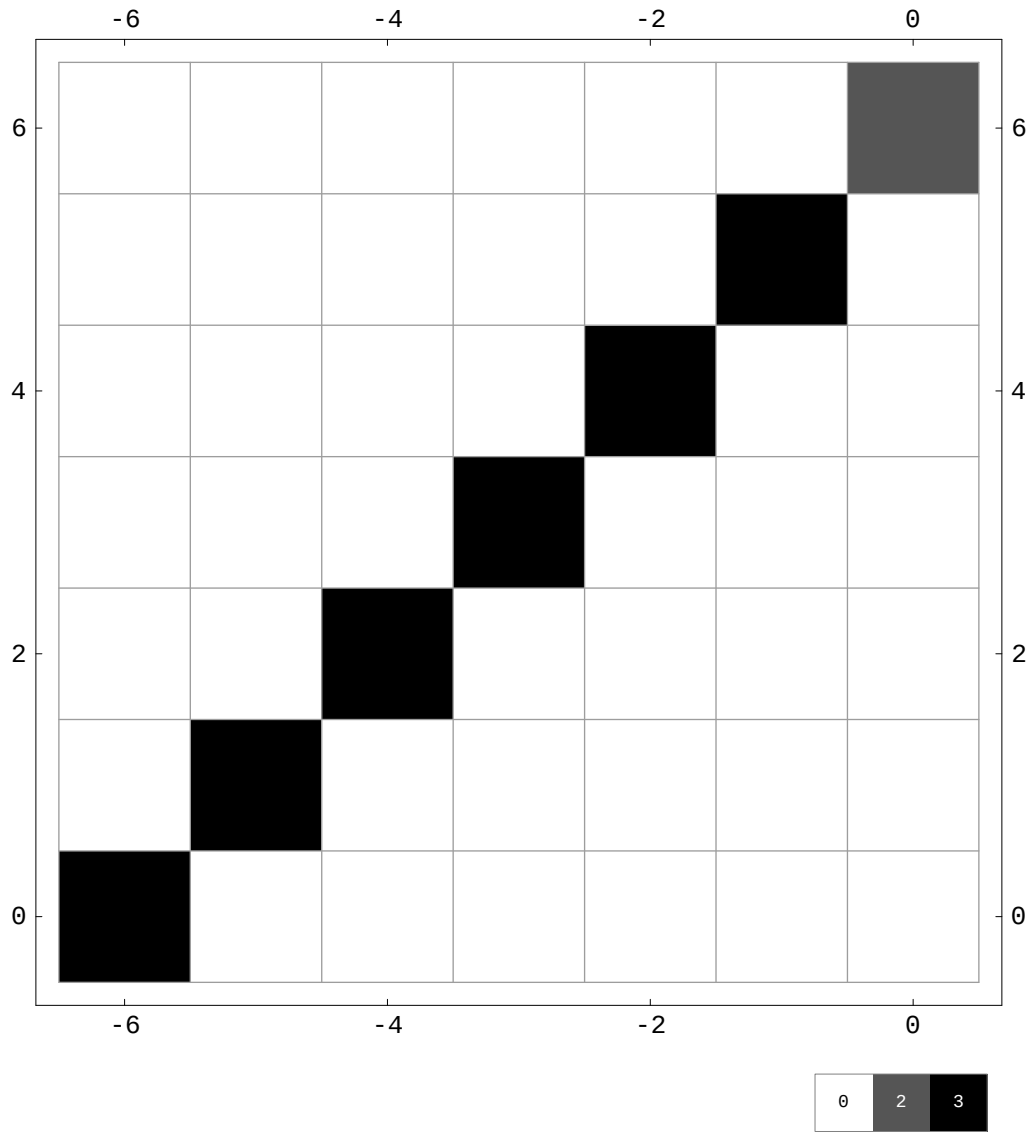

$\mathfrak{d}(2,1,0,36)$

$\mathfrak{D}(18,1,0,30)$

$K(37,18,1,30)$

$x_0 = 37$

$\mathrm{lk}(\mathfrak{b}(12,5)) = 2$

$K(12,5;3,2)$

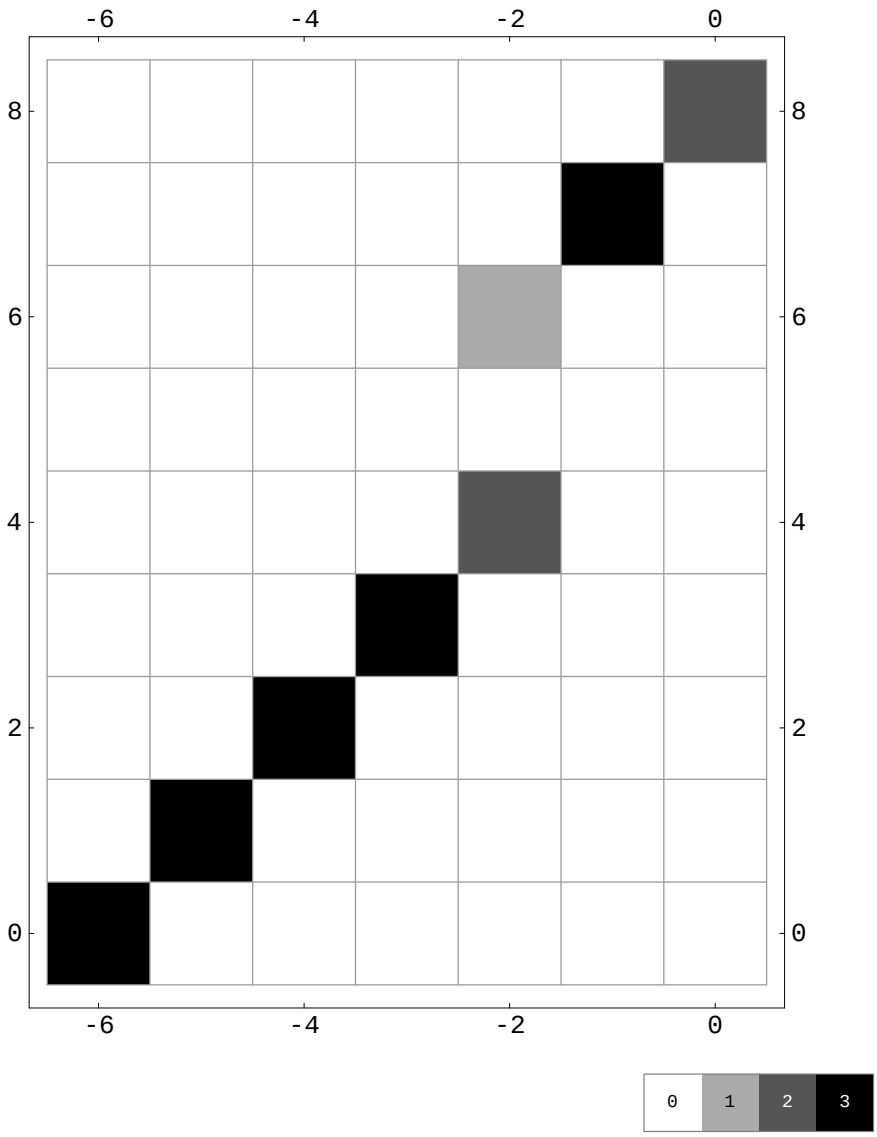

$\mathfrak{d}(2,1,6,18)$

$\mathfrak{D}(9,19,0,35)$

$K(37,9,19,35)$

$x_0 = 20$

$\mathrm{lk}(\mathfrak{b}(12,5)) = 2$

$K(16, 5; 6, 1)$

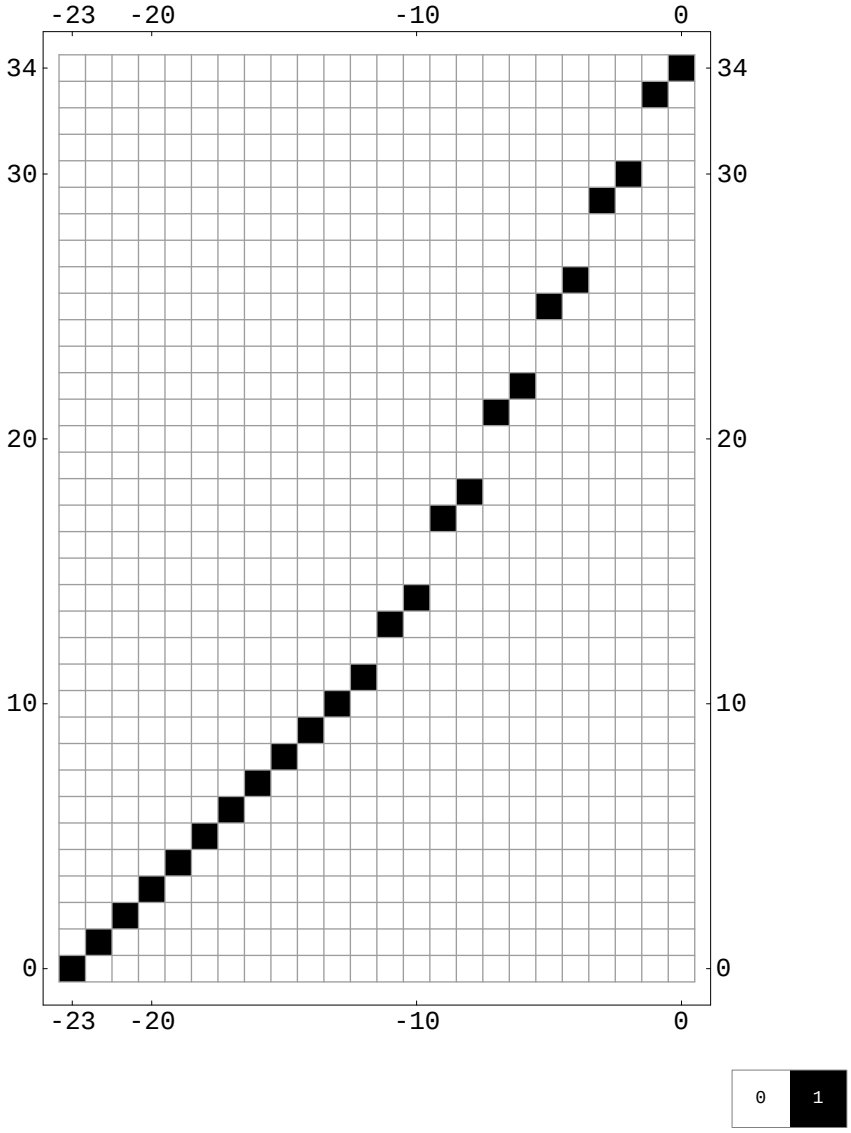

$\mathfrak{d}(2, 3, 0, 48)$

$\mathfrak{D}(12, 22, 1, 7)$

$K(47, 12, 22, 7)$

$x_0 = 41$

$\mathrm{lk}(\mathfrak{b}(16, 5)) = 4$

$K(16,5;3,2)$

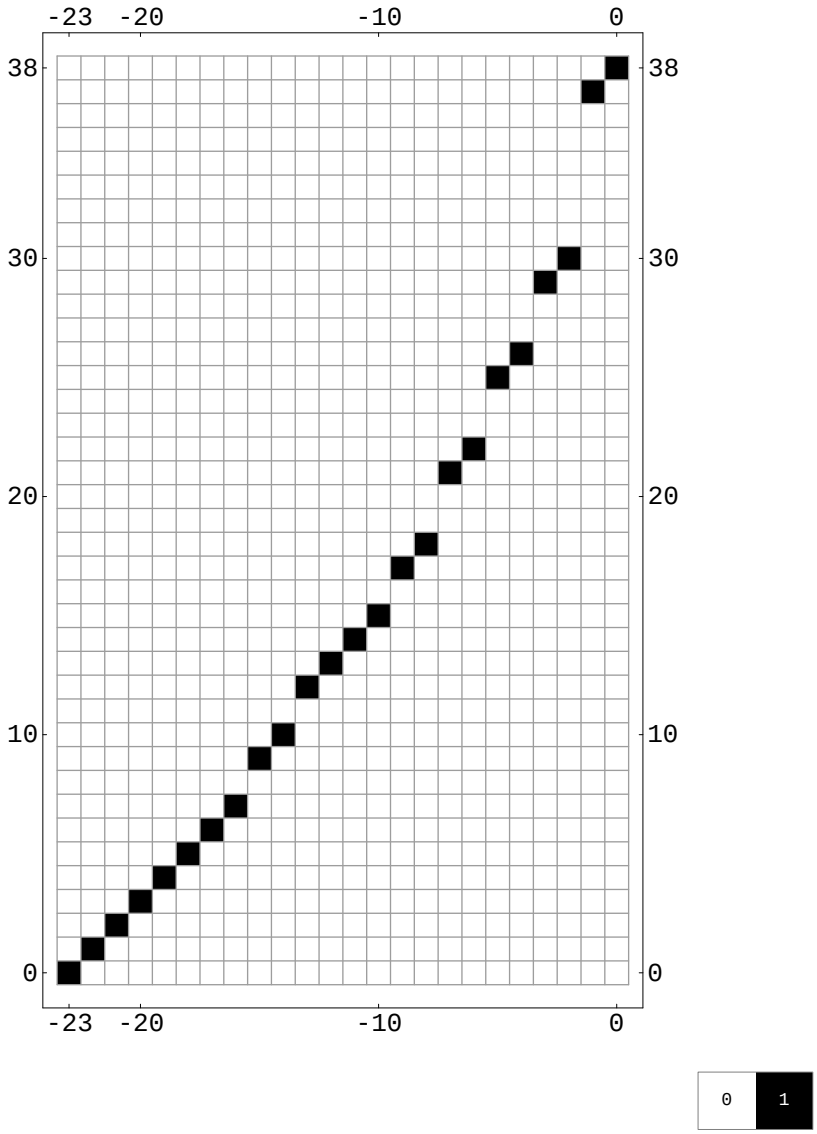

$\mathfrak{d}(2,3,8,24)$

$\mathfrak{D}(6,23,12,37)$

$K(47,6,23,37)$

$x_0 = 19$

$\mathrm{lk}(\mathfrak{b}(16,5)) = 4$

$K(18, 5; 6, 1)$

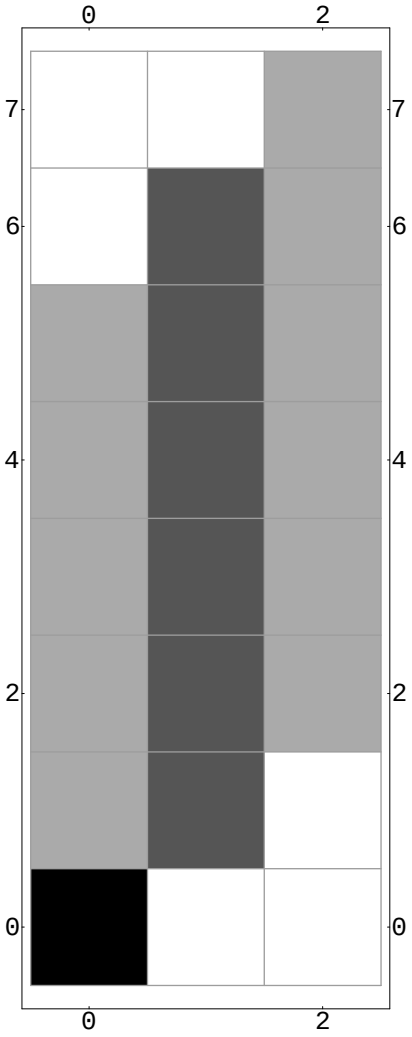

$\mathfrak{d}(2, 4, 0, 54)$

$\mathfrak{D}(13, 18, 5, 7)$

$K(49, 13, 18, 7)$

$x_0 = 26$

$\mathrm{lk}(\mathfrak{b}(18, 5)) = 1$

$K(18, 5; 3, 2)$

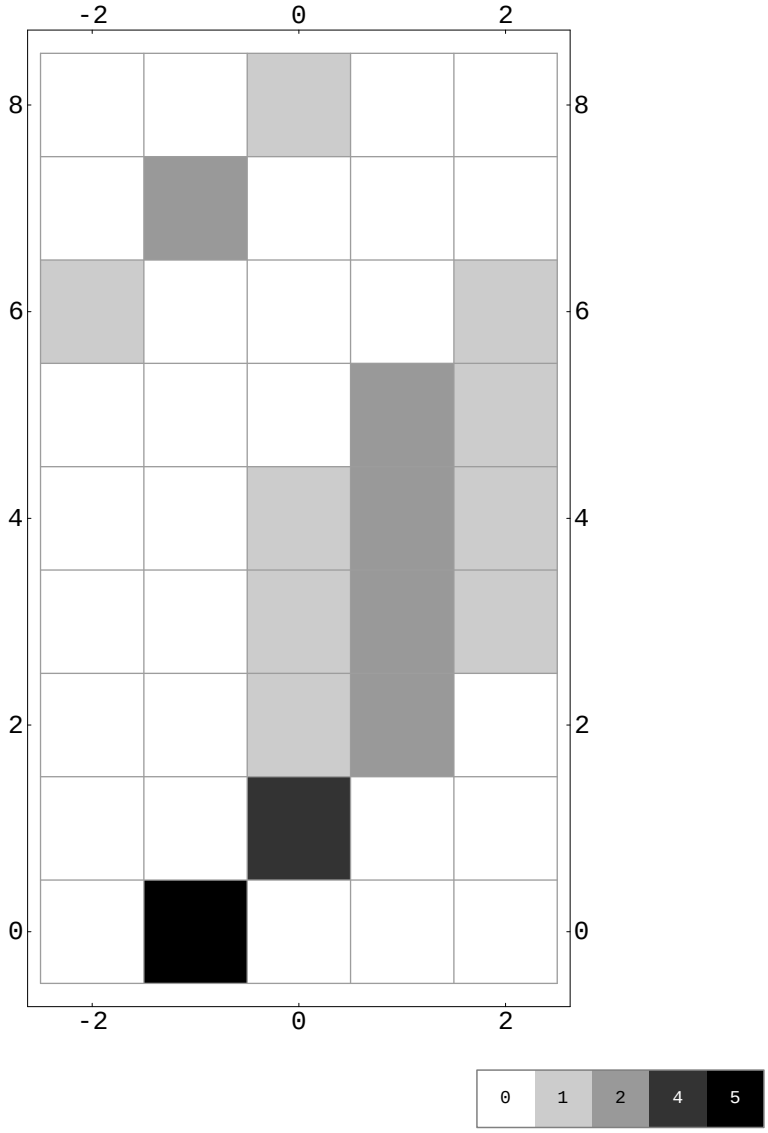

$\mathfrak{d}(2, 4, 9, 27)$

$\mathfrak{D}(8, 24, 11, 41)$

$K(51, 8, 24, 41)$

$x_0 = 16$

$\mathrm{lk}(\mathfrak{b}(18, 5)) = 1$

$K(22, 5; 6, 1)$

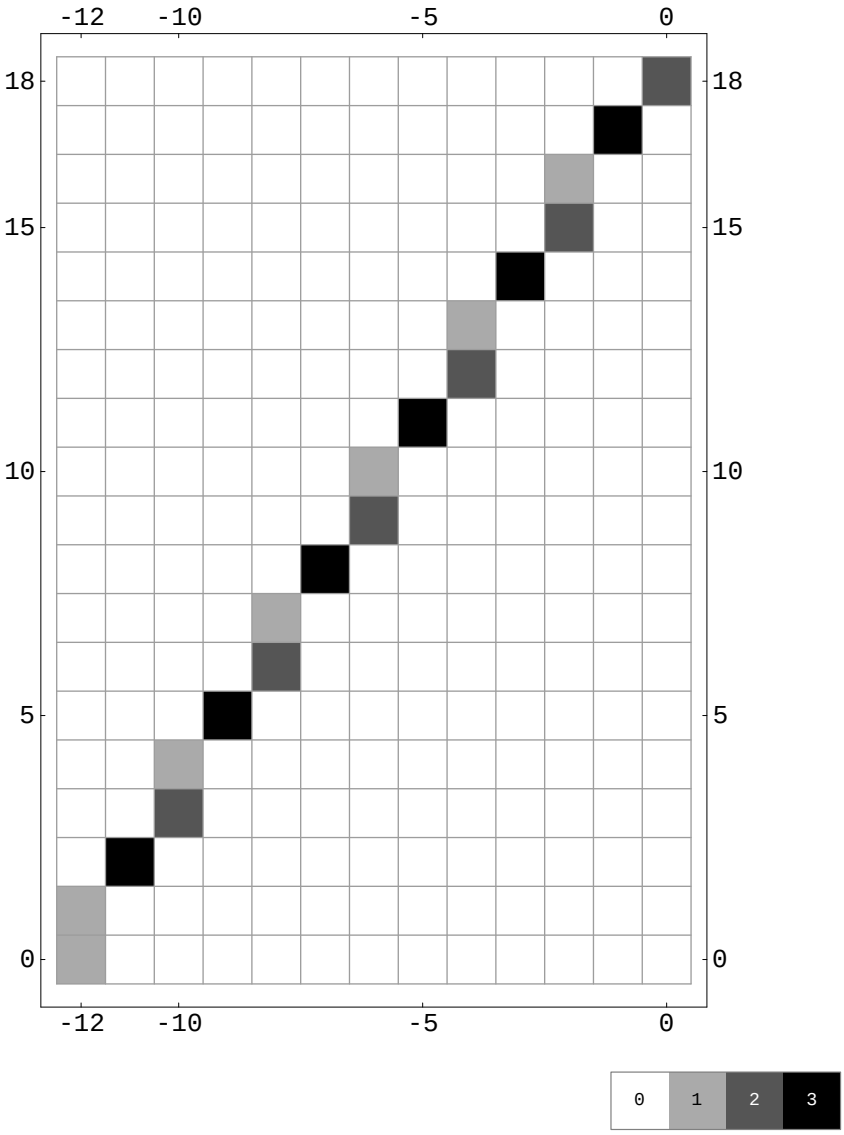

$\mathfrak{d}(2, 6, 0, 66)$

$\mathfrak{D}(18, 7, 30, 30)$

$K(73, 18, 7, 30)$

$x_0 = 43$

$\mathrm{lk}(\mathfrak{b}(22, 5)) = 3$

$K(22, 5; 3, 2)$

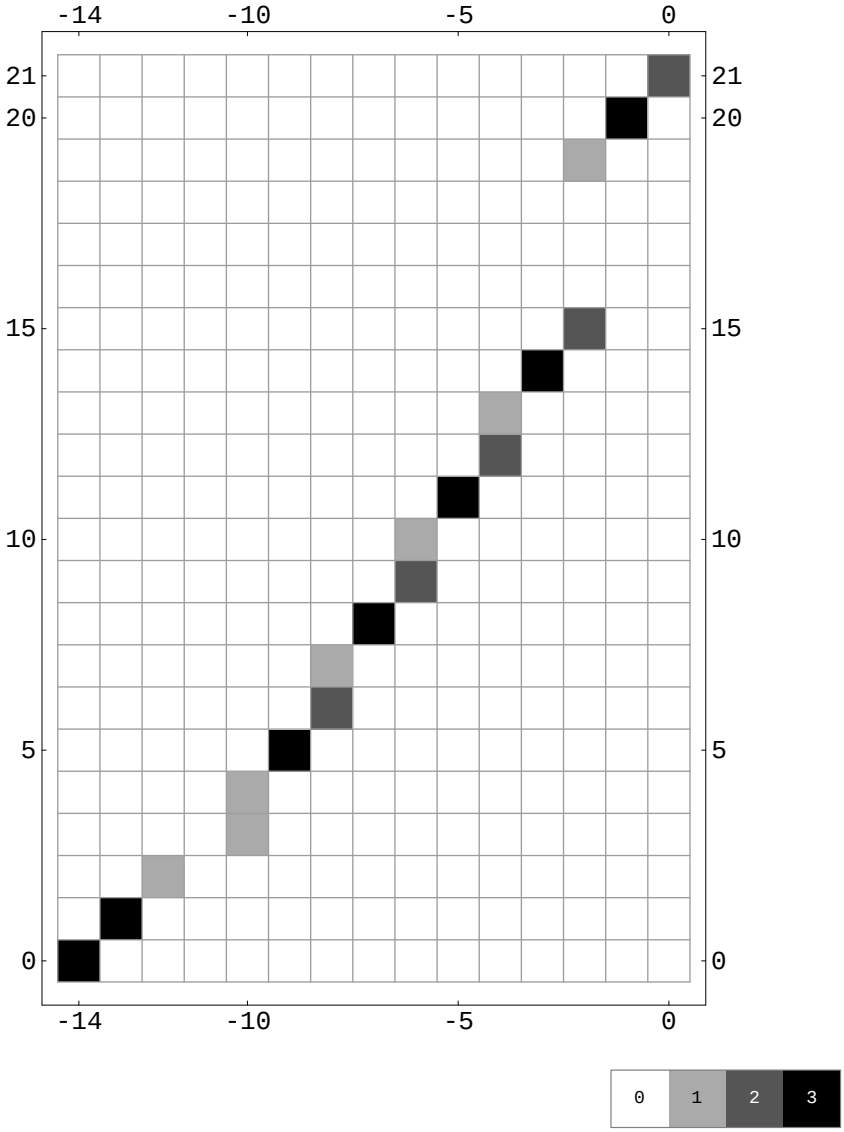

$\mathfrak{d}(2, 6, 11, 33)$

$\mathfrak{D}(9, 40, 15, 53)$

$K(73, 9, 40, 53)$

$x_0 = 23$

$\mathrm{lk}(\mathfrak{b}(22, 5)) = 3$

$K(24, 5; 6, 1)$

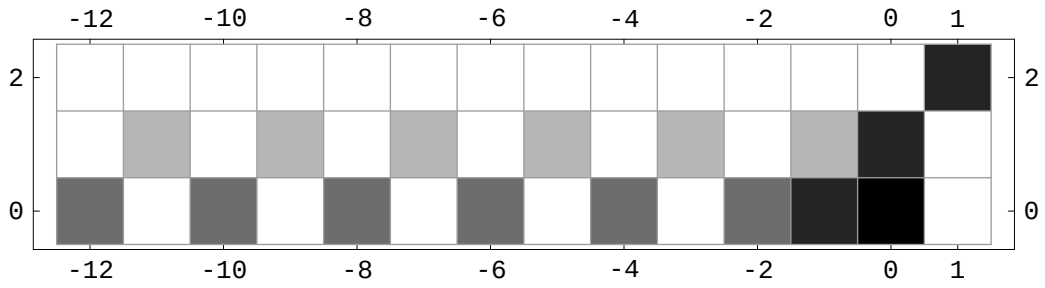

$\mathfrak{d}(2, 7, 0, 72)$

$\mathfrak{D}(18, 13, 36, 30)$

$K(85, 18, 13, 30)$

$x_0 = 37$

$\mathrm{lk}(\mathfrak{b}(24, 5)) = 0$

$K(24, 5; 3, 2)$

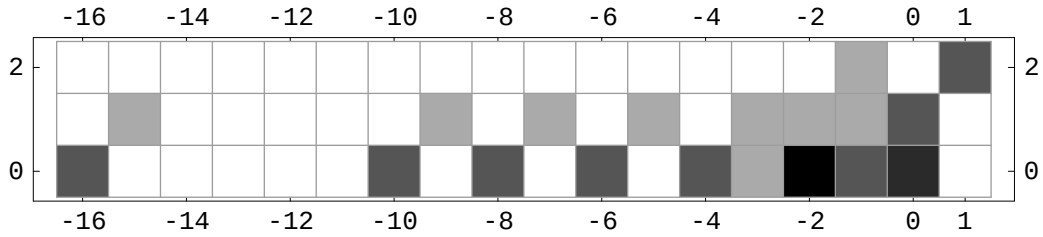

$\mathfrak{d}(2, 7, 12, 36)$

$\mathfrak{D}(9, 49, 18, 59)$

$K(85, 9, 49, 59)$

$x_0 = 20$

$\mathrm{lk}(\mathfrak{b}(24, 5)) = 0$

$K(26, 5; 6, 1)$

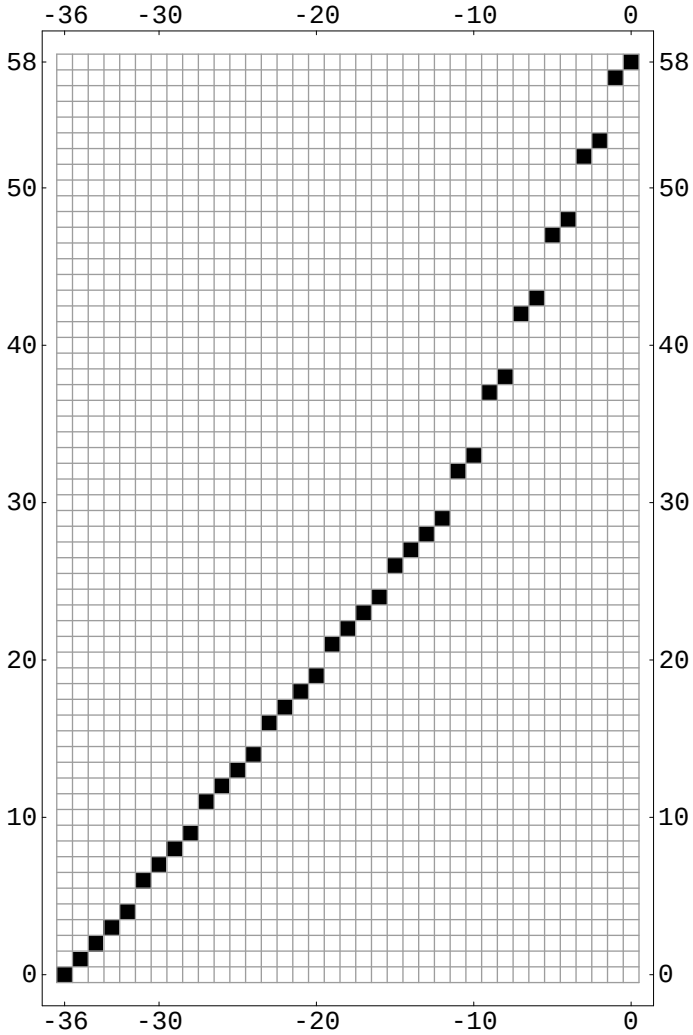

$\mathfrak{d}(2, 8, 0, 78)$

$\mathfrak{D}(13, 42, 5, 56)$

$K(73, 13, 42, 56)$

$x_0 = 38$

$\mathrm{lk}(\mathfrak{b}(26, 5)) = 5$

$K(26, 5; 3, 2)$

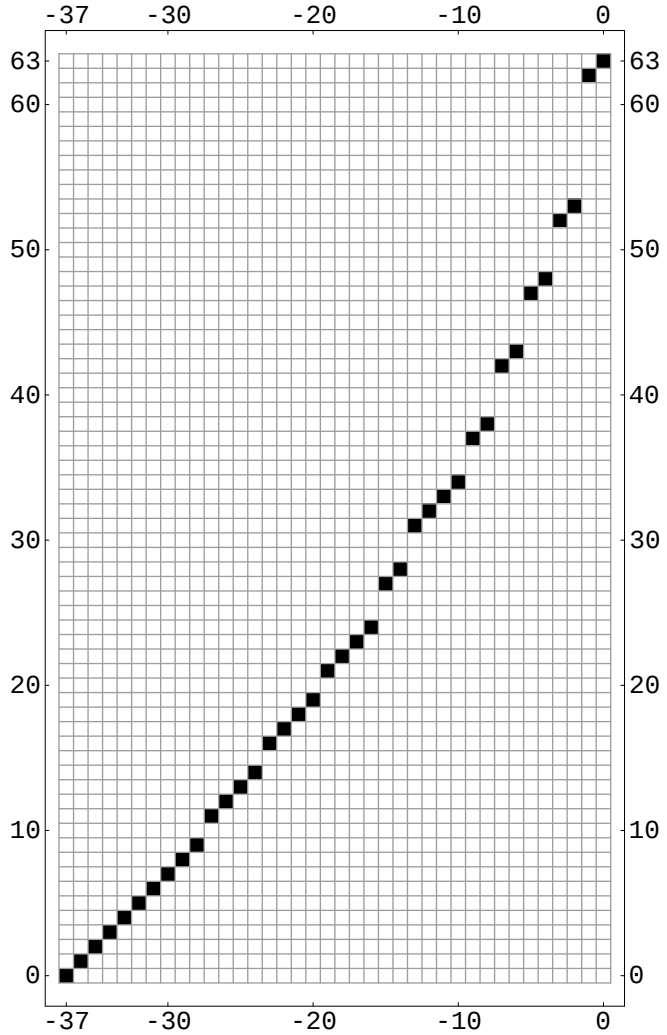

$\mathfrak{d}(2, 8, 13, 39)$

$\mathfrak{D}(8, 36, 23, 53)$

$K(75, 8, 36, 53)$

$x_0 = 22$

$\mathrm{lk}(\mathfrak{b}(26, 5)) = 5$

$K(28, 5; 6, 1)$

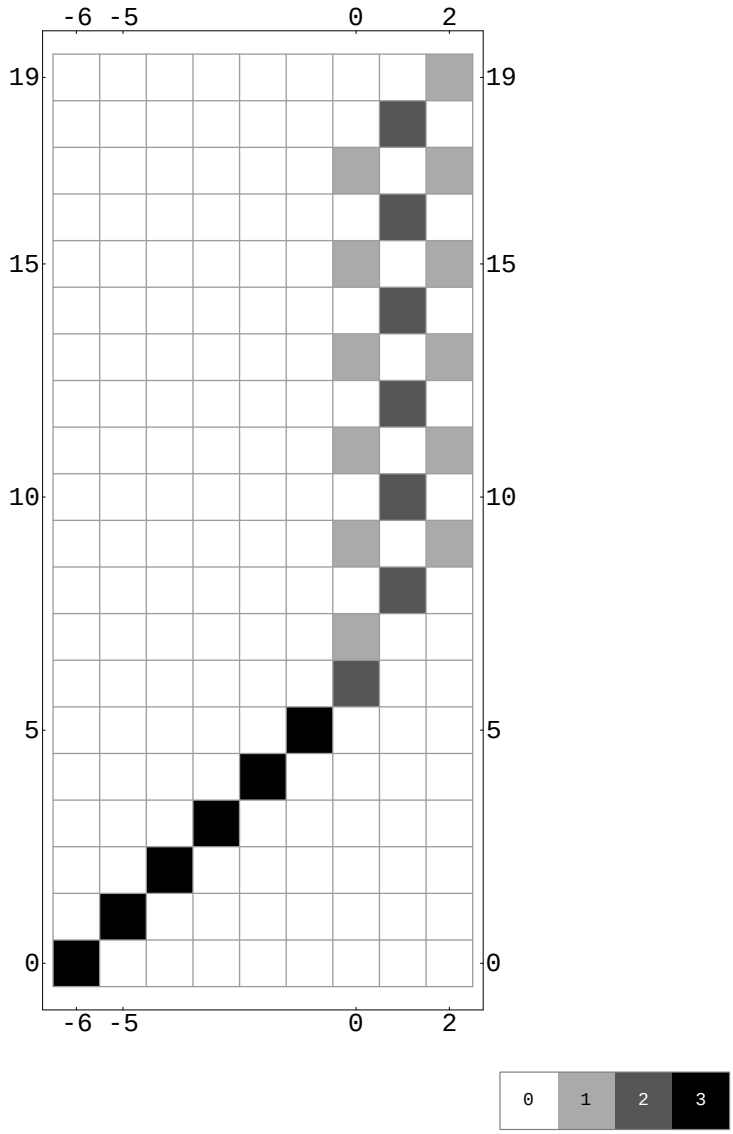

$\mathfrak{d}(2, 9, 0, 84)$

$\mathfrak{D}(18, 1, 48, 30)$

$K(85, 18, 1, 30)$

$x_0 = 37$

$\mathrm{lk}(\mathfrak{b}(28, 5)) = 2$

$K(28, 5; 3, 2)$

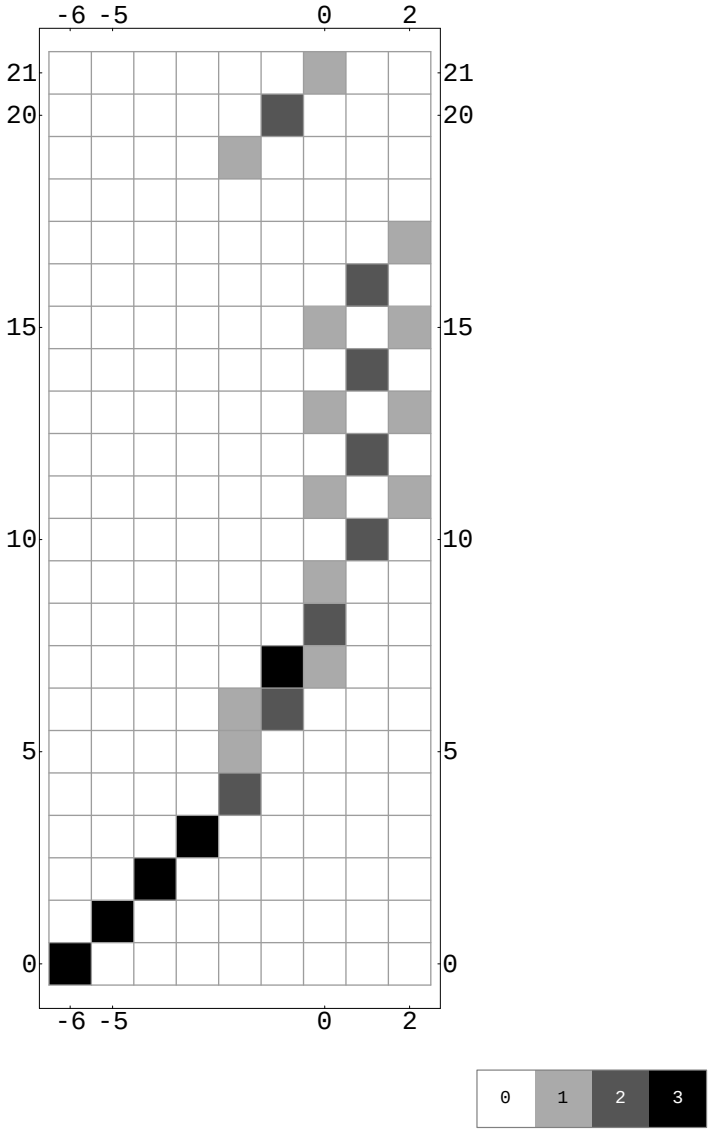

$\mathfrak{d}(2, 9, 14, 42)$

$\mathfrak{D}(9, 43, 24, 59)$

$K(85, 9, 43, 59)$

$x_0 = 20$

$\mathrm{lk}(\mathfrak{b}(28, 5)) = 2$

$K(16, 7; 6, 1)$

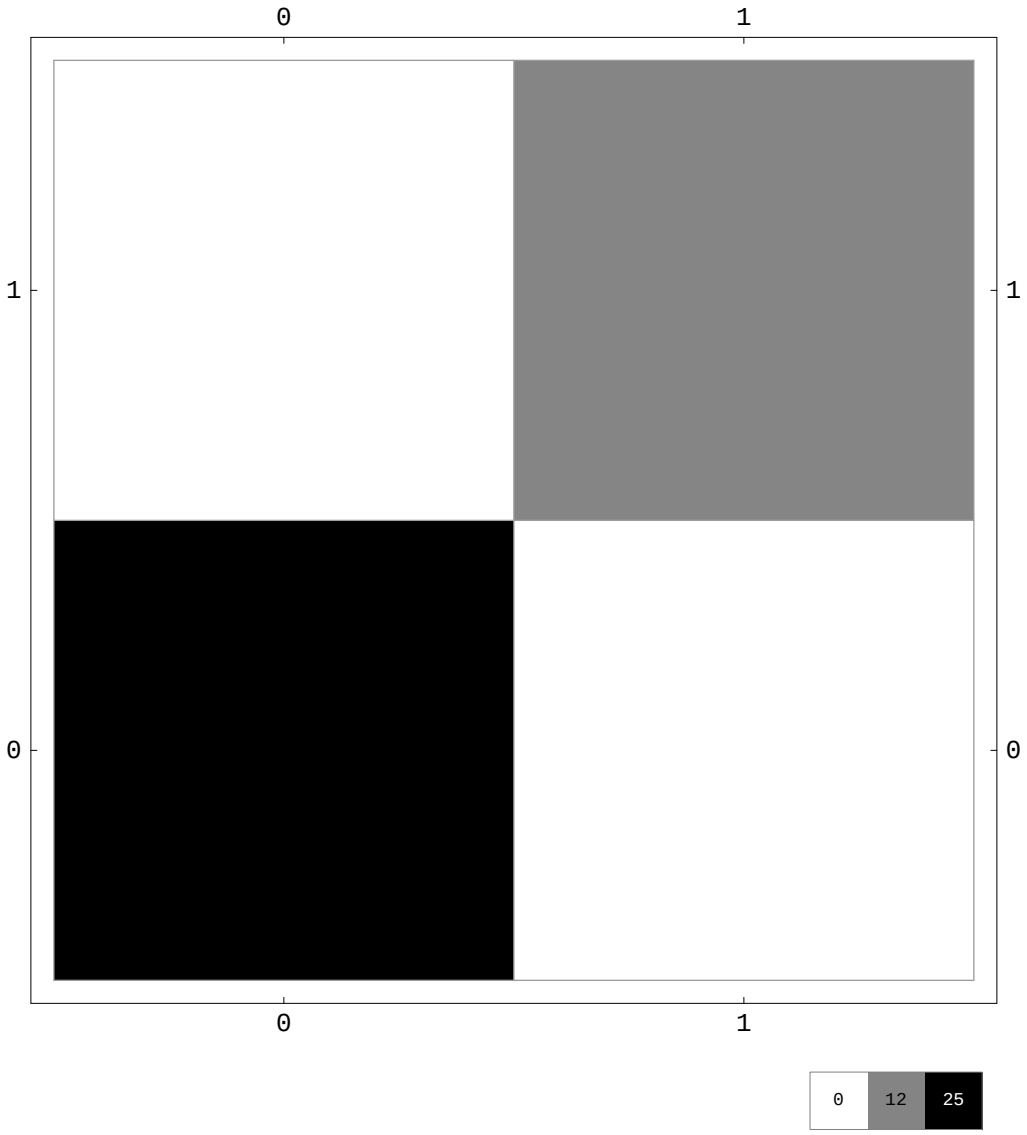

$\mathfrak{d}(3, 1, 0, 48)$

$\mathfrak{D}(24, 1, 0, 42)$

$K(49, 24, 1, 42)$

$x_0 = 43$

$\mathrm{lk}(\mathfrak{b}(16, 7)) = 0$

$K(16, 7; 3, 2)$

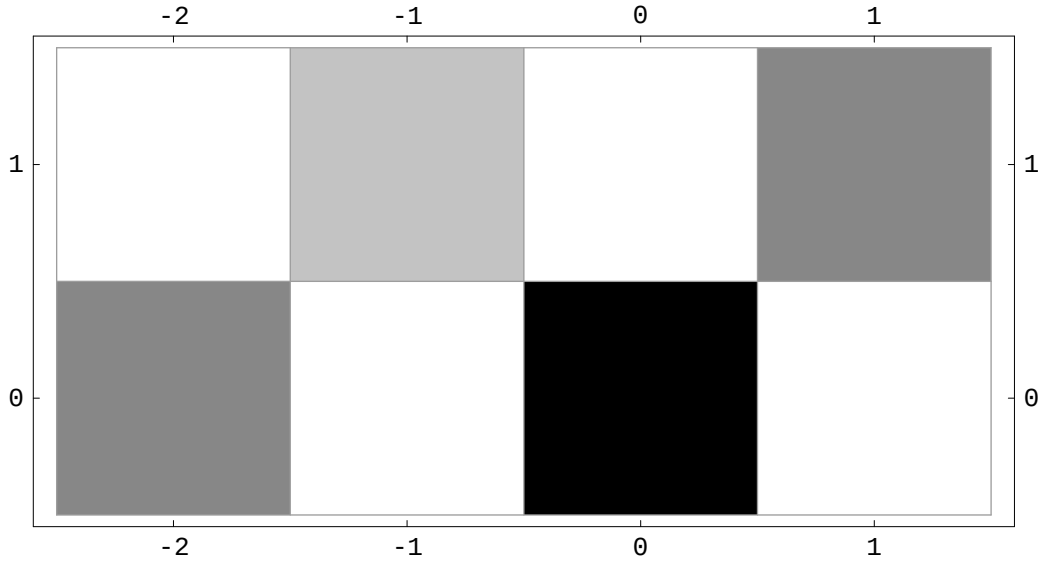

$\mathfrak{d}(3, 1, 8, 24)$

$\mathfrak{D}(12, 25, 0, 47)$

$K(49, 12, 25, 47)$

$x_0 = 23$

$\mathrm{lk}(\mathfrak{b}(16, 7)) = 0$

$K(18, 7; 6, 1)$

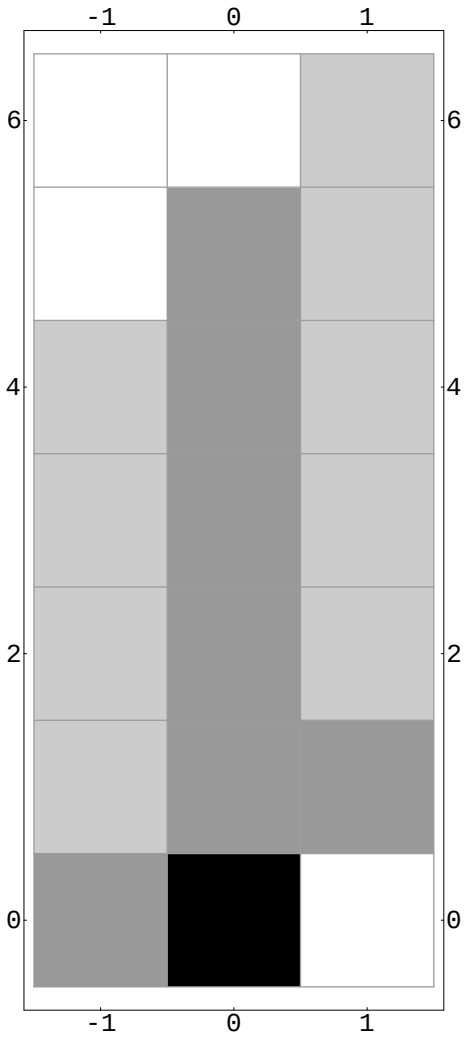

$\mathfrak{d}(3, 2, 0, 54)$

$\mathfrak{D}(19, 6, 5, 31)$

$K(49, 19, 6, 31)$

$x_0 = 32$

$\mathrm{lk}(\mathfrak{b}(18, 7)) = -1$

$K(18, 7; 3, 2)$

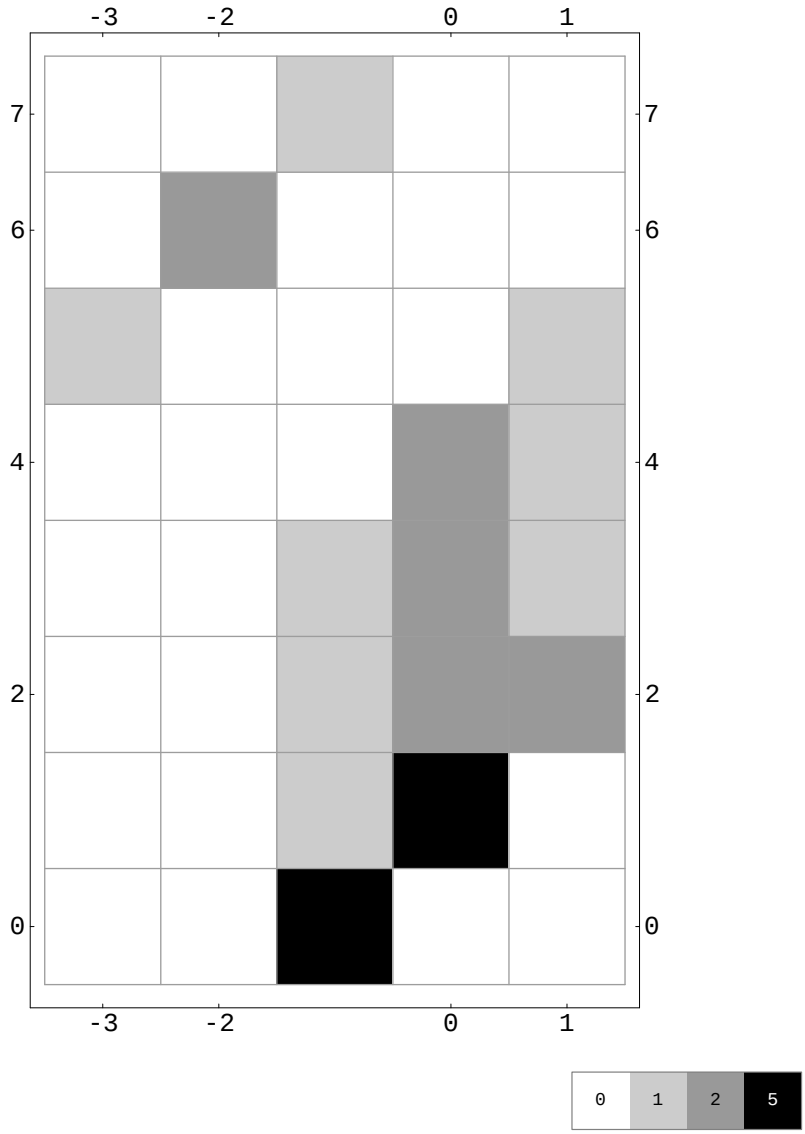

$\mathfrak{d}(3, 2, 9, 27)$

$\mathfrak{D}(11, 24, 5, 47)$

$K(51, 11, 24, 47)$

$x_0 = 19$

$\mathrm{lk}(\mathfrak{b}(18, 7)) = -1$

$K(20, 7; 6, 1)$

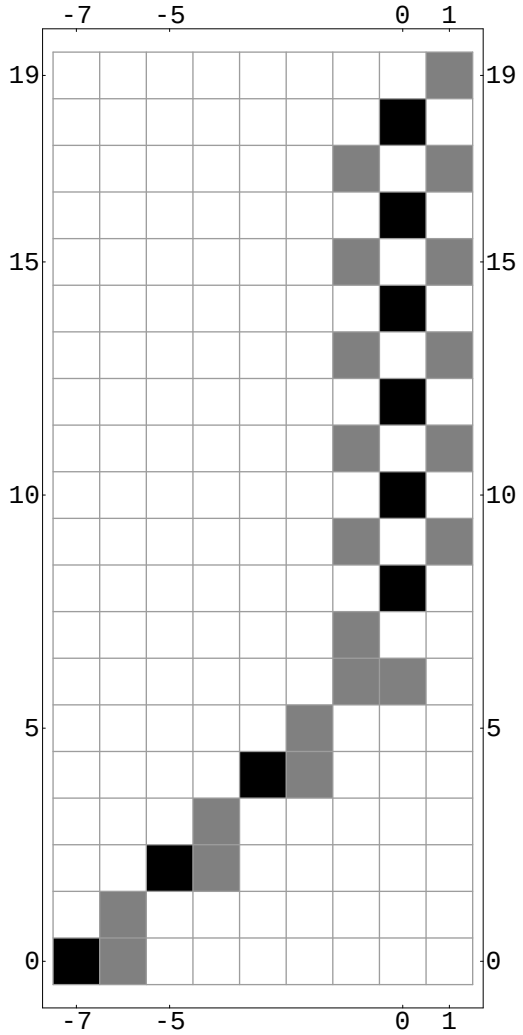

$\mathfrak{d}(3, 3, 0, 60)$

$\mathfrak{D}(24, 13, 12, 42)$

$K(73, 24, 13, 42)$

$x_0 = 43$

$\mathrm{lk}(\mathfrak{b}(20, 7)) = -2$

$K(20, 7; 3, 2)$

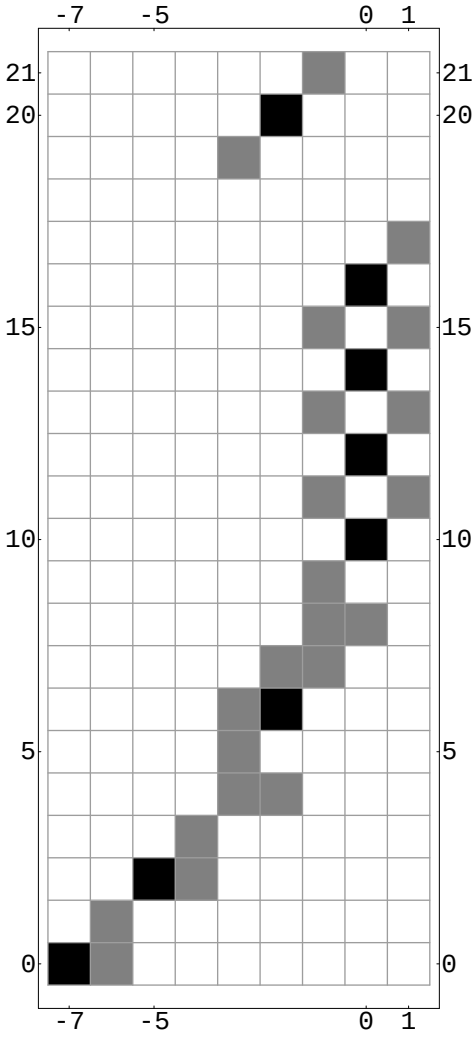

$\mathfrak{d}(3, 3, 10, 30)$

$\mathfrak{D}(12, 43, 6, 59)$

$K(73, 12, 43, 59)$

$x_0 = 23$

$\mathrm{lk}(\mathfrak{b}(20, 7)) = -2$

$K(22, 7; 6, 1)$

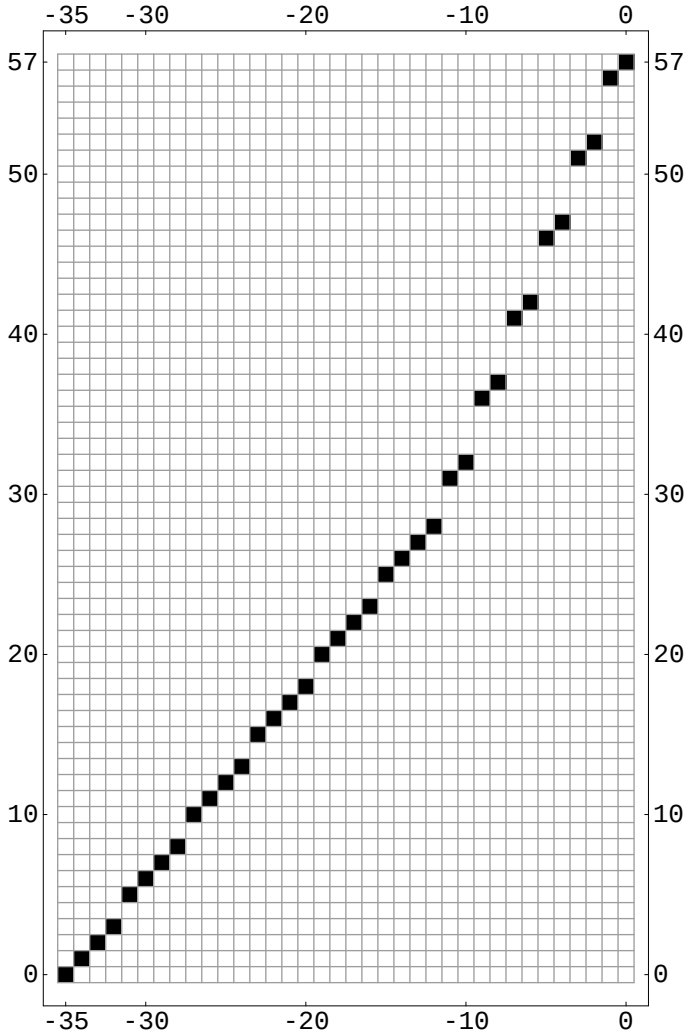

$\mathfrak{d}(3, 4, 0, 66)$

$\mathfrak{D}(18, 5, 30, 42)$

$K(71, 18, 5, 42)$

$x_0 = 65$

$\mathrm{lk}(\mathfrak{b}(22, 7)) = 5$

$K(22,7;3,2)$

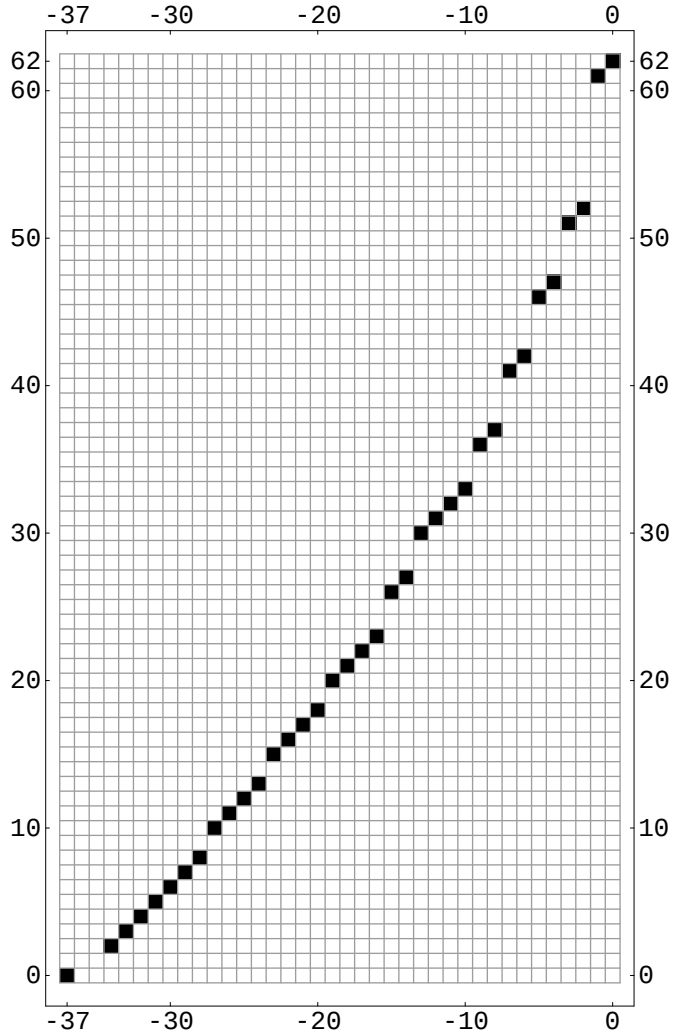

$\mathfrak{d}(3,4,11,33)$

$\mathfrak{D}(9,38,15,55)$

$K(71,9,38,55)$

$x_0 = 31$

$\mathrm{lk}(\mathfrak{b}(22,7)) = 5$

$K(24, 7; 6, 1)$

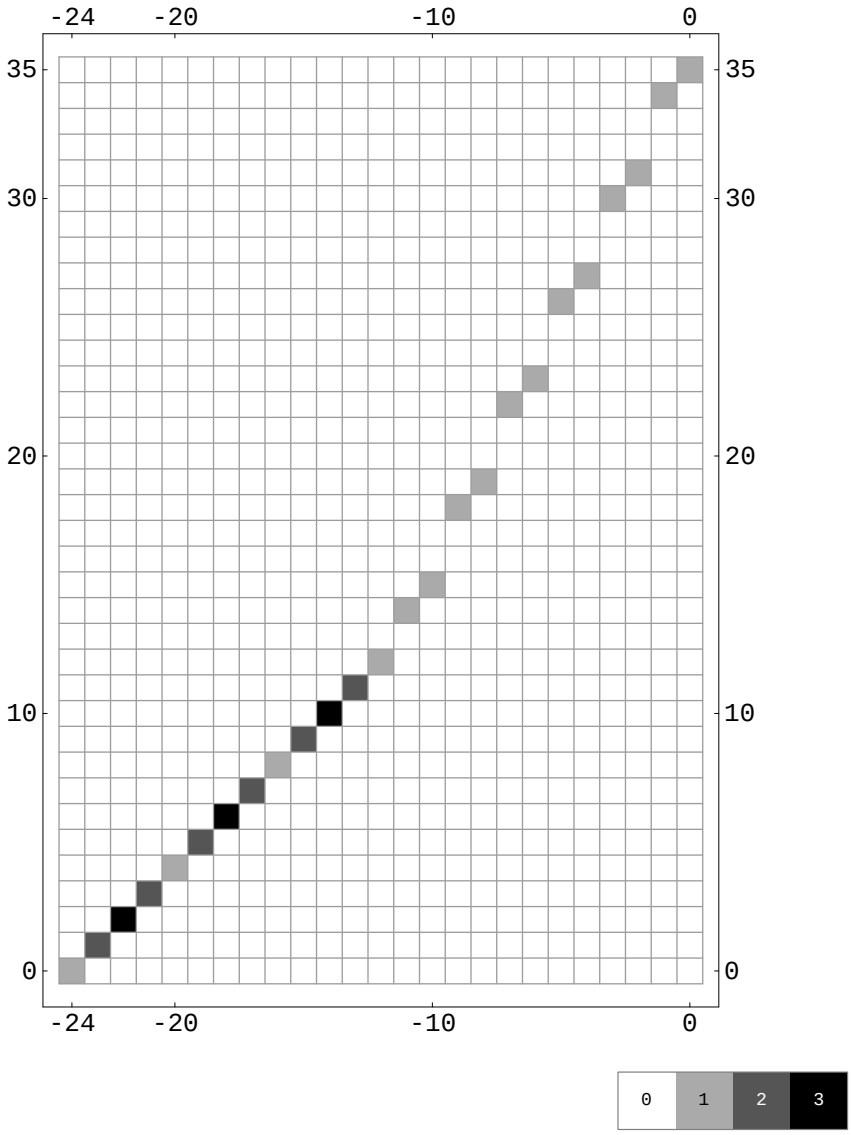

$\mathfrak{d}(3, 5, 0, 72)$

$\mathfrak{D}(24, 1, 24, 42)$

$K(73, 24, 1, 42)$

$x_0 = 67$

$\mathrm{lk}(\mathfrak{b}(24, 7)) = 4$

$K(24, 7; 3, 2)$

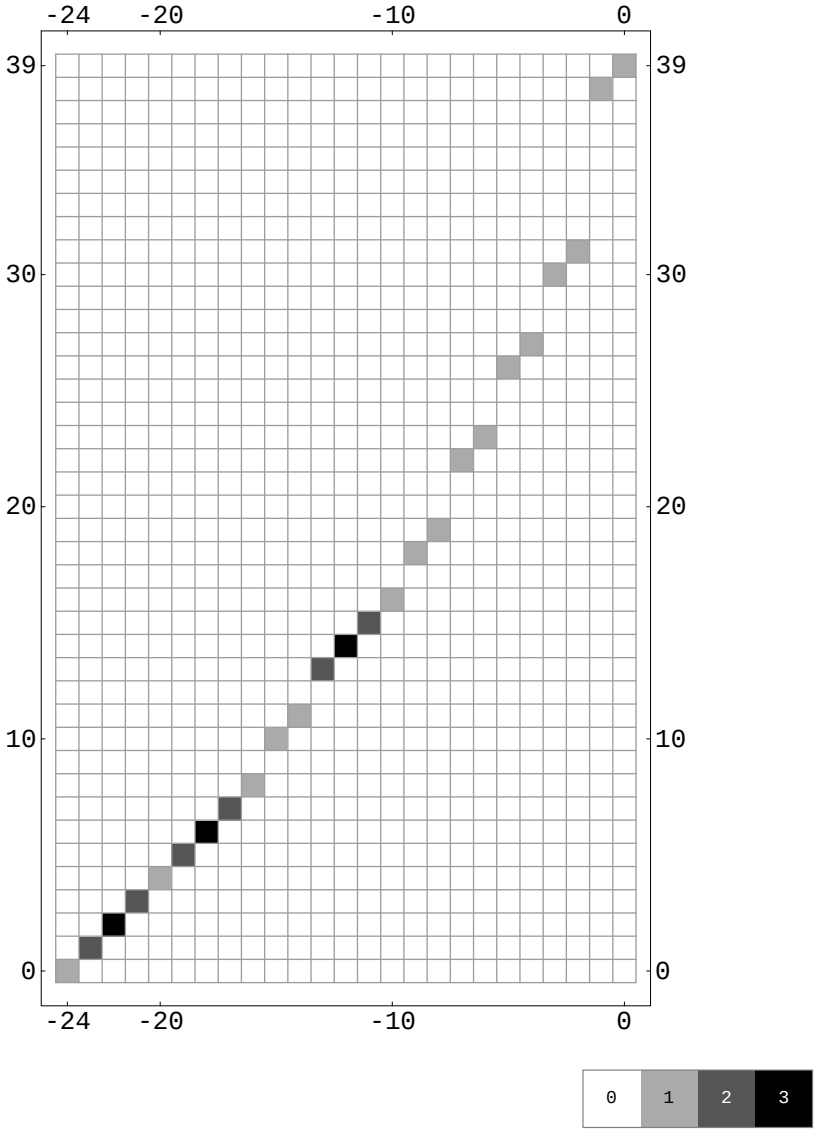

$\mathfrak{d}(3, 5, 12, 36)$

$\mathfrak{D}(12, 37, 12, 59)$

$K(73, 12, 37, 59)$

$x_0 = 35$

$\mathrm{lk}(\mathfrak{b}(24, 7)) = 4$

$K(26, 7; 6, 1)$

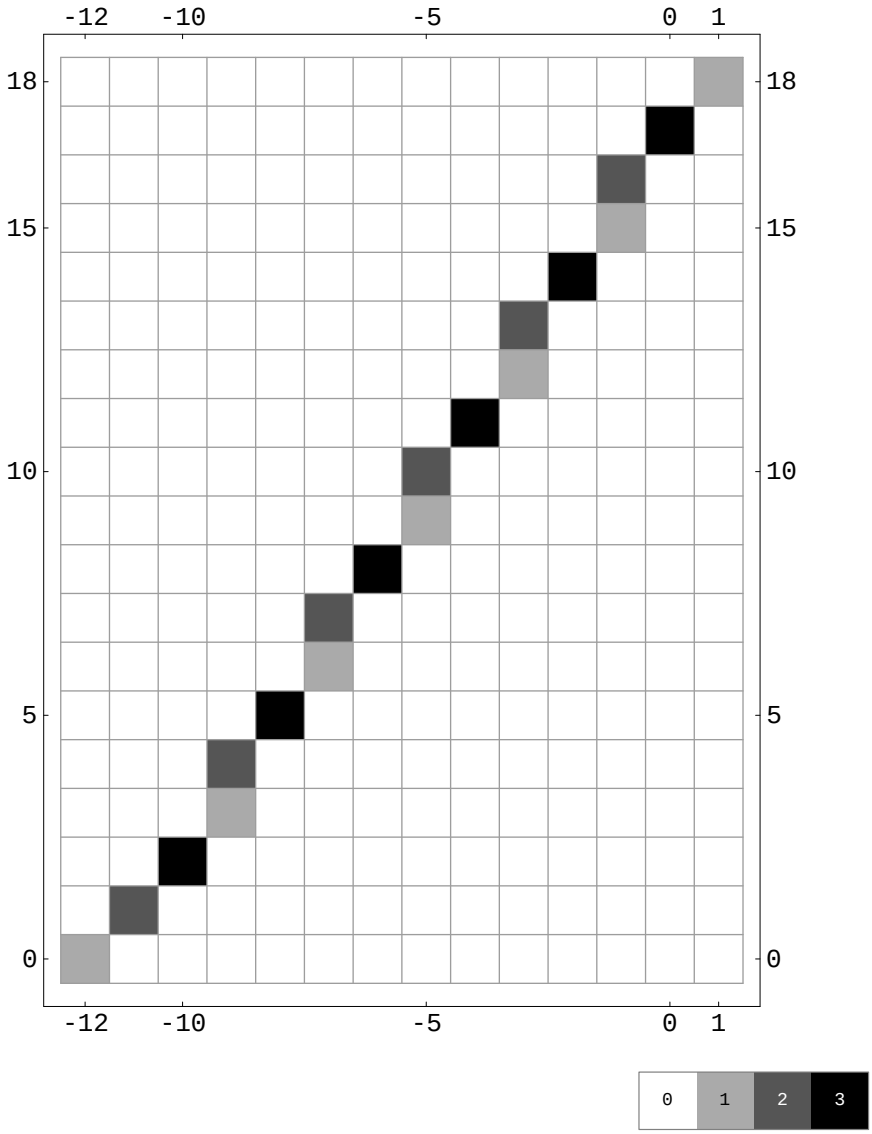

$\mathfrak{d}(3, 6, 0, 78)$

$\mathfrak{D}(19, 30, 5, 7)$

$K(73, 19, 30, 7)$

$x_0 = 44$

$\mathrm{lk}(\mathfrak{b}(26, 7)) = 3$

$K(26, 7; 3, 2)$

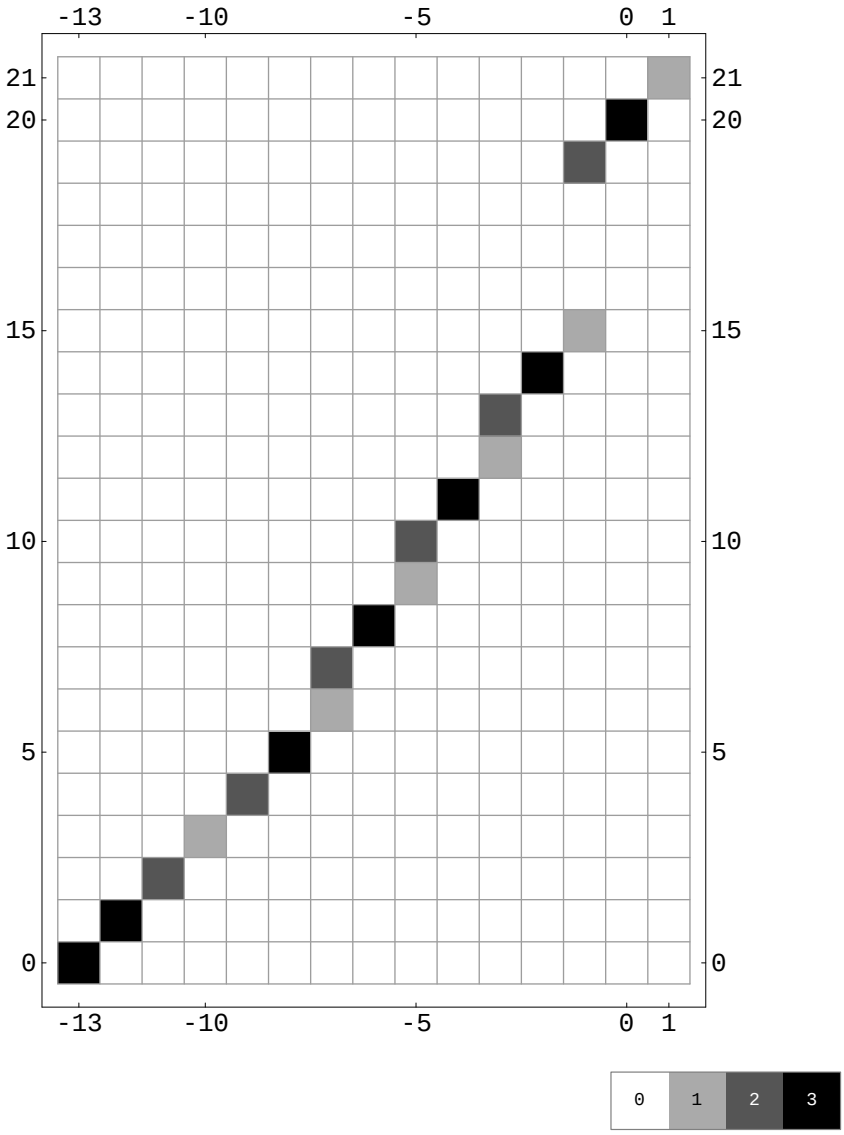

$\mathfrak{d}(3, 6, 13, 39)$

$\mathfrak{D}(11, 36, 17, 59)$

$K(75, 11, 36, 59)$

$x_0 = 25$

$\mathrm{lk}(\mathfrak{b}(26, 7)) = 3$

$K(30, 7; 6, 1)$

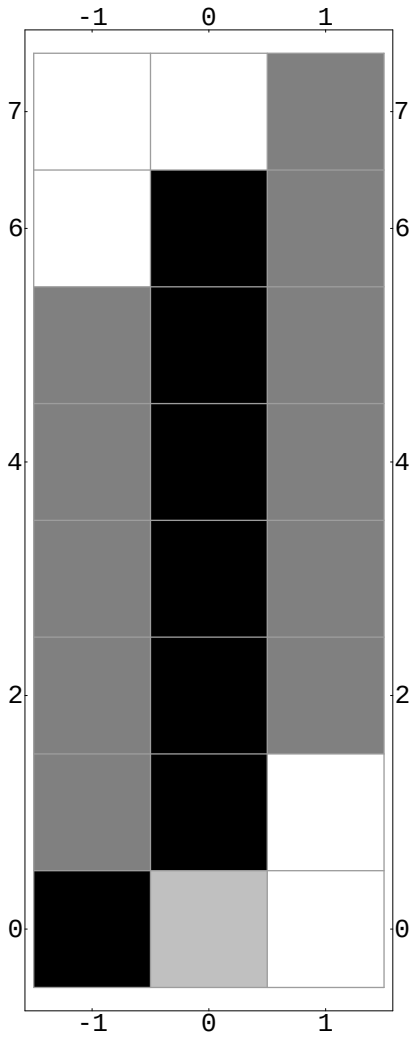

$\mathfrak{d}(3, 8, 0, 90)$

$\mathfrak{D}(24, 7, 42, 42)$

$K(97, 24, 7, 42)$

$x_0 = 49$

$\mathrm{lk}(\mathfrak{b}(30, 7)) = 1$

$K(30, 7; 3, 2)$

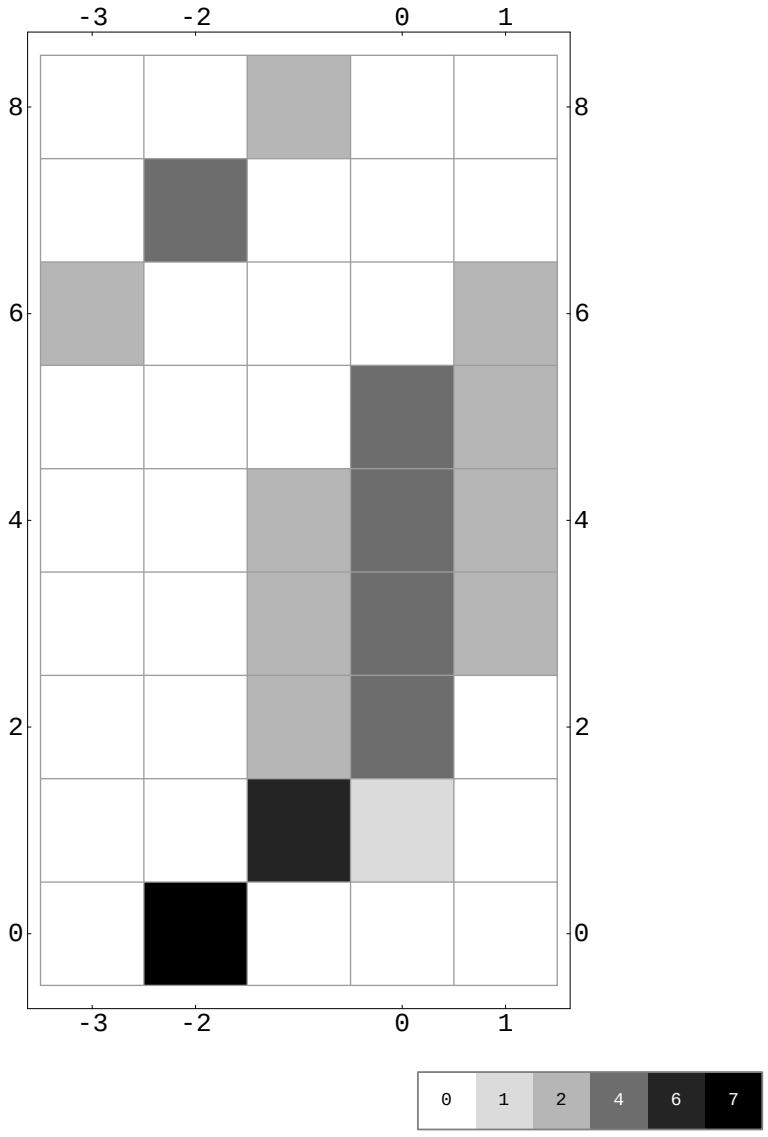

$\mathfrak{d}(3, 8, 15, 45)$

$\mathfrak{D}(12, 52, 21, 71)$

$K(97, 12, 52, 71)$

$x_0 = 26$

$\mathrm{lk}(\mathfrak{b}(30, 7)) = 1$

$K(20, 9; 6, 1)$

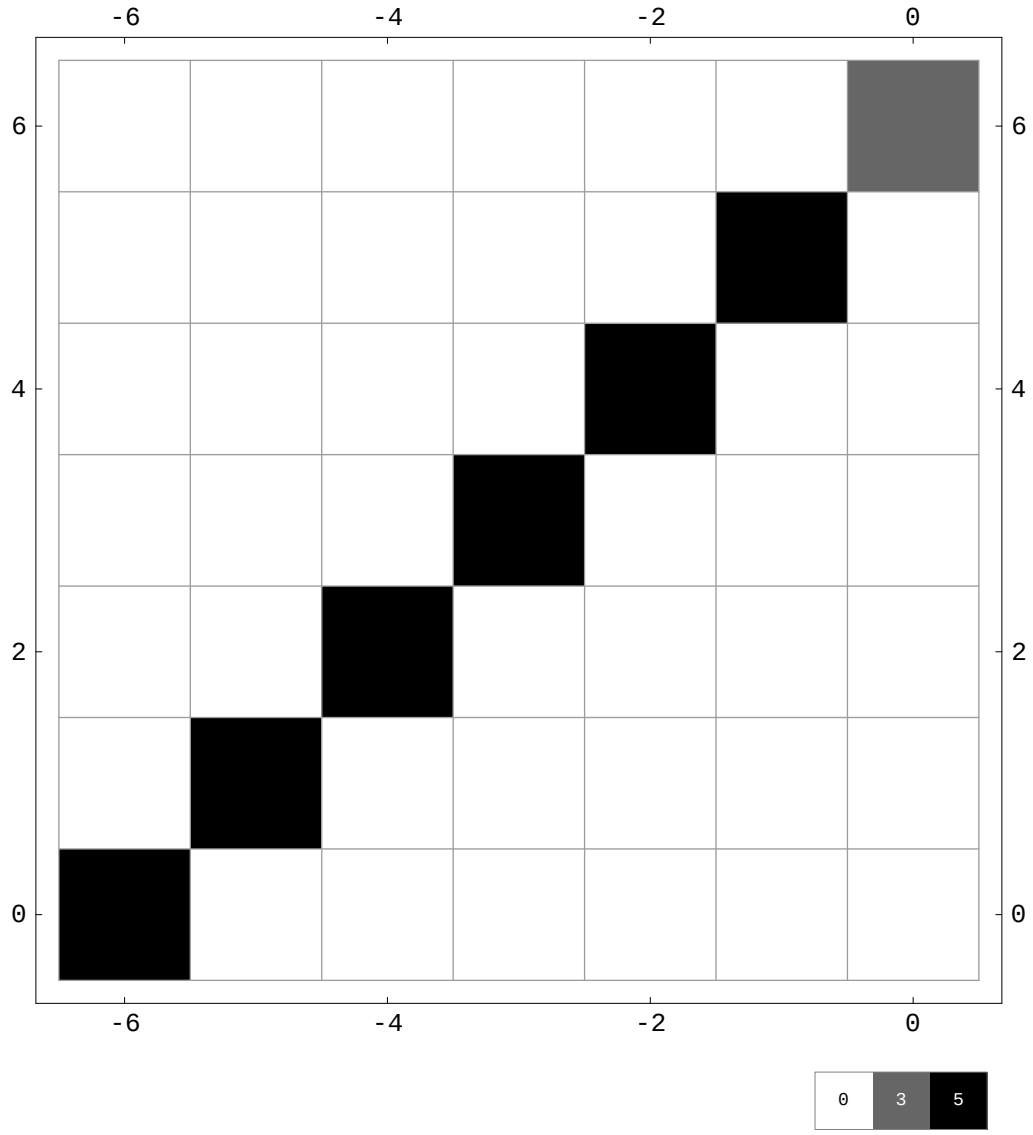

$\mathfrak{d}(4, 1, 0, 60)$

$\mathfrak{D}(30, 1, 0, 54)$

$K(61, 30, 1, 54)$

$x_0 = 61$

$\mathrm{lk}(\mathfrak{b}(20, 9)) = 2$

$K(20, 9; 3, 2)$

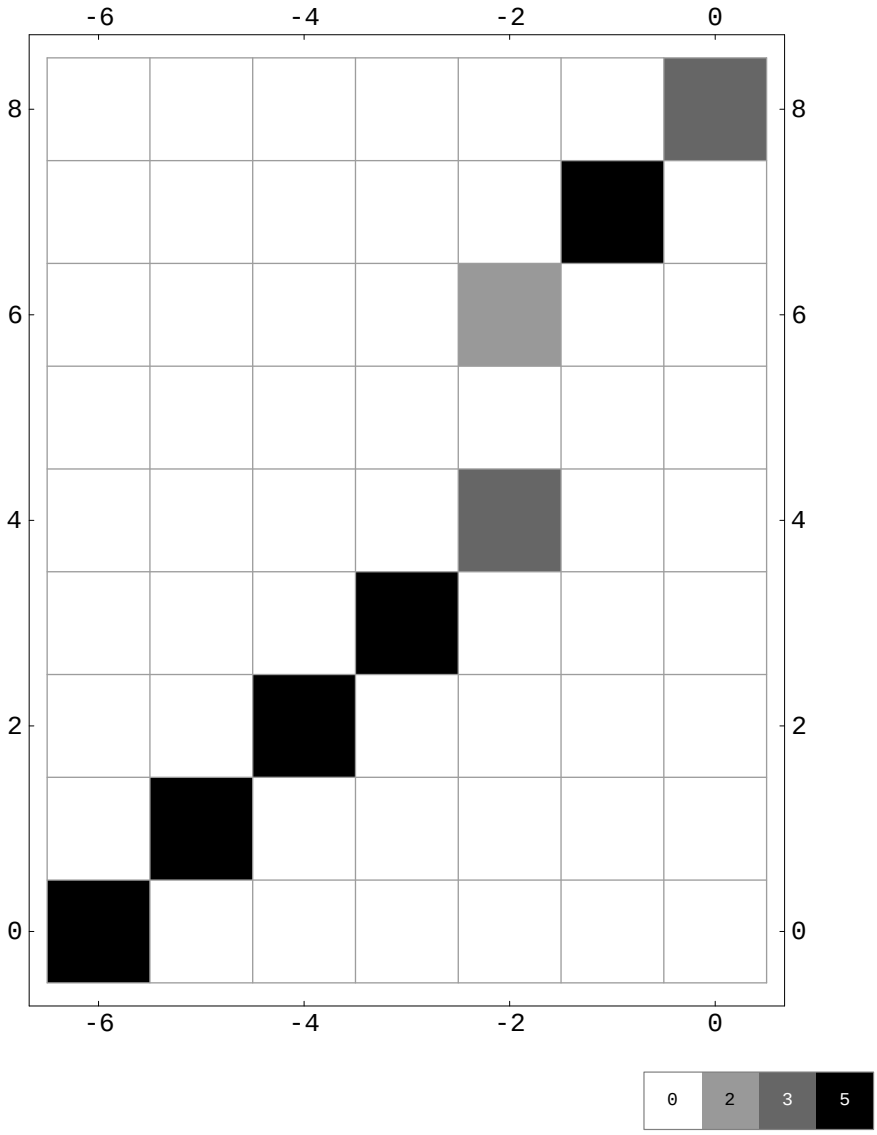

$\mathfrak{d}(4, 1, 10, 30)$

$\mathfrak{D}(15, 31, 0, 59)$

$K(61, 15, 31, 59)$

$x_0 = 32$

$\mathrm{lk}(\mathfrak{b}(20, 9)) = 2$

$K(28, 9; 6, 1)$

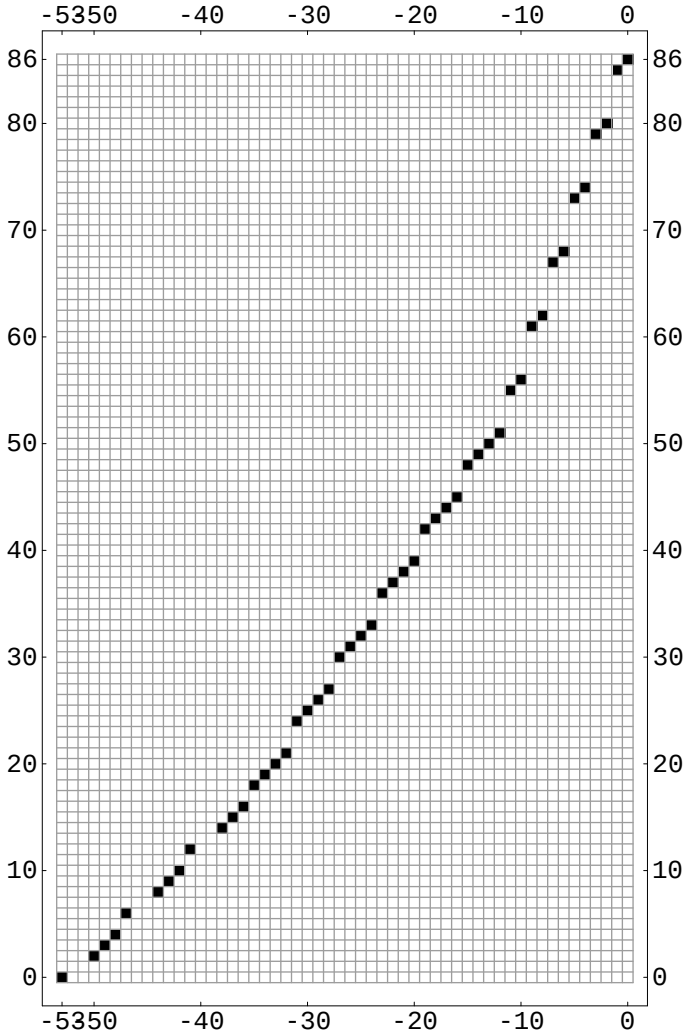

$\mathfrak{d}(4, 5, 0, 84)$

$\mathfrak{D}(24, 11, 36, 54)$

$K(95, 24, 11, 54)$

$x_0 = 89$

$\mathrm{lk}(\mathfrak{b}(28, 9)) = 6$

$K(28, 9; 3, 2)$

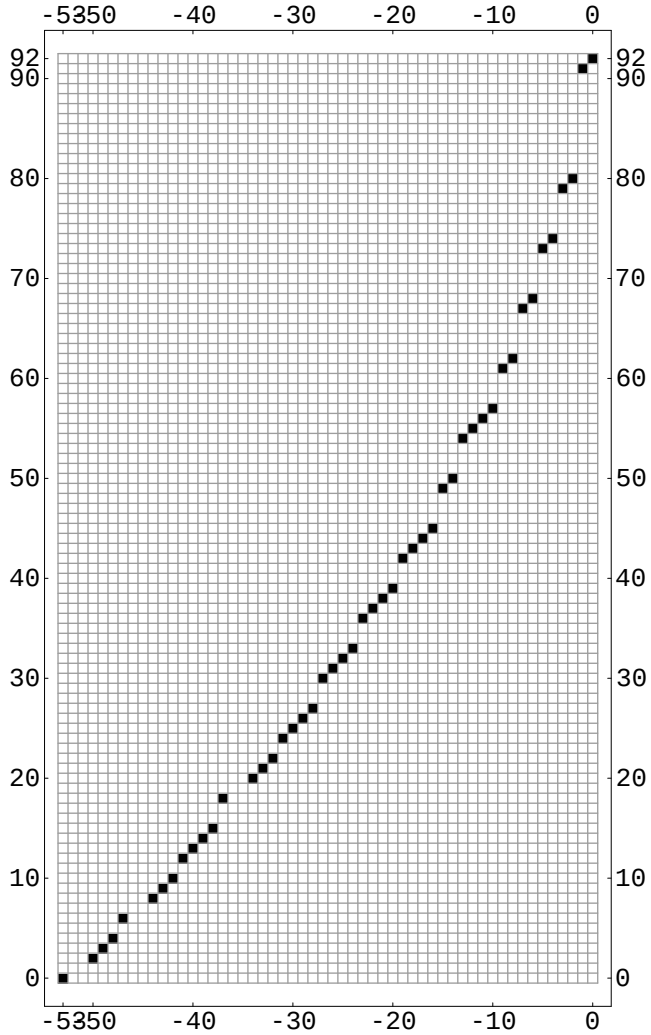

$\mathfrak{d}(4, 5, 14, 42)$

$\mathfrak{D}(12, 53, 18, 73)$

$K(95, 12, 53, 73)$

$x_0 = 43$

$\mathrm{lk}(\mathfrak{b}(28, 9)) = 6$

$K(24, 11; 6, 1)$

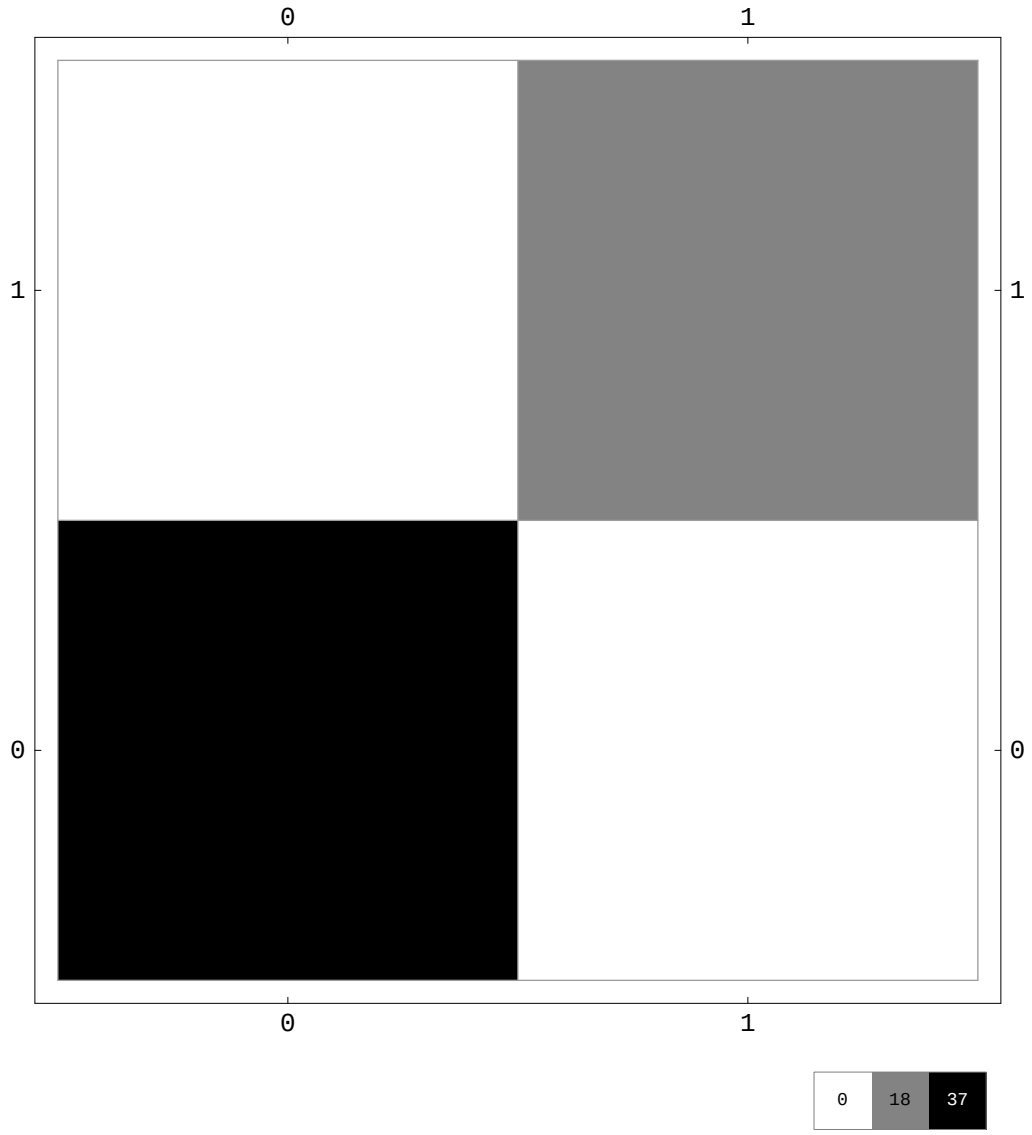

$\mathfrak{d}(5, 1, 0, 72)$

$\mathfrak{D}(36, 1, 0, 66)$

$K(73, 36, 1, 66)$

$x_0 = 67$

$\mathrm{lk}(\mathfrak{b}(24, 11)) = 0$

$K(24, 11; 3, 2)$

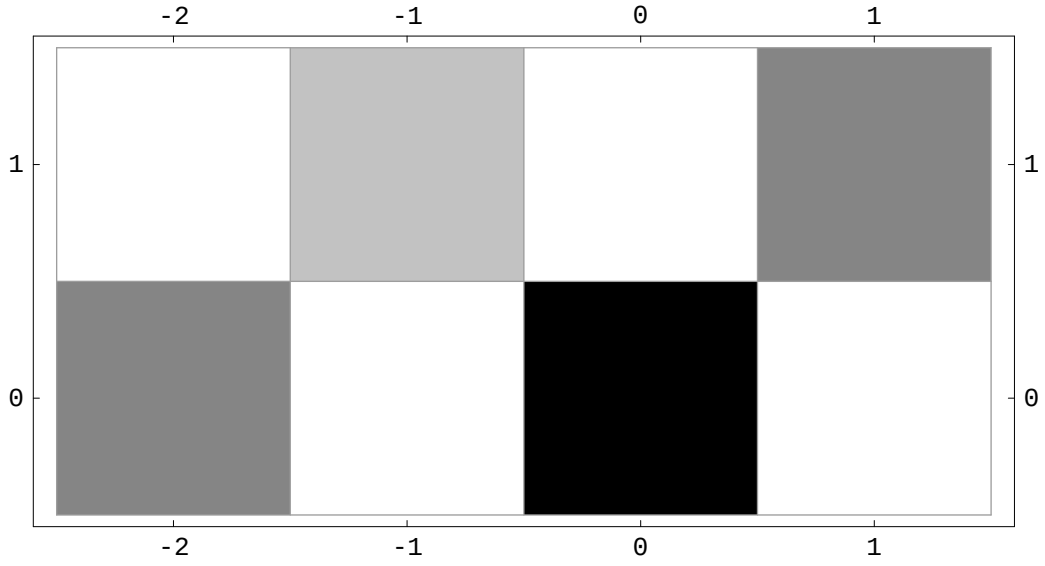

$\mathfrak{d}(5, 1, 12, 36)$

$\mathfrak{D}(18, 37, 0, 71)$

$K(73, 18, 37, 71)$

$x_0 = 35$

$\mathrm{lk}(\mathfrak{b}(24, 11)) = 0$

$K(26, 11; 6, 1)$

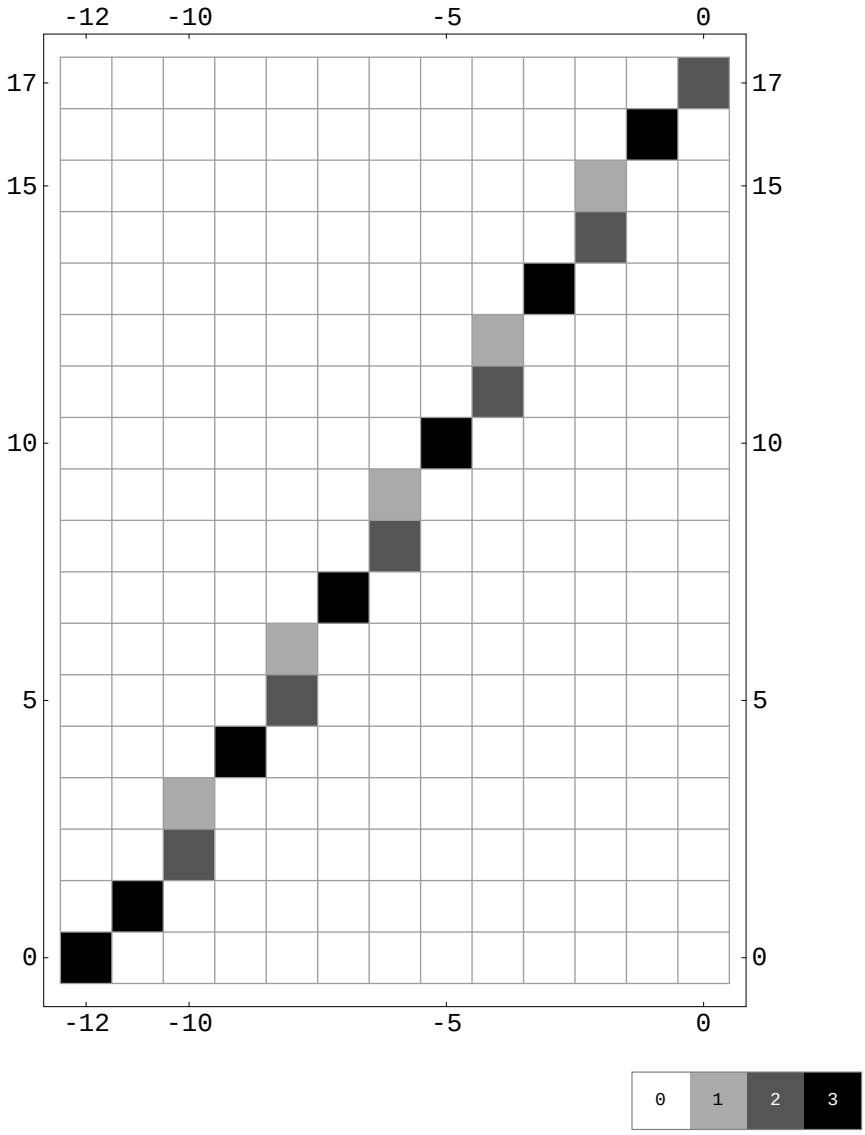

$\mathfrak{d}(5, 2, 0, 78)$

$\mathfrak{D}(31, 6, 5, 55)$

$K(73, 31, 6, 55)$

$x_0 = 68$

$\mathrm{lk}(\mathfrak{b}(26, 11)) = 3$

$K(26, 11; 3, 2)$

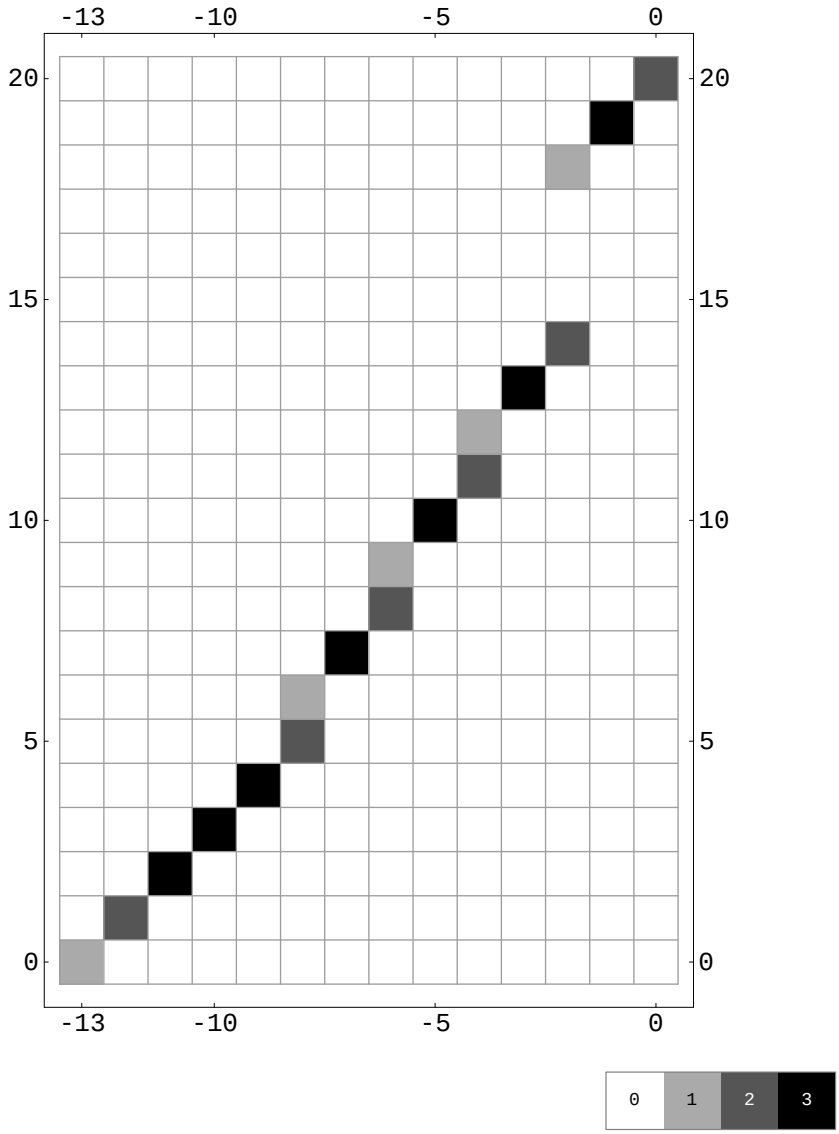

$\mathfrak{d}(5, 2, 13, 39)$

$\mathfrak{D}(17, 36, 5, 71)$

$K(75, 17, 36, 71)$

$x_0 = 37$

$\mathrm{lk}(\mathfrak{b}(26, 11)) = 3$

$K(28, 11; 6, 1)$

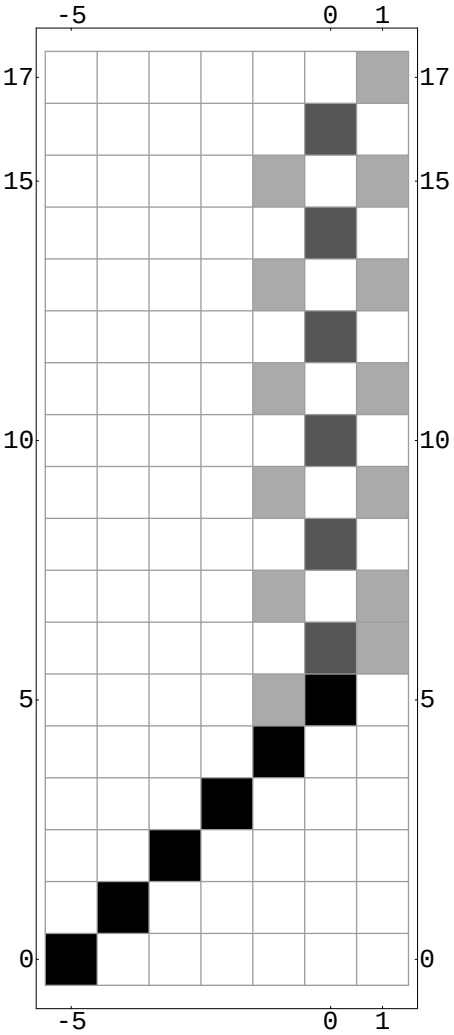

$\mathfrak{d}(5, 3, 0, 84)$

$\mathfrak{D}(30, 22, 1, 43)$

$K(83, 30, 22, 43)$

$x_0 = 49$

$\mathrm{lk}(\mathfrak{b}(28, 11)) = -2$

$K(28, 11; 3, 2)$

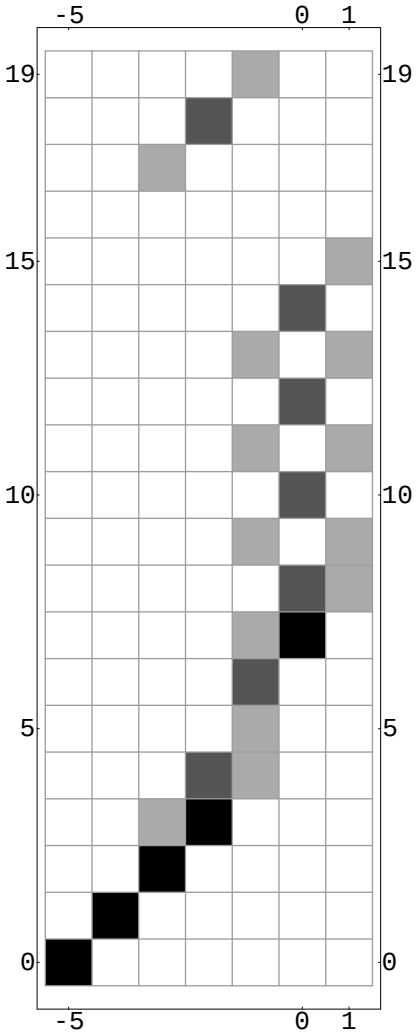

$\mathfrak{d}(5, 3, 14, 42)$

$\mathfrak{D}(15, 41, 12, 73)$

$K(83, 15, 41, 73)$

$x_0 = 26$

$\mathrm{lk}(\mathfrak{b}(28, 11)) = -2$

$K(30, 11; 6, 1)$

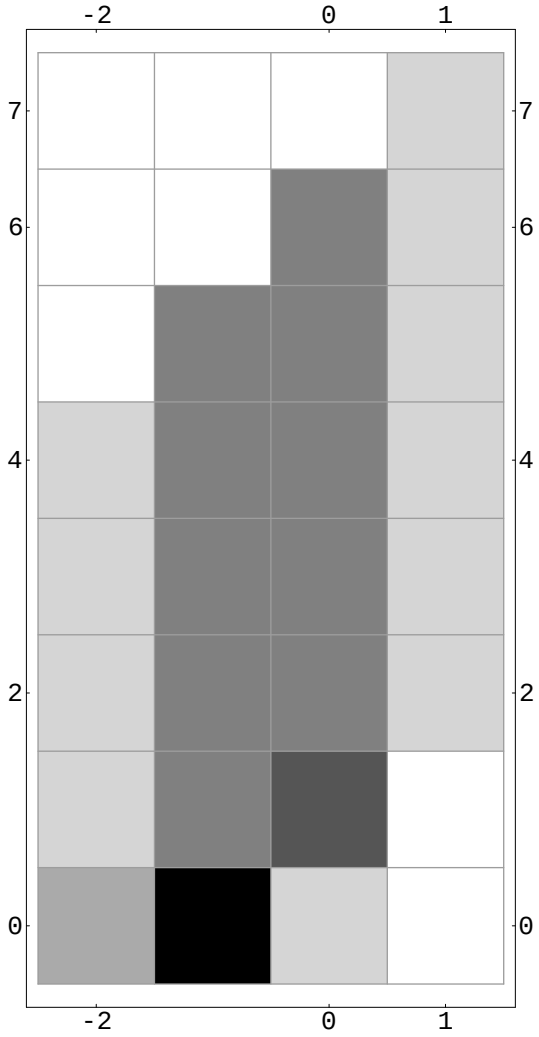

$\mathfrak{d}(5, 4, 0, 90)$

$\mathfrak{D}(36, 7, 18, 66)$

$K(97, 36, 7, 66)$

$x_0 = 73$

$\mathrm{lk}(\mathfrak{b}(30, 11)) = 1$

$K(30, 11; 3, 2)$

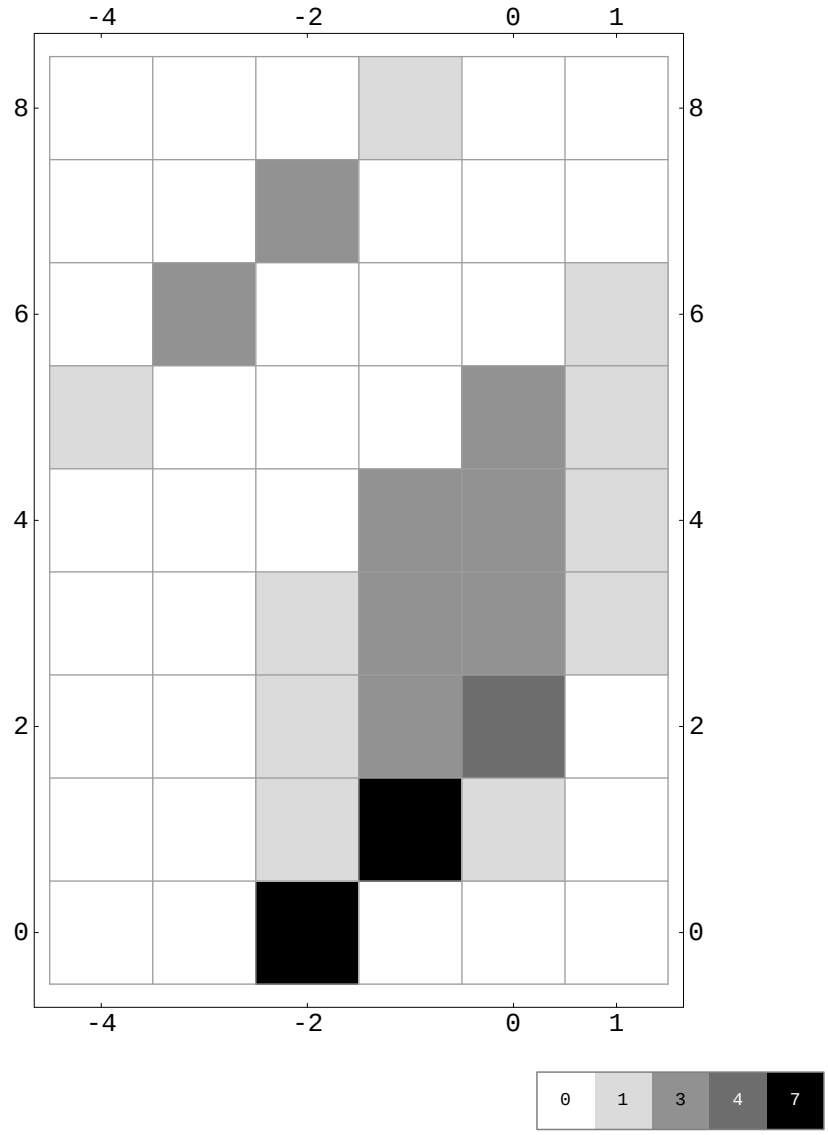

$\mathfrak{d}(5, 4, 15, 45)$

$\mathfrak{D}(18, 52, 9, 83)$

$K(97, 18, 52, 83)$

$x_0 = 38$

$\mathrm{lk}(\mathfrak{b}(30, 11)) = 1$

$K(28, 13; 6, 1)$

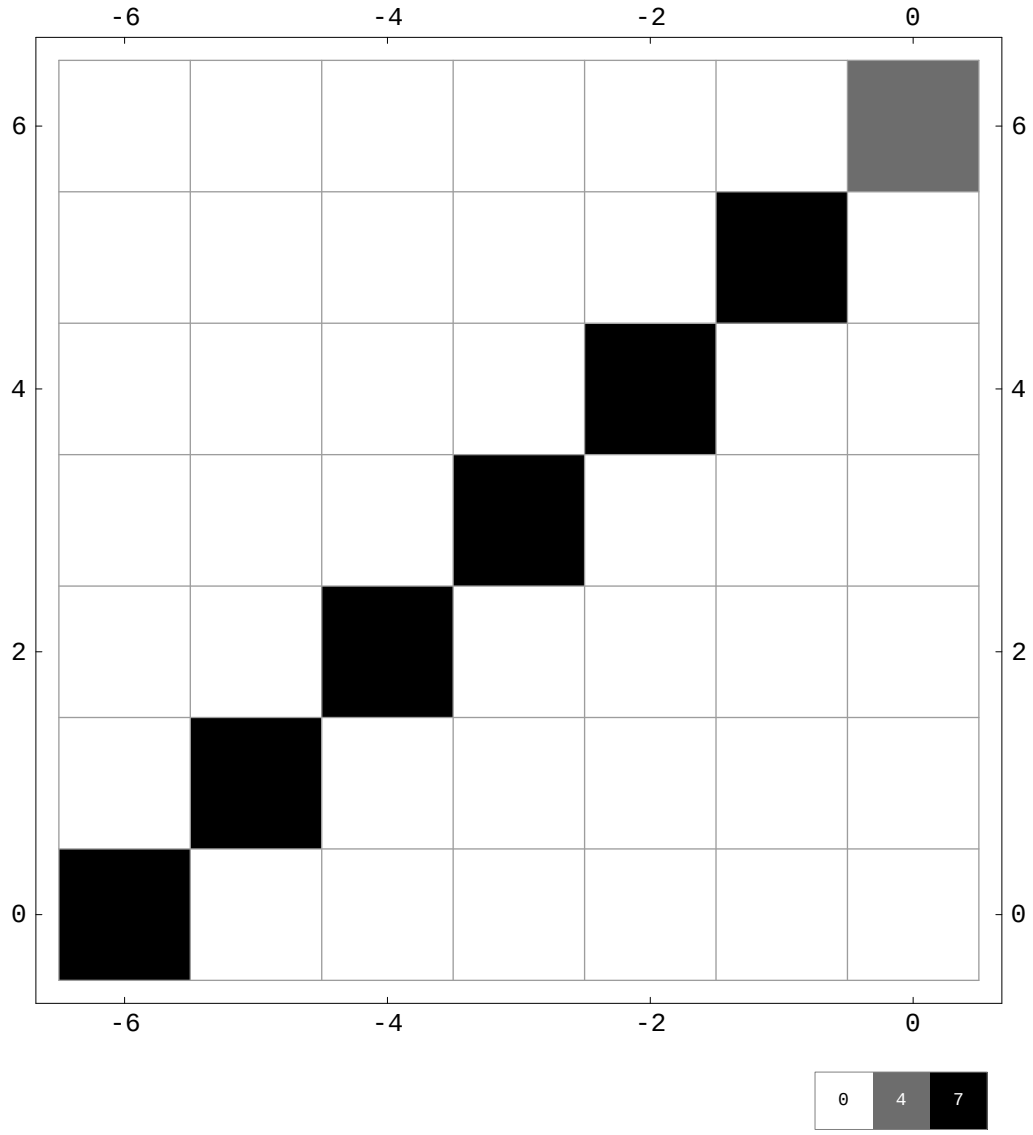

$\mathfrak{d}(6, 1, 0, 84)$

$\mathfrak{D}(42, 1, 0, 78)$

$K(85, 42, 1, 78)$

$x_0 = 85$

$\mathrm{lk}(\mathfrak{b}(28, 13)) = 2$

$K(28, 13; 3, 2)$

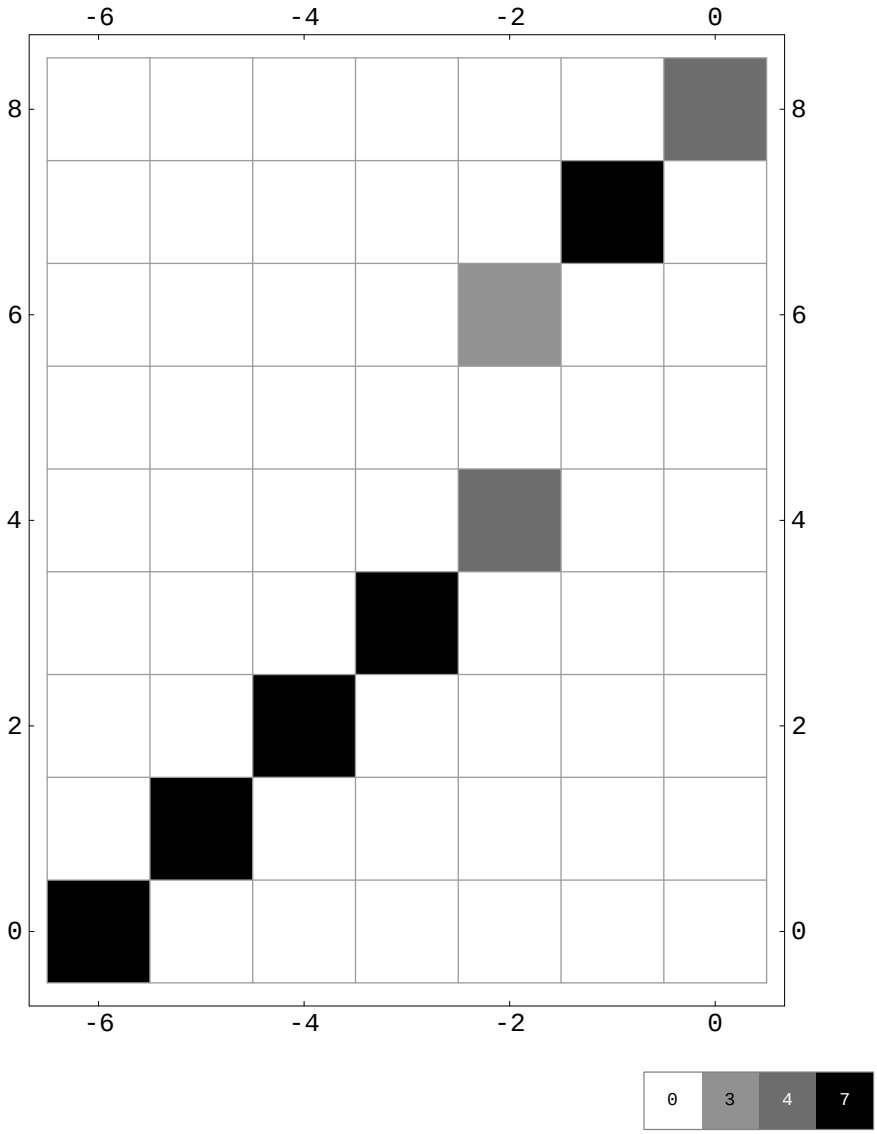

$\mathfrak{d}(6, 1, 14, 42)$

$\mathfrak{D}(21, 43, 0, 83)$

$K(85, 21, 43, 83)$

$x_0 = 44$

$\mathrm{lk}(\mathfrak{b}(28, 13)) = 2$

Bibliography

[BN06] Dror Bar-Natan. The knot atlas, 2006.

[BZ03] Gerhard Burde and Heiner Zieschang. *Knots*, volume 5 of *de Gruyter Studies in Mathematics*. Walter de Gruyter & Co., Berlin, second edition, 2003.

[CK03] Doo Ho Choi and Ki Hyoung Ko. Parametrizations of 1-bridge torus knots. *J. Knot Theory Ramifications*, 12(4):463–491, 2003.

[Doy05] Gabriel Doyle. solve11knot — a perl program for calculating the knot floer homology of a doubly pointed genus one heegaard knot diagram, 2005.

[Eft05] Eaman Eftekhary. Longitude Floer homology and the Whitehead double. *Algebr. Geom. Topol.*, 5:1389–1418 (electronic), 2005.

[Fuj96] Hirozumi Fujii. Geometric indices and the Alexander polynomial of a knot. *Proc. Amer. Math. Soc.*, 124(9):2923–2933, 1996.

[GMM05] Hiroshi Goda, Hiroshi Matsuda, and Takayuki Morifuji. Knot Floer homology of $(1, 1)$-knots. *Geom. Dedicata*, 112:197–214, 2005.

[GS99] Robert E. Gompf and András I. Stipsicz. 4-*manifolds and Kirby calculus*, volume 20 of *Graduate Studies in Mathematics*. American Mathematical Society, Providence, RI, 1999.

[Hed] Matthew Hedden. Knot floer homology of whitehead doubles. In preparation.

[Hed05] Matthew Hedden. *On knot Floer homology and cabling*. PhD thesis, Columbia University, 2005.

[HO] Matthew Hedden and Philip Ording. The Ozsváth-Szabó and Rasmussen concordance invariants are not equal. arXiv:math.GT/0512348.

[Kho00] Mikhail Khovanov. A categorification of the Jones polynomial. *Duke Math. J.*, 101(3):359–426, 2000.

[KM93] P. B. Kronheimer and T. S. Mrowka. Gauge theory for embedded surfaces. I. *Topology*, 32(4):773–826, 1993.

[Lee] Eun Soo Lee. An endomorphism of the Khovanov invariant. arXiv:math.GT/0210213.

[Lic97] W. B. Raymond Lickorish. *An introduction to knot theory*, volume 175 of *Graduate Texts in Mathematics*. Springer-Verlag, New York, 1997.

[MS91] Kanji Morimoto and Makoto Sakuma. On unknotting tunnels for knots. *Math. Ann.*, 289(1):143–167, 1991.

[OS03a] Peter Ozsvath and Zoltan Szabo. Heegaard floer homology and alternating knots. *Geom. Topol.*, 7:225, 2003.

[OS03b] Peter Ozsváth and Zoltán Szabó. Knot Floer homology and the four-ball genus. *Geom. Topol.*, 7:615–639 (electronic), 2003.

[OS04a] Peter Ozsváth and Zoltán Szabó. Heegaard diagrams and holomorphic disks. In *Different faces of geometry*, Int. Math. Ser. (N. Y.), pages 301–348. Kluwer/Plenum, New York, 2004.

[OS04b] Peter Ozsváth and Zoltán Szabó. Holomorphic disks and genus bounds. *Geom. Topol.*, 8:311–334 (electronic), 2004.

[OS04c] Peter Ozsváth and Zoltán Szabó. Holomorphic disks and knot invariants. *Adv. Math.*, 186(1):58–116, 2004.

[OS04d] Peter Ozsváth and Zoltán Szabó. Holomorphic disks and three-manifold invariants: properties and applications. *Ann. of Math. (2)*, 159(3):1159–1245, 2004.

[OS05] Peter Ozsváth and Zoltán Szabó. On knot Floer homology and lens space surgeries. *Topology*, 44(6):1281–1300, 2005.

[Rasa] Jacob A. Rasmussen. Khovanov homology and the slice genus. arXiv:math.GT/0402131.

[Rasb] Jacob A. Rasmussen. Knot polynomials and knot homologies. arXiv:math.GT/0504045.

[Ras03] Jacob Andrew Rasmussen. *Floer homology and knot complements*. PhD thesis, Harvard University, 2003.

[Sch56] Horst Schubert. Knoten mit zwei Brücken. *Math. Z.*, 65:133–170, 1956.

[Shu06] A. Shumakovitch. Khoho — a program for computing and studying khovanov homology, 2006.

[Sti79] John Stillwell. The compound crossing number of a knot. *Austral. Math. Soc. Gaz.*, 6(1):1–10, 1979.

[Wol05] Wolfram Research, Inc. Mathematica, version 5.2, 2005.